January 2015

N-Cadherin Expression And EMT Progression In Arsenic- And Cadmium-Transformed Urotsa

Elizabeth Sandquist

N-CADHERIN EXPRESSION AND EMT PROGRESSION IN ARSENIC- AND CADMIUM-TRANSFORMED UROTSA

by

Elizabeth J. Sandquist
Bachelor of Science, University of North Dakota, 2010

A Dissertation
Submitted to the Graduate Faculty

of the

University of North Dakota

in partial fulfillment of the requirements

for the degree of

Doctor of Philosophy

Grand Forks, North Dakota
August
2015

This dissertation, submitted by Elizabeth Sandquist in partial fulfillment of the requirements for the Degree of Doctor of Philosophy from the University of North Dakota, has been read by the Faculty Advisory Committee under whom the work has been done and is hereby approved.

Scott H. Garrett

Seema Somji

Van A. Doze

John B. Shabb

Katherine A. Sukalski

This dissertation is being submitted by the appointed advisory committee as having met all of the requirements of the School of Graduate Studies at the University of North Dakota and is hereby approved.

Wayne Swisher
Dean of the School of Graduate Studies

June 30, 2015
Date

PERMISSION

Title	N-cadherin Expression and EMT Progression in Arsenic- and Cadmium-transformed UROtsa
Department	Biochemistry and Molecular Biology
Degree	Doctor of Philosophy

In presenting this dissertation in partial fulfillment of the requirements for a graduate degree from the University of North Dakota, I agree that the library of this University shall make it freely available for inspection. I further agree that permission for extensive copying for scholarly purposes may be granted by the professor who supervised my dissertation work or, in his absence, by the Chairperson of the department or the dean of the School of Graduate Studies. It is understood that any copying or publication or other use of this dissertation or part thereof for financial gain shall not be allowed without my written permission. It is also understood that due recognition shall be given to me and to the University of North Dakota in any scholarly use which may be made of any material in my dissertation.

Elizabeth J Sandquist
June 26, 2015

TABLE OF CONTENTS

LIST OF FIGURES viii

LIST OF TABLES xii

ACKNOWLEDGEMENTS xiii

ABSTRACT xiv

CHAPTER

I. INTRODUCTION 1

Environmental Background in Bladder Cancer 1

Arsenic Causes Bladder Cancer 2

Evidence of Arsenic Carcinogenicity 3

Potential Mechanisms of Cancer Induction by Arsenic 5

Cadmium Causes Bladder Cancer 12

Evidence of Cadmium Carcinogenicity 13

Potential Mechanisms of Cancer Induction by Cadmium 14

Cadmium- and Arsenic-transformed UROtsa Cells 20

N-cadherin 26

Bladder Cancer Characteristics and Research Needs 33

Hypothesis and Rationale 37

II. METHODS 39

Cell culture 39

AZC and HDACi 40

Heterotransplant Tumors 40

Real Time RT-PCR 41

Western Blot Analysis 42

Immunofluorescence 43

Immunohistochemistry 43

Chromatin Immunoprecipitation 44

Flow Cytometry 45

III. RESULTS 46

N-cadherin Induction in As^{3+}- and Cd^{2+}-transformed UROtsa Cells 46

EMT Progression in As^{3+}- and Cd^{2+}-transformed UROtsa Cells 59

IV. DISCUSSION 76

Model Systems of Bladder Cancer *in vivo* 76

Bladder Cancer Stem Cells 78

Characterization of EMT in UROtsa Transformants 85

Regulation of N-cadherin 92

APPENDIX 95

Expression of N-cadherin Splice Variants 96

P-cadherin Expression 97

Eukaryotic Elongation Factor 1A2 Expression 98

NR2F1 and NR2F2 Induction in As^{3+}- and Cd^{2+}-transformed UROtsa Cells ... 101

Microarray Validation by Short-term As^{3+} Exposure 104

Neurotrophin-3 Expression in As^{3+}- and Cd^{2+}-transformed UROtsa Cells 105

Ephrin Receptor A4 Induction in As^{3+}- and Cd^{2+}-transformed UROtsa Cells .. 110

Ets Variant 7 Induction in As^{3+}- and Cd^{2+}-transformed UROtsa Cells 112

ITM2C Expression 114

Abbreviations 115

BIBLIOGRAPHY 120

LIST OF FIGURES

Figure Page

1.1 Metabolism of Arsenate 7

1.2 N-cadherin is consistently induced in As^{3+}- and Cd^{2+}-transformed UROtsa cells 26

1.3 *In situ* and papillary urothelial carcinoma 35

1.4 Varying levels of invasive urothelial carcinoma 36

3.1 N-cadherin expression is elevated in As^{3+}- and Cd^{2+}-transformed UROtsa cells 46

3.2 N-cadherin is highly expressed in As^{3+} isolate #6 47

3.3 N-cadherin is expressed at cell-cell junctions 48

3.4 N-cadherin mRNA and protein levels are unchanged in subcutaneous heterotransplant tumors derived from As^{3+}- and Cd^{2+}-transformed isolates 49

3.5 Immunohistochemical analysis demonstrates negative staining in subcutaneous heterotransplant tumors derived from As^{3+}-transformed isolates 50

3.6 Immunohistochemical analysis demonstrates negative staining in subcutaneous heterotransplant tumors derived from Cd^{2+}- transformed isolates 51

3.7 N-cadherin is focally expressed in intraperitoneal tumors 52

3.8 The As^{3+} isolate #6 has dramatically increased numbers of N-cadherin-positive cells 53

3.9 Microspheres originating from As^{3+}- and Cd^{2+}-transformed isolates express cancer stem cell marker ALDH1A1, but low levels of N-cadherin 54

3.10 N-cadherin expression is induced in parent UROtsa cells exposed to 1 μM $CdCl_2$ over 30 days 56

3.11 N-cadherin expression is altered by MS-275 exposure, while relatively unchanged following 5'-AZC 57

3.12 Schematic illustration of the N-cadherin promoter 58

3.13 Histone 3 lysine 9 trimethylation is unchanged at Region 1 of the N-cadherin promoter following MS-275, As^{3+}, or Cd^{2+} exposure 58

3.14 Arsenite exposure and MS-275 increase total histone 4 acetylation at Region 2 of the N-cadherin promoter 59

3.15 E-cadherin is unchanged in As^{3+} and Cd^{2+} transformants 60

3.16 E-cadherin is consistently expressed at the cell membrane in As^{3+}- and Cd^{2+}-transformed UROtsa cells 61

3.17 N-cadherin and E-cadherin are co-expressed at the cell membrane in As^{3+}-transformed UROtsa cells 62

3.18 N-cadherin and E-cadherin are co-expressed at the cell membrane in Cd^{2+}-transformed UROtsa cells 63

3.19 E-cadherin is unchanged in subcutaneous heterotransplants 64

3.20 Immunohistochemical analysis demonstrates strong E-cadherin staining in subcutaneous heterotransplant tumors derived from As^{3+}- transformed isolates 65

3.21 Immunohistochemical analysis demonstrates strong E-cadherin staining in subcutaneous heterotransplant tumors derived from Cd^{2+}- transformed isolates 66

3.22 E-cadherin is strongly positive in IP heterotransplant tumors 67

3.23 N-cadherin mRNA is expressed in the transformed UROtsa isolates Cd#5 and As#6 at similar or higher levels than the mesenchymal-like bladder cancer cell lines J82 and TCCSUP 68

3.24 Twist expression is induced in As^{3+} and Cd^{2+} isolates 69

3.25 Snail expression is induced in As^{3+} and Cd^{2+} isolates 69

3.26 Immunostaining for Snail is positive in IP tumors derived from As^{3+} and Cd^{2+} isolates 70

3.27 Vimentin expression is unaltered in As^{3+}-transformed UROtsa cells, while induced in Cd^{2+} isolates 71

3.28 TCF4 expression is induced in As^{3+} and Cd^{2+} isolates 72

3.29 STEAP1 is consistently induced in Cd^{2+}-transformed UROtsa cells *in vitro* and maintained in some subcutaneous tumors 73

3.30 OCLN is consistently induced in Cd^{2+}-transformed UROtsa cells *in vitro* and maintained in select subcutaneous tumors 74

3.31 IL1RN is varied in Cd^{2+}-transformed UROtsa cells *in vitro* and *in vivo* 75

5.1 Expression of total N-cadherin splice variants in As^{3+}- and Cd^{2+}-transformed UROtsa is lower than that of J82 and RT4 cell lines 96

5.2 P-cadherin expression is variable in As^{3+}- and Cd^{2+}-transformed UROtsa cells 97

5.3 eEF1A2 is induced in Cd^{2+} transformants *in vitro* 98

5.4 eEF12 expression is dependent upon Cd^{2+} exposure in non-malignant UROtsa cells 99

5.5 eEF1A2 expression is regulated by histone acetylation state 100

5.6 NR2F1 is induced in As^{3+}- and Cd^{2+}-transformed isolates and corresponding subcutaneous heterotransplants 102

5.7 NR2F2 remains mostly unchanged in As^{3+}- and Cd^{2+}-transformed isolates *in vitro*, but is reduced in subcutaneous tumors 103

5.8 Microarray validation by analysis of short-term As^{3+} exposure 104

5.9 NTF3 is reduced in As^{3+}-transformed UROtsa cells at the mRNA and protein level 105

5.10 NTF3 is induced in Cd^{2+}-transformed UROtsa cells 106

5.11 Neurotrophin-3 expression is increased in As^{3+} and Cd^{2+} subcutaneous tumors 107

5.12 Neurotrophin-3 expression is unchanged following short-term As^{3+} and Cd^{2+} exposure 108

5.13 Neurotrophin-3 expression is altered by histone deacetylase inhibitor and DNA methyltransferase inhibitor treatment 109

5.14 Ephrin Receptor A4 expression is increased in As^{3+} and Cd^{2+} transformants 110

5.15 EPHA4 expression is elevated in As^{3+} and Cd^{2+} subcutaneous tumors 110

5.16 EPHA4 expression is induced after 12 hrs As^{3+} exposure 111

5.17 EPHA4 is induced by MS-275, but not 5'-AZC treatment 111

5.18 Ets variant 1 expression is induced in As^{3+} and Cd^{2+} transformants 113

5.19 ETV7 is reduced in As^{3+} subcutaneous tumors, and relatively unchanged in Cd^{2+} tumors 113

5.20 ITM2C expression is varied in As^{3+} and Cd^{2+} transformants *in vitro*, though reduced in subcutaneous tumors 114

LIST OF TABLES

Table Page

2.1 Primer source information 41

3.1 As^{3+} isolate #6 has the highest percentage of N-cadherin-positive cells 53

4.1 EMT characterization of transformed UROtsa cells with the human bladder cancer cell lines TCCSUP, RT4, and J82..... 91

ACKNOWLEDGEMENTS

I would like to thank Dr. Sens for his support during my graduate career, in which he allowed me to pursue my scientific passions and provided an environment in which I completed substantial, relevant research. I also thank Dr. Garrett and Dr. Somji for exposing me to a variety of molecular biology techniques, and for always being available for support. Dr. Doze gave me the opportunity to study neuroscience beginning as an undergraduate, for which I am thankful. In this lab, I fell in love with research. I am very appreciative to Dr. Shabb and Dr. Sukalski for allowing me to participate in undergraduate education and supporting my career development. Your mentorship has been invaluable to me. I would also like to acknowledge Dr. Dunlevy for her training in immunofluorescence and microscopy, and Dr. Zhou for his assistance in animal techniques and histology. I thank undergraduates Andrew Millbridge, Tyler Titcomb, Elizabeth Hafner, Austin Ganje, and Liana Haven for their contributions to this research.

Thank you to Dr. Meberg and Dr. Pyle, who supported my interest in science as an undergraduate and gave me opportunities to grow. The mentorship provided by my high school teacher Jim Nesius is what got me interested in science, and I thank him for believing in me.

I would not have survived graduate school without the support of my fellow graduate students, especially Katie Collette and Andrea Slusser. I wish them the best and expect great things from them in the future. Last, I am thankful for my family for believing in me and reminding me how awesome science really is

To my husband David. Thank you for your encouragement, patience, and support throughout my graduate career. I can’t wait to see where life takes us next.

ABSTRACT

Environmental agents are common causes of bladder cancer. Specifically, arsenic (As^{3+}) and cadmium (Cd^{2+}) are known carcinogens implicated in the development of bladder cancer. Previous studies from our laboratory have shown that As^{3+} and Cd^{2+} can cause malignant transformation of normal immortalized bladder urothelial cells, which can form tumors when injected subcutaneous or intraperitoneal into nude mice. Microarray analysis of repeated metal transformation in parallel revealed that N-cadherin was the most upregulated gene in As^{3+} transformants, and a top induced gene in Cd^{2+}-transformed cells. The switch from E-cadherin to N-cadherin is a well-known indicator of the epithelial-to-mesenchymal transition occurring in bladder cancer. Further, N-cadherin upregulation is correlated with tumor stage, increased recurrence, and decreased survival in patients. While the factors mediating the decrease in E-cadherin expression are well-established, little is known of the factors regulating the increase in N-cadherin expression. The goal of the present study was to determine how As^{3+} and Cd^{2+} regulate N-cadherin expression, whether this expression is maintained in heterotransplant models, and if N-cadherin is promoting the epithelial-to-mesenchymal transition in As^{3+}- and Cd^{2+}-transformed UROtsa cells *in vitro*. This work has demonstrated that N-cadherin is induced in As^{3+}- and Cd^{2+}-transformed UROtsa cell lines, and that the expression is maintained in intraperitoneal, but not subcutaneous, tumor xenografts. Further, tumor-initiating cells derived from transformed UROtsa cells did not express N-cadherin. This

suggests that tumor microenvironment and heterogeneity of cell populations are important factors for the use of animal models in cancer research. The As^{3+} and Cd^{2+} UROtsa cell lines represent the initial phases of EMT in bladder cancer, and may demonstrate a unique EMT pathway specific to heavy metal carcinogens. Transcriptional regulation of N-cadherin, which is mostly unknown, may be elucidated by the investigation of the transcription factor Twist and epigenetic regulation, particularly histone acetylation.

CHAPTER I

INTRODUCTION

Environmental Background in Bladder Cancer

The first link between environmental agents and bladder cancer was discovered by Ludwig Rehn in1895, in which he found an increased incidence of bladder cancer in workers using aniline at a dye manufacturer in Frankfurt, Germany (Dietrich & Dietrich, 2001; Rehn, 1895). The findings of Rehn initiated the study of occupational bladder carcinogens and spurred the development of occupational toxicology. Later in 1937, 2-naphthylamine, an aromatic amine, was found to be the bladder cancer-causing agent (Hueper, Wiley, & Wolfe, 1938). By the 1950's, subsequent studies of industrial workers lead to the discovery of multiple other aromatic amines which cause bladder cancer. Exposure to carcinogenic aromatic amines was found in the rubber, textile, and chemical industries (Johansson & Cohen, 1997).

Slowly, regulations were instituted which have limited occupational exposure to these bladder carcinogens. With this reduction, cigarette smoking is now the main cause of bladder cancer in the United States (Freedman, Silverman, Hollenbeck, Schatzkin, & Abnet, 2011). There is an approximately 3 times higher risk for bladder cancer in smokers versus non-smokers (Zeegers, Tan, Dorant, & Van Den Brandt, 2000). While the precise mechanism is unclear, aromatic amines, unsaturated aldehydes, and cadmium in cigarettes are known carcinogens (Johansson & Cohen, 1997; Vineis & Pirastu, 1997). Smokers are exposed to 1.7 µg cadmium per cigarette, and have double the body burden

of cadmium compared to non-smokers (ATSDR, 2012). Cigarettes also contain arsenic at levels up to 1.4 µg per cigarette (C. Smith, Livingston, & Doolittle, 1997).

Bladder cancer due to arsenic exposure was initially discovered in Taiwan, where residents drank water from artesian wells containing high amounts of the metal. Arsenic-induced bladder cancer has been confirmed by a number of studies since then.

Evidence of bladder carcinogenesis due to cadmium exposure is seen in Belgium, where increasing levels of blood cadmium were correlated with cancer risk (Kellen, Zeegers, Hond, & Buntinx, 2007). However, the evidence for cadmium-induced bladder cancer is less than that of arsenic.

Chronic infection with the parasite *Schistosoma haematobium* is also known to cause bladder cancer, predominantly squamous cell carcinoma (Mostafa, Sheweita, & O'Connor, 1999). Chronic infections in addition to that of *Schistosoma haematobium* may also promote bladder cancer, though direct links have yet to be proven (Abol-Enein, 2008).

Arsenic Causes Bladder Cancer

The general public is exposed to arsenic primarily by the oral route through food and drinking water (ATSDR, 2007). Oral ingestion of inorganic arsenic is known to cause skin, kidney, liver, lung, and prostate cancer in addition to that of bladder. Average dietary consumption of inorganic arsenic in the United States is 10.22 µg/day (MacIntosh et al., 1997), while exposure through drinking water is about 5 µg/day (ATSDR, 2007). The current limit of arsenic in drinking water is 10 ppb (EPA, 2001). Arsenic can leach from the soil into ground and surface water. Releases into the environment are mainly

from anthropogenic sources including nonferrous metal mining and smelting, pesticide use, coal and wood combustion, and waste combustion (ATSDR, 2007).

Evidence of Arsenic Carcinogenicity

Numerous epidemiological studies have proven the link between arsenic and bladder cancer. The discovery of arsenic-induced bladder cancer in Taiwan was initiated by the high incidence of blackfoot disease, a peripheral artery disease caused by arsenic exposure (Tseng, 1977). Upon investigation of these blackfoot-endemic regions, it was found that residents of this area also had high rates of bladder cancer (C. J. Chen, Chuang, Lin, & Wu, 1985). High exposure to arsenic in drinking water was later confirmed as the cause of bladder cancer in this region.

Following initial reports of increased bladder cancer in Taiwan (C J Chen, Chen, Wu, & Kuo, 1992; C J Chen, Chuang, You, Lin, & Wu, 1986; C. J. Chen et al., 1985; C. J. Chen & Wang, 1990; Chiou et al., 1995; L. Wang et al., 2012), evidence arose of bladder cancer due to arsenic in drinking water in Argentina (Hopenhayn-Rich et al., 1996) and Chile (A. H. Smith, Goycolea, Haque, & Biggs, 1998). More recent studies have shown links between arsenic in drinking water and bladder cancer in Tunisia (Feki-Tounsi et al., 2013b) and Pakistan (Wadhwa, Kazi, Afridi, Tüzen, & Citak, 2013). Studies of bladder cancer in Chile show that the effects of arsenic exposure have a long latency period, as increased bladder cancer mortality rates did not appear until 10 years following exposure to arsenic-contaminated drinking water (Marshall et al., 2007). Even 40 years later, bladder cancer odds ratios were elevated compared to the general population (Steinmaus et al., 2013). In Taiwan, studies report reduced bladder cancer incidence and mortality only after twenty years of exposure cessation through installation of tap water systems

(C.-C. Su, Lu, Tsai, & Lian, 2011; C.-Y. Yang, Chiu, Chang, Ho, & Wu, 2005), though rates remained elevated compared to the general population.

Epidemiological studies have been performed in the United States to determine if bladder cancer rates in Taiwan and other countries may be used to extrapolate risk at lower concentrations typically seen in the United States, as well as in populations of differing ethnicity. Previous studies showed increased bladder cancer risk at exposures over 300 mg/L (C. Chen et al., 2009; Chiou et al., 1995) Studies in Utah, Michigan, and Idaho with arsenic concentrations of 0-166 µg/L in drinking water found no change in bladder cancer risk, incidence, or mortality rates (Han, Weissfeld, Davis, & Talbott, 2009; Lewis, Southwick, Ouellet-Hellstrom, Rench, & Calderon, 1999; Meliker et al., 2010; Meliker, Wahl, Cameron, & Nriagu, 2007). In 2004, a nationwide study found no correlation between arsenic exposures of 3-60 µg/L and bladder cancer mortality rates (Lamm et al., 2004). A meta-analysis of 9 studies for bladder cancer risk also found no significant difference, though it suggested that the influence of cigarette smoking should be evaluated at these lower exposure levels (J. S. Tsuji, Alexander, Perez, & Mink, 2014). Finally, an epidemiological study in Taiwan that was re-evaluated to exclude high arsenic exposures found that bladder cancer risk does not increase until 100-200 µg/L in drinking water (Lamm et al., 2014).

Animal models of arsenic-induced bladder cancer have been difficult to replicate. Past studies with inorganic exposure alone have not found increased incidence of bladder tumors, except in whole-life exposure. Mice exposed to inorganic arsenic prior to breeding, during pregnancy, lactation, and after weaning through adulthood show increased levels of urinary hyperplasia (Tokar, Diwan, Ward, Delker, & Waalkes, 2011).

There are mixed results with organic arsenic carcinogenicity models. Exposure to dimethylarsenic acid for 2 years at 12.5, 50, and 200 mg/L in drinking water causes a significant increase in bladder tumors and urothelial hyperplasia (Wei et al., 2002; Wei, Wanibuchi, Yamamoto, Li, & Fukushima, 1999) and dietary exposure to 100 mg/L DMA causes urothelial cell papilloma and carcinoma in rats (Arnold, Eldan, Nyska, van Gemert, & Cohen, 2006). However, DMA in the diet does not cause cancer in mice at exposures up to 500 ppm (Arnold et al., 2006).

There are cases in which arsenic acts as a co-carcinogen in animal models. Gestational exposure to 85 mg/L inorganic arsenic in mice followed by postnatal tamoxifen treatment increases formation of urinary bladder transitional cell tumors and bladder hyperplasia compared to either treatment individually (Waalkes, Liu, Ward, & Diwan, 2006). Increased urinary bladder proliferative lesions are also seen for transplacental inorganic arsenic exposure followed by postnatal diethylstilbestrol treatment (Waalkes et al., 2006). DMA treatment enhances tumor induction in diethylnitrosamine, *N*-butyl-*N*-(4-hydroxybutyl)nitrosamine, *N*-methyl-*N*-nitrosourea, dihydroxy-di-*N*-propylnitrosamine, and *N*-*N'*-dimethylhydrazine-treated rats (S. Yamamoto et al., 1995).

Potential Mechanisms of Cancer Induction by Arsenic

The mechanism by which arsenic causes bladder cancer has yet to be elucidated. The general theory is that inorganic arsenic undergoes metabolism to reactive metabolites which cause cytotoxicity. In response, the urothelium undergoes regenerative proliferation, leading to development of tumors. (Arnold et al., 2014; Cohen, Arnold, Beck, Lewis, & Eldan, 2013). Inorganic arsenic undergoes a series of reductions and

methylations leading to the formation of reactive metabolites including oxygenated compounds of trivalent and pentavalent arsenic, as well as thiolated pentavalent arsenic compounds. Inorganic pentavalent arsenate is converted to trivalent arsenite (AsIII) mainly in the blood and liver by arsenate reductase, followed by transport into cells (Figure 1.1). Inorganic arsenic may be transported by a number of proteins including aquaporin (Z. Liu et al., 2002), phosphate transporters (Rosen, 2002) and glucose transporters (Drobná et al., 2010). Inside the cell, arsenic methyltransferase converts trivalent arsenite to pentavalent monomethylarsonic acid (MMAV). Monomethylarsonic acid is then reduced to trivalent monomethylarsenous acid (MMAIII) by monomethylarsonic acid reductase and oxidatively methylated by monomethylamine methyltransferase to form dimethylarsenic acid (DMAV) (Cohen, Arnold, Eldan, Lewis, & Beck, 2006). The liver is the main site of methylation and reduction, though arsenite may be metabolized in other tissues (Vahter, 2002). Monomethylarsenic acid and DMA(V) are the predominant metabolites found in the urine following inorganic arsenic exposure (Vahter, 2002). In mice exposed to arsenate, both DMA(V) and inorganic arsenic may be found in the urine, though DMA(V) is the major metabolite (Hughes et al., 2003; Kenyon et al., 2008). However, humans generate more MMA(V) than other animals (Hernández-Zavala et al., 2008). Rats metabolize DMA(V) to trimethylarsenic oxide, while humans do not, an important factor to consider when using rats as a model for arsenic metabolism and carcinogenesis (Cohen et al., 2006).

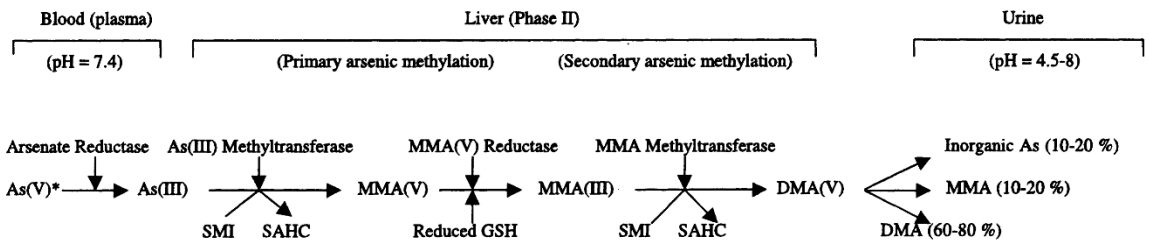

Figure 1.1 Metabolism of arsenate. Adapted from (Y. Chen et al., 2003). As(V): Arsenate, As(III): Arsenite, MMA(V): Monomethylarsonic acid, MMA(III): Monomethylarsenous acid, DMA(V): Dimethylarsenic acid

Trivalent and pentavalent arsenicals, both organic and inorganic, are cytotoxic, though the species differ in potency, and cytotoxicity dependent upon its concentration and potential to react with sulfhydryl groups (Cohen et al., 2006; Yager et al., 2013). Trivalent arsenicals are considered more toxic due to their greater transport efficiency into the cell and enhanced binding affinity to sulfhydryl groups (Cohen et al., 2006). Dimethylarsonous acid, DMA(V), and As(III) are the most toxic to bladder cells (Cohen et al., 2002; Styblo et al., 2000)

The mechanisms which mediate arsenic cytotoxicity can include genotoxicity, oxidative stress, and dysregulation of cell signaling pathways. Trivalent arsenicals bind selectively to sulfhydryl-containing proteins including metallothionein, rat hemoglobin, and zinc finger proteins (Demicheli et al., 2011; G. Jiang, Gong, Li, Cullen, & Le, 2003; Kitchin & Wallace, 2008; Yan, Wang, Weinfeld, Cullen, & Le, 2009; X. Zhou et al., 2011). The effect of this interaction on cytotoxic mechanisms therefore is dependent upon cell type and arsenic species (Cohen et al., 2013).

While arsenic is not mutagenic, it causes genotoxicity through inhibition of DNA repair systems or the generation of reactive oxygen species (ROS) that are damaging to DNA (Klein, Leszczynska, Hickey, & Rossman, 2007; Nesnow et al., 2002). Methylated

arsenic metabolites interact with zinc finger proteins involved in DNA repair and damage signaling, inhibiting base excision repair and nucleotide excision repair (Hartwig et al., 2002). Further, arsenic-induced bladder cancer risk is increased in individuals with a variant of XRCC3, a double-strand break repair gene (Andrew et al., 2009). DNA damage induced by MMA(III) and DMA(III) is prevented by treatment with ROS inhibitors Tiron, melatonin, and the vitamin E analog Trolox (Nesnow et al., 2002).

Oxidative stress due to arsenic exposure is damaging to lipids and proteins, in addition to DNA. Trivalent arsenicals, particularly DMA(III), cause lipid peroxidation and the protein oxidation *in vitro* (Shi, Shi, & Liu, 2004; T.-C. Wang, Jan, Wang, & Gurr, 2007). Sodium arsenite and MMA(III) induce ROS in the immortalized human urothelial cell line UROtsa which is reverted by catalase or superoxide dismutase. Oxidative DNA damage is observed, as well as induction of Hsp70 and metallothionein, a protein which protects the cell against metal toxicity and oxidative stress (Eblin et al., 2006; Michael R Rossi et al., 2002). Glutathione is a major antioxidant of the cell (Forman, Zhang, & Rinna, 2009), and is the electron donor for the reduction of arsenate to arsenite (Scott, Hatlelid, MacKenzie, & Carter, 1993). A decrease in glutathione and an increase of glutathione disulfide, the oxidized peptide created during ROS detoxification, is an indicator of chronic oxidative stress (Lu, 2009). Glutathione is a tripeptide containing a cysteine residue available for arsenite binding (Scott et al., 1993). In mice and humans exposed to arsenic-containing water for prolonged periods, liver glutathione is decreased, accompanied by an induction in glutathione disulfide (Hall et al., 2013; Santra, Maiti, Chowdhury, & Mazumder, 2000). Low arsenite exposure in UROtsa cells stimulates an accumulation of ubiquitin-conjugated protein that is increased

upon reduction of cellular glutathione, suggesting that glutathione may prevent disruption of the ubiquitin-proteasome pathway caused by arsenic (Bredfeldt, Kopplin, & Gandolfi, 2004). Thioredoxin, an electron donor for the reduction of MMA(V) to MMA(III), is also an important cell antioxidant (Kitchin & Wallace, 2008). Thioredoxin activity is decreased following As(III) and MMA(V) exposure in hepatocytes (S. Lin et al., 2001), which may mediate arsenic-induced apoptosis (Arnér & Holmgren, 2000; Shi et al., 2004).

Several epigenetic modifications are altered in arsenic-induced carcinogenesis, including DNA methylation and histone acetylation, to enhance expression of tumor-promoting genes. It is believed that methylation during arsenic biotransformation by arsenic methyltransferase depletes availability of the methyl donor S-adenosyl methionine (SAM), reducing DNA methylation activity to cause a global hypomethylated state (Bustaffa, Stoccoro, Bianchi, & Migliore, 2014). However, while hypomethylation is a prominent global characteristic of arsenic transformation, many cell types and specific genes do not demonstrate hypomethylation, including UROtsa cells transformed with MMA(V). This study found that alterations in DNA methylation occurr non-randomly at hundreds of gene promoters to alter gene expression. Further, the DNA methylation changes are permanent, as removal of arsenic does not alter DNA methylation levels, gene expression, or malignant phenotype (Jensen, Novak, Wnek, Gandolfi, & Futscher, 2009).

Urothelial cancers from arsenic-contaminated areas show gene-specific hypermethylation of death-associated protein kinase (DAPK), a member of the apoptosis pathway downstream of interferon-γ, TNF-α, and Fas signaling. Hypermethylation of the

DAPK promoter is correlated with tumor invasiveness, grade, and recurrence. Hypermethylation of the DAPK promoter is associated with decreased expression (W. T. Chen, Hung, Kang, Huang, & Chai, 2007). In SV-HUC-1 cells exposed to sodium arsenite, promoter hypermethylation of the tumor suppressor RECK leads to decreased expression of the gene, a tumor invasion and angiogenesis suppressor (Y. Huang, Hung, Chen, Yu, & Chai, 2011). Urothelial cancers from blackfoot disease-endemic areas also show decreased RECK protein levels compared to cancers from non-endemic regions (Y. C. Huang et al., 2011). Additionally, urothelial carcinomas from a blackfoot disease area show elevated expression of cyclin D1 that is confirmed in arsenite-treated SV-HUC-1 cells. Further, cyclin D1 expression is dependent upon DNA methylation state (Y. C. Huang et al., 2011). Hypermethylation of the CTBP1 promoter has been observed in HUC-1 cells exposed to transforming levels of sodium arsenite, accompanied by increased expression of the gene which is involved in regulation of epithelial phenotype (Grooteclaes & Frisch, 2000; Michailidi et al., 2015; Peinado, Olmeda, & Cano, 2007). Conversely, arsenite causes hypermethylation of the HER2 and NFκB2 promoters, increasing gene expression (Michailidi et al., 2015). In another study, chronic sodium arsenite exposure to immortalized human urothelial cells causes hypomethylation and overexpression of lipocalin-2, an oncogene that promotes metastasis through the LCN2/MMP9 complex and enhancement of the epithelial-to-mesenchymal transition (H. H. Wang et al., 2014).

Assessment of the histone acetylation state of 13,000 promoters in arsenite-transformed UROtsa cells and normal UROtsa cells exposed to transforming levels of MMA(III) reveals changes in histone H3 acetylation, which enhances DNA

hypermethylation at these regions to alter the expression state of the associated gene (Jensen, Novak, Eblin, Gandolfi, & Futscher, 2008).

Alterations in histone acetylation are also believed to promote carcinogenesis in bladder (Bustaffa et al., 2014). Quantitative mass spectrometric analysis of histone epigenetic state following arsenite or MMA(III) exposure to UROtsa cells discovered a global decrease in acetylation at several H3 and H4 lysine residues (Chu et al., 2011). MYST1, a histone 4 lysine 16 acetyltransferase plays a role in urothelial resistance to arsenic cytotoxicity. UROtsa cells lacking the MYST1 gene show increased sensitivity to arsenite and MMA(III), along with dose- and time-dependent decreases in global H4K16 acetylation (Jo et al., 2009). In another study, low level MMA(III) exposure increases expression and activity of histone deacetylases, leading to reduced global histone acetylation in UROtsa cells (Ge et al., 2013).

In a review of genomic dose-response information in models of arsenic carcinogenesis, common pathways altered by chronic low exposure include oxidative stress, proteotoxicity, inflammation, proliferative signaling, DNA repair, cell cycle G2/M checkpoint control, and induction of apoptosis (Xie et al., 2010). The arsenic-transformed UROtsa cells demonstrate permanent induction of pathways involved in mismatch repair, amino acid metabolism, glycolysis/gluconeogenesis and alkaloid biosynthesis and repression of apoptosis and endocytosis pathways (unpublished data). Global gene expression analysis has also been performed on 1T1 bladder cells exposed to As(III), MMA(III), and DMA(III) for 24 hrs. Among all arsenicals, the NRF2-mediated oxidative stress response, cholesterol biosynthesis, and interleukin-10 signaling pathways are altered (Dodmane et al., 2013). Indeed, NRF2-repressed UROtsa cells demonstrate

increased sensitivity to sodium arsenite and MMA(III), while NRF2 overexpression promotes a tolerance to arsenic cytotoxicity (X.-J. Wang et al., 2007). In another study of As(III) and MMA(III) treated cells, the p53 signaling pathway is deregulated in both treatments, while changes in cell cycle regulation and DNA damage response are unique to As(III) exposure (Dodmane et al., 2013). UROtsa cells exposed to 50 nM MMA(III) are malignantly transformed after 3 months. While subtle changes in gene expression occurr over the first 2 months, the same pathways are substantially altered at 3 months. These include oxidative stress, cell proliferation, anti-apoptosis, MAPK and inflammation pathways (Medeiros et al., 2012).

Proteomic analysis of primary and immortalized uroepithelial cells treated with arsenite trioxide for 3 weeks shows alterations in proteins involved with nucleotide binding, lipid metabolism, protein folding, biosynthesis, transcription, DNA repair, cell cycle control, and signal transduction (S. Chen et al., 2010). Genomic analysis of mouse urine exposed to arsenate in drinking water for up to 12 weeks discovered enhanced epithelial-to-mesenchymal transition, inflammation, and proliferation pathways, while in a study of rat urothelium after exposure to DMA(III) for 28 days, changes were seen in genes for apoptosis, cell cycle regulation, oxidative stress response, and cancer control processes (Clewell et al., 2011; Sen, Wang, Hester, Robertson, & Wolf, 2005).

Cadmium Causes Bladder Cancer

Cadmium was demonstrated to have negative consequences for human health in 1955, when outbreaks in Japan of Itai-Itai disease, translated as “it hurts-it hurts”, were linked to cadmium exposure. Releases of cadmium effluent from a nearby zinc mine contaminated rice paddies, which provided the main source of food for residents in the

area. Toxicity is characterized by renal injury due to tubular and glomerular dysfunction and bone injury consisting of osteomalacia and osteoporosis. Initial femoral pain spreads throughout the body, ultimately causing the patient to become bed-ridden (Inaba et al., 2005).

Exposure to cadmium in humans is mainly through diet and cigarette smoking (NTP, 2011). The largest contribution to dietary cadmium is leafy vegetables including lettuce and spinach, potatoes and grain, peanuts, soybeans, and sunflower seeds (ATSDR, 2012; FDA, 2008). Liver and shellfish also contain higher levels of cadmium (ATSDR, 2012; Satarug & Moore, 2004). Occupational exposure to cadmium may occur in zinc and iron ore smelting, welding cadmium-coated steel, working with solders containing cadmium, and handling or producing cadmium powders (NTP, 2011). The estimated cadmium intake is 0.35 µg/kg/day in males and 0.30 µg/kg/day in females (Choudhury et al., 2001). Cadmium is found in the Earth's crust and is distributed in dust, volcanic emissions, and forest fires along with other natural phenomena (ATSDR, 2012). However, anthropogenic production is the main source of cadmium in the environment. Zinc, copper, and lead smelting, coal and oil-fired broilers, and industrial waste incinerators release cadmium into the environment. Application of phosphate fertilizers and waste leaching from landfills also releases cadmium into the soil and water (EPA, 1985).

Evidence of Cadmium Carcinogenicity

Cadmium is classified as a carcinogen (IARC, 1993), though the evidence for bladder cancer induction by cadmium is less than that of arsenic. In a study of bladder cancer cases in Belgium, increasing levels of blood cadmium are correlated with bladder cancer

risk (Kellen et al., 2007). However, a study of cancer incidence in northeastern Belgium and southeastern Netherlands found no correlation between long-term emission of cadmium by zinc smelters and bladder cancer incidence (Verhoeven et al., 2011). A study of Tunisian men also found that blood cadmium levels are significantly higher in cases of bladder cancer and that cadmium levels are correlated with smoking and age (Feki-Tounsi et al., 2013a). Urinary metallothionein-bound cadmium is significantly elevated in transitional cell carcinoma patients as measured by inductively coupled plasma mass spectrometry (Wolf, Strenziok, & Kyriakopoulos, 2009). In addition, a study based in Montreal, Quebec, Canada implicates occupational exposure to cadmium compounds to bladder cancer risk (Siemiatycki, Dewar, Louise, & Gérin, 1997). One difficulty in epidemiological studies of cadmium-induced carcinogenesis is the confounding factor of cigarette smoking. In fact, no studies have found a significant association between cadmium and bladder cancer in non-smokers (Feki-Tounsi & Hamza-Chaffai, 2014). Future experiments with larger sample size and non-smoking populations will help to determine the role of cadmium in bladder cancer.

While animal studies confirm cadmium as a carcinogen, no cadmium exposure studies have demonstrated the development of bladder cancer specifically in animals. However, *in vitro* exposure to cadmium chloride malignantly transforms urothelial cells as indicated by anchorage independent cell growth and tumor formation in nude mice (Sens et al., 2004).

Potential Mechanisms of Cancer Induction by Cadmium

The manner by which cadmium causes bladder cancer, and all cancers in general, remains unknown. As with arsenic-induced bladder cancer, the likely mechanism of

cancer induction by cadmium is that of initial cytotoxicity followed by regenerative proliferation and the development of tumors. The processes involved in each step, however, are likely unique due to the inherent differences in cadmium and arsenic. Changes observed during cadmium carcinogenesis include aberrant gene expression, DNA damage repair inhibition, impairment of apoptosis, and oxidative stress (Feki-Tounsi & Hamza-Chaffai, 2014).

Following absorption at the small intestine, ingested cadmium accumulates predominantly in the kidney and to a lesser extent in liver (Satarug, Baker, Reilly, Moore, & Williams, 2002; Sumino, Hayakawa, Shibata, & Kitamura, 1975), and has a biological half-life of at least 15-20 years (ATSDR, 2012; Jin, Lu, & Nordberg, 1998). Metallothionein, a cysteine-rich antioxidant protein, plays an important role in cadmium accumulation, as cadmium has the ability to bind protein thiol groups (Carballo, Castineiras, Dominguez-Martin, Garcia-Santos, & Niclos-Gutierrez, 2013). Metallothionein readily binds cadmium in the liver, preventing its excretion. In metallothionein-null mice, absorption and distribution of the metal is unaffected, however, elimination through the bile is inhibited, causing accumulation of cadmium-bound metallothionein in the body (Klaassen, Liu, & Choudhuri, 1999). Though metallothionein accumulates cadmium in the kidney, it is protective against nephrotoxicity. In metallothionein-null mice, renal toxicity iss enhanced compared to controls (J. Liu, Liu, Habeebu, & Klaassen, 1998). Metallothionein expression is also induced upon cadmium exposure in the kidney and bladder (Chung, Nartey, & Cherian, 1986; Sens et al., 2003)

Mechanisms of cadmium transport have not been fully elucidated. Cadmium has no known biological function and utilizes transporters for zinc, iron, and calcium. Known cadmium transporters include divalent metal transporter 1 (*SLC11A2*) (Park, Cherrington, & Klaassen, 2002), ZIP8 (*SLC39A8*) (Dalton et al., 2005), and ZIP14 (*SLC39A14*) (Girijashanker et al., 2008). Recent studies have implicated megalin as a transporter of cadmium-bound metallothionein (Wolff, Abouhamed, Verroust, & Thévenod, 2006). Cadmium transport and accumulation is enhanced upon deficiency of the dietary metals zinc, iron, and calcium (Ueda et al., 1987; Vesey, 2010), such that nutritional state must be considered in studies of cadmium toxicity and transport.

Due to the lack of animal models, mechanisms of cadmium-induced bladder cancer have been investigated *in vitro*. Inhibition of apoptosis is one manner in which cadmium causes carcinogenesis. In normal cells, cadmium often induces apoptosis initially, followed by resistance upon malignant transformation. Cadmium-transformed prostate epithelial cells exhibit enhanced resistance to apoptosis induced by cadmium, accompanied by down-regulation of several caspase family members and overexpression of anti-apoptotic genes (W. Achanzar, Webber, & Waalkes, 2002). Cadmium exposure to the nontransformed prostate epithelial cell line RWPE-1 induces apoptosis in 65% of cells; however, the surviving 35% have elevated levels of metallothionein (W. E. Achanzar, Achanzar, Lewis, Webber, & Waalkes, 2000). This suggests that metallothionein may promote the survival of cadmium-exposed cells. Similarly, alveolar epithelial cells subjected to repeated *in vitro* exposure to cadmium demonstrate increased resistance to apoptosis caused by the oxidant hydrogen peroxide, along with elevated expression of Metallothionein 1 and 2 (Eneman et al., 2000). Indeed, similar results are

observed in transformation of UROtsa cells by arsenite and cadmium. The UROtsa cell line exposed to toxic levels of sodium arsenite and cadmium chloride experience both apoptosis and necrosis. Meanwhile, UROtsa cells malignantly transformed with arsenite and cadmium display increased resistance to arsenite- and cadmium-induced toxicity, and are more likely to undergo necrosis, suggesting that apoptosis inhibition may promote heavy metal carcinogenesis. In both parent UROtsa and Cd^{2+}-transformed cells, cadmium exposure induce metallothionein. However, there is no difference in the level of induction between the normal and transformed cells, indicating that metallothionein does not play a role in arsenic or cadmium transformation (Somji, Zhou, Garrett, Sens, & Sens, 2006).

Cadmium may induce cytotoxicity and carcinogenesis by interfering with cysteine-containing proteins such as the tumor suppressor p53. In human breast cancer MCF-7 cells, p53 induction by DNA-damaging agents is inhibited by cadmium (Méplan, Mann, & Hainaut, 1999). While initial exposure to cadmium induces p53 expression in human prostate epithelial cells, continued exposure reduces levels to those below baseline (W. E. Achanzar et al., 2000).

Bladder-specific mechanisms of cadmium carcinogenesis has been investigated by this lab in regard to aberrant gene expression. Transformation of the UROtsa cell line by chronic cadmium exposure results in permanent induction of genes associated with mismatch and nucleotide excision repair, DNA replication, amino acid metabolism, glycolysis/gluconeogenesis, and sphingolipid metabolism. Repressed pathways included apoptosis, the Jak-STAT signaling pathway, and Wnt signaling (unpublished data).

Oxidative stress has not been studied in cadmium-induced bladder cancer specifically, but are common traits of cadmium carcinogenicity in other tissues.

Cadmium exposure induces numerous radical species, including hydrogen peroxide, superoxide anions, and hydroxyl anions (Bertin & Averbeck, 2006). Oxidative stress due to cadmium has been observed both *in vitro* and in animal studies (Joseph et al., 2001; Koizumi, Shirakura, Kumagai, Tatsumoto, & Suzuki, 1996; Nigam, Shukla, & Agarwal, 1999; Shih et al., 2004). In a study of the general population, urinary cadmium levels are correlated to increased serum γ-glutamyltransferase and decreased vitamin C, carotenoids, and vitamin E (Lee, Lim, Song, Boo, & Jacobs, 2006). However, cadmium is not a Fenton metal, indicating that oxidative stress is generated indirectly by cadmium (Bertin & Averbeck, 2006).

Cadmium may induce oxidative stress indirectly by reducing the levels or activity of antioxidant enzymes, increasing the cell's vulnerability to ROS (Waisberg, Joseph, Hale, & Beyersmann, 2003). Second, cadmium may displace iron from ferritin and apoferritin, making iron available for ROS-producing Fenton reactions (Casalino, Sblano, & Landriscina, 1997; Price & Joshi, 1983). Cadmium may also induce oxidative stress by interfering with oxidative metabolism in mitochondria (Bertin & Averbeck, 2006; Nigam et al., 1999). Cadmium-mediated oxidative stress leads to mutations and damage to DNA, as well as lipids in several organs and cell types (Bertin & Averbeck, 2006). 8-hydroxydeoxyguanosine formation, indicative of premutagenic lesions due to oxidative stress, and DNA strand breaks are caused by cadmium exposure in HeLa and lymphoblastoid cells (Dally & Hartwig, 1997; Mikhailova, Littlefield, Hass, Poirier, & Chou, 1997). In addition to their damaging effects, ROS may act as signaling molecules (Bertin & Averbeck, 2006). Reactive oxygen species generated by cadmium activates extracellular signal-regulated kinases (ERK) and AKT to induce the pro-angiogenic

molecule hypoxia-inducible factor-1 in human bronchial epithelial cells (Jing et al., 2012). In BALB/c-3T3 cells transformed with cadmium chloride, ROS mediates the upregulation of proto-oncogenes c-fos, c-jun, and c-myc (Joseph et al., 2001). The relative importance of ROS in cadmium carcinogenesis is still unclear. In a study of rat liver epithelial cells transformed by chronic cadmium exposure, initial induction of ROS is abolished well before malignant transformation (Qu et al., 2005).

Cadmium may mediate carcinogenesis through the inhibition of various DNA damage repair mechanisms, including base excision repair, nucleotide excision repair, and mismatch repair (Giaginis, Gatzidou, & Theocharis, 2006), though alterations in these processes have not been studied in bladder cancer specifically. Cadmium has been found to inhibit numerous steps of base excision repair. Cadmium reduces the activity of 8-oxoG glycosylase, an enzyme involved in the initiation of repair (Potts, Bespalov, Wallace, Melamede, & Hart, 2001). It also suppresses the activity of 8-oxo-2'-deoxyguanosine 5-triphosphate pyrophosphohydrolase, an enzyme which prevents incorporation of mutagenic 8-oxo-dGTP (Bialkowski, Bialkowska, & Kasprzak, 1999). Ape-1 endonuclease and exonuclease action is inhibited by cadmium *in vitro*, as well as DNA polymerase β (Popenoe & Schmaeler, 1979) and DNA ligase 1 (McNeill, Narayana, Wong, & Wilson, 2004; S. W. Yang, Becker, & Chan, 1996).

Studies on the effect of cadmium exposure on nucleotide excision repair reveal that the metal inhibits initial phases of this process (Giaginis et al., 2006). Transcription factor IIIA, an enzyme important in the initiation of nucleotide excision repair, is impaired in its ability to bind DNA by cadmium. It is thought that cadmium binds to cysteines within the zinc finger protein to inhibit DNA binding (Hanas & Gunn, 1996). Cadmium reduces the

DNA binding ability of XPA, another initiator of nucleotide excision repair, likely due to sensitivity of the zinc finger protein to cadmium (Asmuss, Mullenders, Eker, & Hartwig, 2000).

There is evidence that cadmium suppresses initial phases of mismatch repair by inhibiting MSH2-MSH6-dependent activity, attenuating the complex's DNA binding affinity and reducing its ability to distinguish mismatched duplexes (Clark & Kunkel, 2004). Cadmium also inhibits DNA mismatch-repair-mediated cell cycle arrest following alkylation damage (Lützen, Liberti, & Rasmussen, 2004). However, the mechanisms of protein inhibition in mismatch repair does not appear to be due to the targeting of zinc finger motifs (Giaginis et al., 2006).

Cadmium- and Arsenic-transformed UROtsa Cells

Immortalized human bladder cancer-derived cell lines are widely available and well characterized, however, they do not allow for investigation of the initial stages of carcinogenesis, and the cancer-inducing agent is unknown. The UROtsa cell line originates from urothelial cells derived from the left ureter of a 12-year-old girl, which was then immortalized with a temperature-sensitive SV40 large T-antigen gene. UROtsa cell morphology resembls primary urothelial cells, growing in tightly packed colonies in the shape of irregular polygonal cells with a low nucleus to cytoplasmic ratio.

Multinucleated and long fusiform cells ae observed at low frequency. The cells do not grow in soft agar and are unable to form tumors in nude mice, indicating that they are not neoplastically transformed. The cells were immortalized with a temperature-sensitive T-antigen such that incubation at elevated temperature would reduce growth rates, possibly providing an *in vitro* model system that more closely resembled that of human

urothelium. The temperature-sensitive trait of the SV40 T-antigen was lost and UROtsa cell growth rate was unchanged at elevated temperatures (Petzoldt, Leigh, Duffy, Sexton, & Masters, 1995). Further, characterization proves that the immortalized UROtsa cell line is a close model of normal human epithelium, with the ability to resemble the intermediate or basal cell layer depending upon serum growth conditions.

UROtsa cells cultured on serum-containing growth medium demonstrate a basal cell phenotype with a flattened appearance and grow as a monolayer with no tendency to stratify. The cells have numerous desmosomal connections and moderate lateral digitations, a high nuclear to cytoplasmic ratio, and presence of intermediate filaments. No tight junctions nor gap junctions are observed between the apical poles of the cells. UROtsa cells cultured on a serum-free growth medium resemble the transitional epithelium, with multilayered formations of cells, abundant intermediate filaments, and a more polarized epithelial morphology. The cells contain frequent desomosomal connection and extensive interdigitation. Freeze-fracture analysis reveals the presence of gap junctions and tight junction sealing strands between cells. The immortalized UROtsa cell line also expresses metallothioneins and heat shock protein profiles in agreement with *in situ* urothelial expression (M R Rossi et al., 2001).

This lab was the first to malignantly transform urothelial cells with cadmium and arsenic *in vitro*, providing a model system for the confirmation of epidemiological studies and further investigation of carcinogenic mechanisms and biomarker identification. During transformation, both serum-fed and serum free cultures were used. Immortalized UROtsa cells were fed medium containing 1 μM sodium arsenite or cadmium chloride over a period of up to three months. Several rounds of cytotoxicity followed by regrowth

of remaining cells occurred, after which growth rates began to increase far in excess over the parental UROtsa cells. The transformed cells appeared morphologically similar to the parent, though the serum-free cultures lost the ability to stratify. The transformed cells formed colonies in soft agar, though the serum-fed cells were more efficient. Furthermore, UROtsa cells transformed by cadmium and arsenic in serum-free media were able to form tumors when injected subcutaneously into nude mice (Sens et al., 2004).

The tumor heterotransplants provide a useful tool for the study of arsenic- and cadmium-induced bladder cancer, as animal models for these cancers are difficult to produce. The subcutaneous tumor heterotransplants generated from arsenic-transformed cells are composed of infiltrating masses or nests of moderately differentiated cells, with differentiation increasing from the periphery towards the center of the masses. The tumor histology resembles that of invasive urothelial cell carcinoma along with regions of squamous differentiation. Tumors derived from the cadmium transformants are similar to the arsenic heterotransplants, but with less squamous differentiation (Sens et al., 2004).

Global analysis of changes in gene expression in the transformed isolates allows for the investigation of metal-specific carcinogenic mechanisms and biomarkers for bladder cancer staging, and prediction of progression and recurrence. Multiple independently-transformed isolates were subjected to microarray analysis; that is, additional isolates were derived from the parent UROtsa cell line with identical exposures (Garrett, Somji, Sens, & Zhang, 2014). Multiple independently-transformed isolates allow for assessment of variability and determination of commonly altered pathways, eliminating non-specific gene expression. Tumor heterogeneity is an important issue in cancer research, both

within individual tumors and within a single tumor (M Gerlinger & Swanton, 2010; Marco Gerlinger et al., 2014; Sjöblom, 2008). Furthermore, UROtsa cells metabolize inorganic arsenic to MMA(III) (Bredfeldt et al., 2004) and the different metabolites of arsenic may give rise to a variety of changes. By comparing and contrasting changes in gene expression in arsenic- and cadmium-transformed cells, the carcinogenesis pathways unique to each metal may be elucidated, as well as common mechanisms of bladder cancer progression.

Subcutaneous tumors derived from arsenic-transformed UROtsa cells display a squamous phenotype, including expression of keratin 6 and 16 which are indicative of early features of squamous differentiation (Cao et al., 2010). Subcutaneous tumors derived from cadmium-transformed UROtsa cells display mild to prominent squamous differentiation, as well (Somji et al., 2010). Keratin-6a, a gene involved in urothelial proliferation and wound repair, is upregulated in cadmium-transformed UROtsa cells *in vitro* and in mouse heterotransplant tumors. In the normal UROtsa cell line, keratin-6a expression iss induced by insulin and EGF, suggesting that keratin-6a may be a marker for cancer cells with an activated growth factor pathway (Somji et al., 2008). Keratin 6, 16, and 17 are correlated with areas of squamous differentiation in Cd heterotransplants. Subcutaneous tumors derived from arsenic-transformed UROtsa cells demonstrate intense focal staining for keratin 7 and 19. In general, cadmium and arsenic transformation of UROtsa cells display similar patterns of keratin 6, 7, 16, 17 and 19 *in vitro* and in tumors (Somji et al., 2011). Other studies have found that keratin 5/6 expression may distinguish reactive urothelial atypia from urothelial carcinoma *in situ*

and the non-invasive compartment of high-grade papillary urothelial carcinoma (Edgecombe, Nguyen, Djordjevic, Belanger, & Mai, 2012).

While metallothionein does not appear to play a large role in cancer initiation, its induction due to heavy metals may be valuable as a biomarker of cancer progression. Patterns of Metallothionein 1/2 in arsenic- and cadmium-transformed UROtsa heterotransplants are similar to that of human high-grade bladder cancers, which is focal in its expression (X. D. Zhou, Sens, Sens, et al., 2006). Metallothionein-3, which is expressed in 96% of high-grade urothelial cancers, is observed in tumor heterotransplants derived from arsenic- and cadmium-transformed UROtsa cells, as well (X. D. Zhou, Sens, Garrett, et al., 2006), indicating that the metallothionein proteins may be useful as a biomarker of high-grade bladder cancer.

SPARC, a protein involved in extracellular matrix synthesis and the promotion of changes in cell shape, is decreased in arsenic- and cadmium-transformed UROtsa cell lines and subcutaneous tumor heterotransplants. While the epithelial component of cells is negative for SPARC, positive staining is observed in stromal cells. Negative epithelial with positive stromal expression of SPARC is confirmed in human bladder cancer specimens, as well (Jennifer Larson et al., 2010). In SPARC-null mice, development of urothelial preneoplasia, neoplasia, and metastasis is increased, along with a reduction in survival. SPARC also regulates chemical carcinogen-associated inflammation, ROS, and cell proliferation (Said, Frierson, Sanchez-Carbayo, Brekken, & Theodorescu, 2013).

Neuron-specific enolase is induced in arsenic- and cadmium-exposed UROtsa cells, as well as the transformed cell lines and tumor heterotransplants, suggesting a role in

carcinogenesis. Protein expression was localized to the nucleus, suggesting alternatives to its commonly known role in glycolysis (Soh et al., 2012).

Microarray analysis of the arsenic-transformed isolates reveal 328 genes commonly induced and 91 repressed that had at least two-fold change for each isolate compared with the control. In the cadmium-transformed isolates, 285 genes are commonly induced, with 215 repressed. (Garrett et al., 2014). The microarray consisted of six arsenic-transformed and seven cadmium-transformed biological replicates. To assess statistical significance of the numbers of commonly induced and repressed genes, a simulation study was designed using randomly generated subsets of genes. The number of significantly induced or repressed genes in common to all isolates was counted, and a new subset of genes was then randomly selected. This simulation was performed 1,000,000 times, and the number of differentially expressed genes never surpassed that found by the microarray (Garrett et al., 2014).

Validation by PCR array was then performed. Genes which demonstrated less than 5% false discovery rate and greater than 3.2-fold change on the microarray were selected for validation. In the microarray, each biological replicate was tested in triplicate. Results from the PCR array were similar to those from the microarray, in which the percent of genes which failed to validate was similar to the 5% false discovery rate utilized in the microarray (Garrett et al., 2014).

To determine whether the number of isolates used for microarray were sufficient to identify common gene sets, a model was developed to predict the number of commonly induced or repressed genes as the number of isolates increased. With the addition of each isolate, the number of common genes decreased. However, when the number of isolates

reached four or five (depending upon the sample set), the number of common genes stabilized, indicating that at this point the list of induced and repressed genes are truly responsive to the cadmium or arsenite treatment. As the cadmium- and arsenic-transformed UROtsa cells contained seven and six isolates, respectively, it was determined that the commonly induced or repressed genes identified were responsive and specific (Garrett et al., 2014).

Of the differentially induced genes confirmed by PCR in the arsenic-transformed isolates, N-cadherin was the top-most consistently induced gene. In cadmium-transformants, N-cadherin is the 5th most consistently induced gene (Figure 1.2) (Garrett et al., 2014).

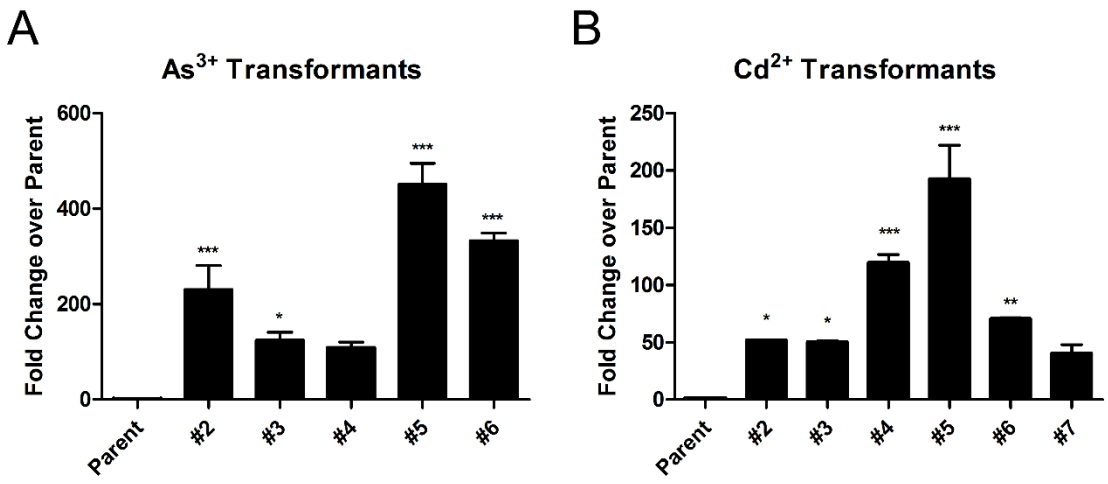

Figure 1.2 N-cadherin is consistently induced in As^{3+}- and Cd^{2+}-transformed UROtsa cells. PCR array validation of microarray results indicates N-cadherin is significantly induced in the majority of As^{3+}-and Cd^{2+}-transformed UROtsa isolates. PCR results represent Mean ±SEM of triplicate determinations. *p<0.05, **p<0.01, ***p<0.001

N-cadherin

Cadherins are proteins that contribute to adherens junctions, named for their calcium-dependent adhesive properties (Jäger et al., 2010). These Type 1 transmembrane proteins

mediate homophilic cell adhesion and include epithelial-cadherin (E-cadherin), neuronal-cadherin (N-cadherin), placental-cadherin (P-cadherin), and retinal cadherin (van Roy, 2014).

N-cadherin is normally expressed in the brain, vascular endothelial cells, and cardiac and skeletal muscle cells. N-cadherin promotes the development of neuroepithelial adherens junctions, axon migration, and synapse formation (Takeichi, 2007). Expression of N-cadherin is a hallmark of the epithelial-to-mesenchymal transition (EMT), a process which occurs in numerous cancers and is believed to promote invasion and metastasis (Wheelock, Shintani, Maeda, Fukumoto, & Johnson, 2008).

During EMT, E-cadherin expression is often lost or decreased, leading to destabilization of adherens junctions and loss of apical-basal polarity (C. Huang, Ke, Costa, & Shi, 2004). E-cadherin is the main cadherin that promotes cell-cell adhesion and polarity in epithelial tissues, supporting their differentiated state (Capaldo & Macara, 2007; Gumbiner, Stevenson, & Grimaldi, 1988). E-cadherin also sequesters β-catenin, preventing activation of the Wnt signaling pathway and expression of oncogenes such as cyclin D1 (Bryan & Tselepis, 2010). As such, the loss of E-cadherin expression in bladder cancer is associated with increased stage, grade, and incidence of recurrence and with decreased survival rate (Baumgart et al., 2007; B. Liu, Miyake, Nishikawa, & Fujisawa, 2015; Muramaki et al., 2012; Muramaki, Miyake, Terakawa, Kusuda, & Fujisawa, 2011; K M Rieger-Christ et al., 2001; Shimazui et al., 1996; Zhao, Dong, Sun, Zhang, & Sun, 2014).

Additional changes include loss of other adhesion complexes and alterations in morphology due to cytoskeletal restructuring (Lamouille, Xu, & Derynck, 2014). Cell

motility is increased, facilitated by an enhanced ability to degrade extracellular matrix proteins. Resistance to senescence and apoptosis is also elevated (Thiery, Acloque, Huang, & Nieto, 2009).

N-cadherin expression during EMT promotes cell affinity for the extracellular matrix and endothelial compartment, promoting cell survival and transendothelial migration (Groen et al., 2011; Qi, Chen, Wang, & Siu, 2005). N-cadherin also interacts with and stabilizes fibroblast growth receptors at the cell surface, enhancing its activity and altering the downstream MAPK/ERK pathway leading to increased invasion (Suyama, Shapiro, Guttman, & Hazan, 2002).

N-cadherin expression has been positively correlated with bladder cancer progression and recurrence. In a study of 161 bladder cancer patients, N-cadherin expression levels are correlated with tumor recurrence following removal of non-muscle-invasive urothelial carcinoma of the bladder (B. Liu et al., 2015). In another study of 115 patients with non-muscle-invasive bladder cancer following tumor removal, positive N-cadherin expression is significantly associated with bladder cancer recurrence and significant reduction in recurrence-free survival. Incidence of recurrence is significantly increased in E-cadherin-negative and N-cadherin-positive tumors, and recurrence-free survival is reduced (Muramaki et al., 2012). Recurrence-free survival is associated with negative N-cadherin expression in a study of urothelial carcinoma of the upper urinary tract after removal of parts of the bladder and kidney (Muramaki et al., 2011). Lascombe *et al.* examined N-cadherin expression in 101 tumors and found that mRNA expression is increased in muscle-invasive versus superficial tumors, but comparable protein levels are not detected (Lascombe et al., 2006). A study of 181 bladder cancer patients stratified by

tumor invasiveness found that N-cadherin expression negatively correlates to survival in all cases, but positively associates with survival in invasive cases (Jäger et al., 2010), and no correlation is found between N-cadherin and stage, grade, lymph node involvement or vascular invasion in a study of 572 bladder cancer patients (Baumgart et al., 2007).

Numerous transcription factors regulate the epithelial-to-mesenchymal transition, including Twist, Snail, Slug, Zeb1, and Zeb2 (Lamouille et al., 2014). Differential expression of Twist, a repressor of E-cadherin, has been noted in bladder cancer, in which elevated Twist expression is correlated with bladder cancer stage, grade, and poorer progression-free survival (Fondrevelle et al., 2009). The roles of other EMT transcription factors in bladder cancer have not been fully elucidated. In a recent immunohistochemical study of transcription factors in 49 samples of urothelial carcinoma, Snail is correlated with local invasiveness, while Slug is associated with both local and muscle invasion capacity, as well as metastasis. Zeb1 is significantly related to invasiveness, but not metastasis (Schulte et al., 2012).

MicroRNAs also regulate EMT, particularly the miR-200 family which promotes the epithelial phenotype and has been explored in bladder cancer. miR-200c is down-regulated in bladder cancer specimens in a study by Liu *et al*., and its overexpression results in decreased cell invasion, migration, and proliferation capabilities (L. Liu et al., 2014). In another study, miR-200 family mRNAs are expressed in bladder cancers displaying an epithelial phenotype, and the transcription factors Zeb1 and 2 are inversely correlated with miR-200c expression. Further, miR-200c reverts EMT, inducing the mesenchymal bladder cancer cell line UMUC3 to undergo epithelial differentiation, further validating the role of miR-200c as a negative regulator of EMT (Adam et al.,

2009). Loss of miR-141 and miR-200b is associated with increased invasion and migration, Vimentin and N-cadherin expression, downregulated E-cadherin, and increased metalloproteases in a study performed with the UM-UC-3 and HTB 9 bladder cancer cell lines (W. Liu et al., 2015).

The EMT status of some human bladder cancer cell lines has been characterized, though a common pattern of EMT progression has not been clarified. The cell lines RT4 and RT112 demonstrate an epithelial phenotype and morphology, with low to no expression of the mesenchymal markers N-cadherin and Vimentin (Matsui et al., 2012). The bladder cancer cell lines 5367 and 253J BV display both epithelial and mesenchymal characteristics, with co-expression of N-cadherin and E-cadherin. Cell line 5367 demonstrates high levels of the pro-EMT transcription factor Slug but low expression of Vimentin, while 253J BV has low Slug expression accompanied with high Snail levels, another pro-EMT transcription factor, and is positive for Vimentin (Hänze, Henrici, Hegele, Hofmann, & Olbert, 2013; Matsui et al., 2012; Wu et al., 2012). TCCSUP lacks E-cadherin, with a moderate increase in N-cadherin expression. Vimentin is low in this cell line, though it demonstrates mesenchymal morphology (Baumgart et al., 2007; Hänze et al., 2013; Matsui et al., 2012). Cell lines J82 and T24 are the most mesenchymal, showing a loss of E-cadherin accompanied by increased N-cadherin, as well as Vimentin expression (Wu et al., 2012). Both cell lines demonstrate increased cell invasion capacity, with T24 the highest (Wallerand et al., 2010).

Very little is known about the regulation of N-cadherin. A few transcription factors have been investigated in the regulation of N-cadherin, though not in the context of urothelial tissue expression. The transcription factor Twist, a basic helix-loop-helix

protein and well-known repressor of E-cadherin expression, may also activate transcription of N-cadherin. In a study by Alexander *et al*. in prostate cancer cells, Twist depletion results in a decrease in N-cadherin expression. Using a luciferase assay, co-expression of Twist and the 5' promoter construct for N-cadherin shows no increase in promoter activity. However, co-expression of Twist with an E-box sequence within the first intron of N-cadherin results in significant increases in promoter activity. Further analysis by electrophoretic mobility shift assay reveals Twist binding at +2,627, within the first intron of N-cadherin (Alexander et al., 2006). This regulation displays similarity with that of E-cadherin, which is regulated at the first and second introns *in vivo* (Stemmler, Hecht, Kinzel, & Kemler, 2003). Further evidence of dual regulatory function is seen in the activation of YB-1 and AKT-2 by Twist (Cheng, Zhang, & Wang, 2008; Shiota et al., 2008). The mechanisms that underlie its dual transcriptional mode are not fully elucidated, though recruitment of epigenetic factors have been implicated (F. Yang et al., 2012).

Activating protein 1 (AP-1), a heterodimer formed of c-Jun and c-Fos, is another potential transcription factor regulating N-cadherin expression. AP-1 regulates transcription of N-cadherin in Schwannoma cells (Martiáñez, Lamarca, Casals, & Gella, 2013). Further, AP-1 activity may be altered in urothelial cells by arsenic exposure. Exposure to four weeks of sodium arsenite in mice induces hyperplasia of the bladder urothelium and an increase in DNA binding of AP-1. In transgenic mice containing an AP-1 luciferase reporter, arsenite exposure promotes AP-1 transactivation. *In vitro* experiments using a human bladder epithelial cell line also demonstrate increased AP-1 DNA binding following arsenite treatment (Simeonova et al., 2000, 2001). In addition,

exposure to methylarsine oxide or iododimethylarsine promotes phosphorylation of c-Jun and AP-1 DNA binding, and was found to be more potent than arsenite in promoting AP-1 activity (Drobná, Jaspers, Thomas, & Stýblo, 2003).

NFκB may also regulate N-cadherin transcription. Electrophoretic mobility shift assays for NFκB DNA binding reveal strong binding activity at the N-cadherin promoter in melanoma cells. Reporter gene assays showed that NFκB binding activates N-cadherin transcription (Kuphal & Bosserhoff, 2006). In UROtsa cells, MMA(III) exposure induces the translocation of NFκB to the nucleus, suggesting that arsenic may induce N-cadherin expression through NFκB to promote bladder cancer progression (Escudero-Lourdes, Medeiros, Cárdenas-González, Wnek, & Gandolfi, 2010).

The transcription factors specificity protein 1 (SP1) and 2 (SP2) show evidence of regulatory function, as well. Electrophoretic mobility shift assays in human osteoblasts indicate that an Sp1/Sp3 binding site regulates N-cadherin expression. Specifically, Sp3 antagonizes Sp1-induced transcription (Le Mée, Fromigué, & Marie, 2005). In a series of experiments studying the anti-proliferative, anti-angiogenic, and pro-apoptotic activity of arsenic trioxide in bladder cancer cells, arsenite-responsive cell lines displayed oxidative stress-dependent decreases in Sp1, Sp3, and Sp4 expression. A number of additional studies in other cell types have also found downregulation of Sp1 following arsenic exposure (Ai et al., 2007; Chou et al., 2005; Y. Zhang et al., 2015). Cadmium is also associated with reduced Sp1 activity (Aiba, Hossain, & Kuo, 2008; Kothinti, Blodgett, Tabatabai, & Petering, 2010; Y. Li, Kimura, Huyck, Laity, & Andrews, 2008; Watkin, Nawrot, Potts, & Hart, 2003; Youn et al., 2005), suggesting that Sp1 and/or Sp3 may

mediate arsenic- and cadmium-induced alterations in N-cadherin expression in the progression of bladder cancer.

Other transcription factors shown to have regulatory activity at the N-cadherin promoter include RBPJ (Fangfei Li et al., 2011), GATA-4 (H. Zhang, Toyofuku, Kamei, & Hori, 2003), SOX-9 (Panda, Miao, Lefebvre, Hendy, & Goltzman, 2001), MZF1 (Le Mée et al., 2005), and SMAD4 (Kang et al., 2014). However, these transcription factors have not been associated with bladder cancer progression or arsenic and cadmium exposure.

Bladder Cancer Characteristics and Research Needs

In 2011, it was estimated that 571,518 individuals were living with bladder cancer in the United States (Howlader et al., 2014). 74,690 new cases of bladder cancer were estimated for 2014 in the United States, with 15,580 deaths due to the disease (Malats & Real, 2015). Bladder cancer is the 9th leading cause of death in the United States. The median age at diagnosis is 73, with bladder cancer more common in men than women (Howlader et al., 2014). The annual cost of bladder cancer was $4 billion in the United States. when estimated in 2010, and it is predicted to rise to $5 billion by 2020 (Yeung, Dinh, & Lee, 2014).

The bladder is composed of a mucosa lined by transitional epithelium, muscularis, and adventitia. The number of layers of the transitional epithelium can vary from six when the bladder is empty, to three when the bladder is distended. (Ross & Pawlina, 2011). The urothelium consists of a basal layer, intermediate layer, and superficial layer, with cells increasing in differentiation from base to surface. Extensive interdigitations of cytoplasmic processes and desmosomes create lateral connections throughout, while

superficial cells are linked by tight junctions to create an impermeable barrier (Jost, Gosling, & Dixon, 1989). The superficial, or umbrella cells, are usually cuboidal and bulge into the lumen. Further, in the distended bladder, umbrella cells flatten and unfold to increase available surface area. The normal urothelium has a very low proliferative capacity, wherein basal cells act as progenitors. Upon pathological damage, both basal and intermediate cells will rapidly regenerate the urothelium (Ho, Kurtova, & Chan, 2012). Underlying the transitional epithelium is the lamina propria, a dense collagenous layer, followed by the muscularis. The muscularis contains longitudinal and circular layers of smooth muscle which aid the movement of urine through the ureter to the bladder (Ross & Pawlina, 2011).

The majority of bladder cancers are transitional cell carcinoma, with less than ten percent composed of squamous cell carcinoma and adenocarcinoma. Small cell carcinoma and sarcoma of the bladder are rare (Cubilla et al., 2004). Transitional cell carcinoma is widely categorized by the extent of its invasion into surrounding tissue. There are two types of non-muscle-invasive transitional cell neoplasms: flat and papillary lesions. Of the flat lesions, carcinoma *in situ* is a known precursor of invasive cancer. This lesion contains cells with irregular, large, hyperchromatic nuclei (See Figure). Most patients have multifocal or diffuse carcinoma *in situ* cells (Figure 1.2.A). Papillary lesions often occur in multiples, and frequently recur following local resection (Figure 1.2.B). Patients with a history of papillary tumors are at risk for developing invasive carcinoma (Al-ahmadie, Lin, & Reuter, 2011). The grading of papillary neoplasms is widely debated, but the current system is based on architectural and cytologic changes in the urothelium. With increasing grade, papillary carcinoma progression rates are

elevated. Invasive urothelial carcinoma includes tumors which invade the muscularis mucosae or the muscularis propria (Figure 1.3). These tumors have variable histology, though depth of invasion is important for staging (Cubilla et al., 2004).

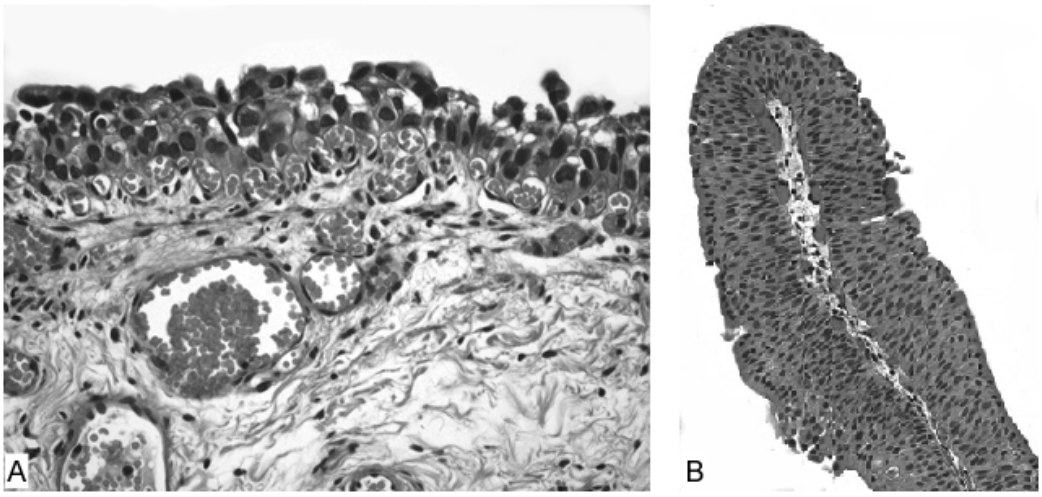

Figure 1.3 *In situ* and papillary urothelial carcinoma. *A*) Urothelial carcinoma *in situ* and B) Papillary urothelial neoplasm of low malignant potential. Adapted from (Al-ahmadie et al., 2011).

Squamous cell carcinoma is characterized by keratin pearls, intercellular bridges, and keratotic cellular debris. At the time of diagnosis, most squamous cell carcinomas are poorly differentiated and deeply invasive, possibly contributing to the poor prognosis of these tumors (Al-ahmadie et al., 2011).

Seventy percent of bladder cancers are confined to the bladder and are non-muscle-invasive. While only 5-10% of those will progress and infiltrate the bladder, half of non-invasive bladder cancers will recur (Simon et al., 2004).

Cancer grade is a prediction of cancer progression, while stage characterizes tumor size and spread. The American Joint Committee on Cancer designated 6 stages of bladder cancer (0a, 0is, I, II, III, and IV) determined by tumor type (papillary or *in situ* and extent

of bladder invasion), presence of lymph node metastasis, and indication of distant metastasis (Rubin & Hansen, 2012).

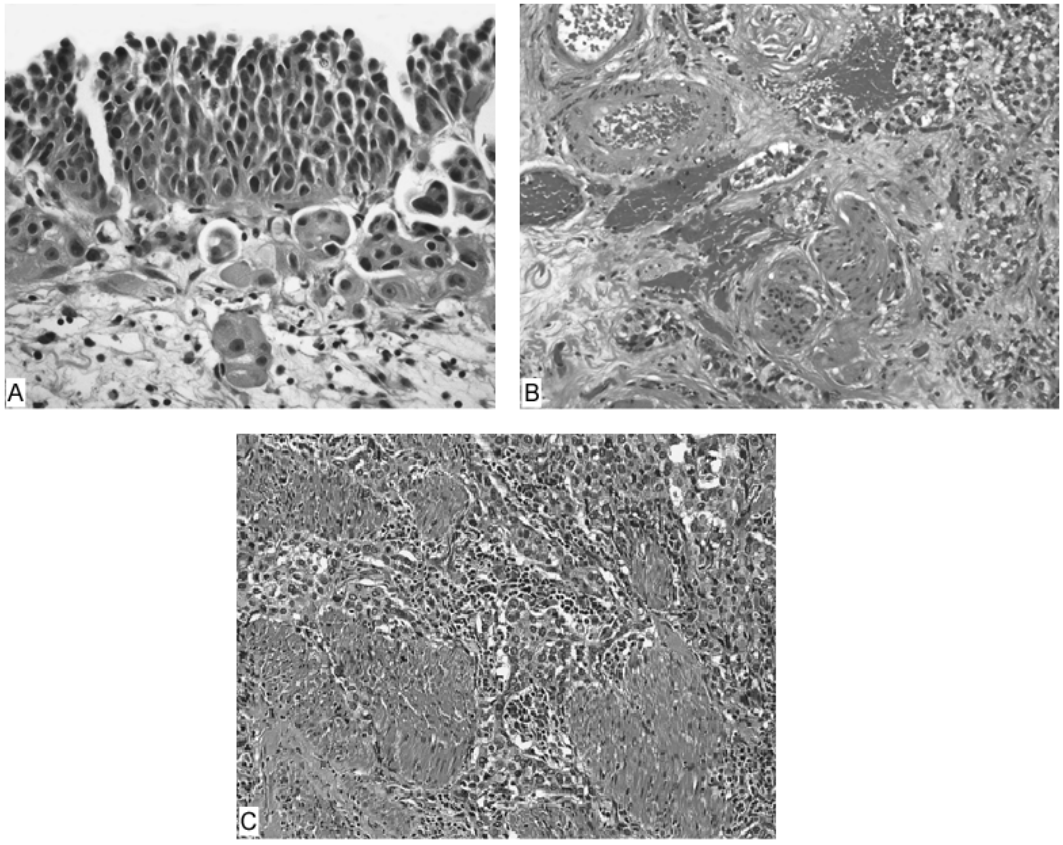

Figure 1.4 Varying levels of invasive urothelial carcinoma. A) Invasion into lamina propria. B) Invasion into deep lamina propria. B) Invasion into muscularis propria. Adapted from (Al-ahmadie et al., 2011).

The most common symptom of bladder cancer is painless hematuria. Cystoscopy is the gold standard for evaluation of bladder cancer, in which tumor location, size, and appearance is determined (Kamat et al., 2013). Transurothelial resection or biopsy is then performed for histological examination of cancer type and stage. Cytology is also used for detection of high grade cancer and to monitor patients for recurrence following treatment. In cytology, cells found in urine are analyzed for abnormalities indicating

neoplasia. The clinical value of cytology for the management of urothelial cancer is variable, as it only has strong sensitivity in high-grade bladder cancers (Al-ahmadie et al., 2011).

Bladder cancer has the highest lifetime cost per person (Yeung et al., 2014), with 60% of costs due to surveillance and treatment of recurrence (Avritscher et al., 2006). Surveillance has been identified as a target for improvement in economical efficacy (Svatek et al., 2014). Tumor biomarkers may be a promising route to determining bladder cancer recurrence. Tumor biomarkers do not add additional invasive procedures, as analysis utilizes previously resected tumors. Upon initial tumor resection, evaluation of biomarkers could provide information about potential recurrence, reducing the number of cystoscopies and allowing for earlier detection of tumor recurrence (Lotan et al., 2010). A number of tissue-based biomarkers have been developed, though none are yet ready for use in clinical settings (Kamat et al., 2013).

Hypothesis and Rationale

This body of work tests the hypothesis that As^{3+} and Cd^{2+} induce bladder cancer through EMT mechanisms. In the first study, the role of N-cadherin, a pro-EMT marker, in bladder cancer caused by As^{3+} and Cd^{2+} will be determined both *in vitro* and in animal models. The finding that N-cadherin was the top-most consistently induced gene in arsenic transformed UROtsa cells and a top induced gene in cadmium transformed isolates suggests that the gene may play an instrumental role in the process of malignant transformation, and that it could be developed as a biomarker of heavy metal-induced bladder cancer. The fact that N-cadherin expression is maintained in transformants

following removal of arsenic and cadmium also implies a mechanism of permanent gene activation, and the role of epigenetic regulation will be explored.

To further establish the role of EMT in As^{3+}- and Cd^{2+}- induced bladder cancer, additional markers of the transition will be characterized. While EMT is considered the mechanism by which cancers progress and become metastatic, the details of the process are unique to cell type and inducing agent, and have not been elucidated in bladder cancer.

The As^{3+}- and Cd^{2+} transformed UROtsa cell lines are a valuable tool for distinguishing the characteristics of bladder cancer induced by heavy metals. Further, this model system demonstrates metal-specific EMT mechanisms of bladder cancer progression. With these tools at hand, sensitive and specific biomarkers may be elucidated to better detect and predict bladder cancer progression.

CHAPTER II

METHODS

Cell Culture

The human urothelial cell line UROtsa was immortalized and cultured as described in Rossi et al. 2001. Briefly, cells were grown in 75 cm^2 cell culture flasks with Dulbecco's modified Eagle's medium (DMEM) (Gibco) supplemented with 5% v/v fetal calf serum (Gibco). Cells were maintained at 37 ^oC in a 5% CO_2/95% air atmosphere. Upon reaching confluency, cells were subcultured at a 1:3 ratio with 0.25% trypsin/ EDTA (Gibco). Cells were fed every three days with growth medium.

UROtsa cells were transformed with arsenite and cadmium as previously described (Sens et al., 2004). Briefly, UROtsa cells were cultured under identical conditions and transformed with 1µM cadmium chloride and sodium (Sigma-Aldrich) in the media. Cells were harvested periodically throughout the transformation. The resulting seven Cd^{2+} and six As^{3+} isolates were expanded ten times at a 1:20 ratio before use. All isolates were able to form colonies in soft agar as described in Sens *et al*. 2004. Cells were maintained in DMEM supplemented with 5% fetal calf serum and 1% glucose and subcultured at a 1:10 ratio.

Human bladder cancer cell lines J82, RT4, and TCCSUP were purchased from ATCC and cultured in DMEM with 10% fetal calf serum,1% glucose, and 2.5% nonessential amino acids.

For short-term heavy metal exposure experiments, the parent UROtsa cell line was passaged with DMEM containing 1 µM sodium arsenite or cadmium chloride for 30 days. Cells were harvested for PCR and Western blot analysis at each passage.

Microspheres were derived from cell monolayer cultures by seeding at low density on low-adherance flasks. The parent UROtsa cells were grown in serum-free DMEM, and transformed isolates were cultured in 20/12 media.

AZC and HDACi

Parent UROtsa cells were seeded 1:10 and treated the following day with 5-Aza-2'-deoxycytidine (5-AZC) (Sigma-Aldrich) or MS-275 (ALEXIS Biochemicals). Cells were exposed to 0.5, 1, 1.5 and 3 µM 5-AZC or 1, 3, and 5 µM MS-275 for three days. Upon reaching confluency, cells were harvested for PCR analysis.

Heterotransplant Tumors

Heterotransplant tumors were formed by subcutaneous (SC) injection of the transformed isolates in nude mice as described in Sens et al. 2004. In short, NCr-*nu/nu* mice were inoculated with 1×10^6 cells in 0.2 ml phosphate-buffered saline. Mice were sacrificed after 10 weeks or if conditions warranted euthanasia. Individual tumors were split for RNA isolation, protein isolation, and immunohistochemistry.

To observe the ability of tumors to colonize internal organs of the peritoneum, transformed cells were implanted into nude mice via intraperitoneal injection as described in Cao et al. (2010). Briefly, 1×10^6 cells in phosphate-buffered saline (PBS) were injected into the lower right quadrant of the abdominal cavity. Mice were euthanized 53 days later when tumors became visible and large in some mice. Following

necropsy, tumors and their associated organs were formalin fixed and paraffin embedded for histology or flash frozen for molecular techniques.

Real Time RT-PCR

Total RNA was isolated using the TRI Reagent protocol (Molecular Research Center, Inc.) and quantified by spectrophotometry (Nanodrop). Tumor samples were snap frozen and ground to a powder with liquid nitrogen before RNA isolation.

One hundred ng of purified RNA was subjected to cDNA synthesis using the iScript cDNA synthesis kit (Bio-Rad) in a total volume of 20 µl. Real time PCR was performed with SYBR Green (Bio-Rad) using 10 ng of cDNA. Amplification was performed using the iCycler MyiQ real time detection system (Bio-Rad) and measured by SYBR Green fluorescence. Primers used are indicated in Table 2.1.

Gene	Company	Catalog No.
ALDH1A1	Qiagen	QT00013286
CD44	Qiagen	QT00073549
CDH1	BioRad	qHsaCED0042076
CDH2	Qiagen	QT00063196
eEF1A2	BioRad	qHsaCID0011054
EPHA4	BioRad	qHsaCID0017961
ETV7	BioRad	qHsaCED0037660
IL1RN	BioRad	qHsaCID0014491
LIMCH1	BioRad	qHsaCID0010779
LPHN2	BioRad	qHsaCID0010674
NR2F1	BioRad	qHsaCED0047128
NR2F2	BioRad	qHsaCID0015621
NTF3	BioRad	qHsaCED0004155
OCLN	BioRad	qHsaCED0038290
Slug	Qiagen	QT00044128
Snai1	Qiagen	QT00010010
STEAP1	BioRad	qHsaCED0046236
TCF4	Qiagen	QT00031829
Twist	Qiagen	QT00011956
UGT8	BioRad	qHsaCID0017816
Vimentin	BioRad	qHsaCID0012604
Zeb1	Qiagen	QT01888446
Zeb2	Qiagen	QT01867586

Table 2.1 Primer source information

Levels of gene expression were determined using quantitative and relative standard curves. Samples were normalized to β-actin (forward, 5-CGACAACGGCTCCGGCATGT-3 and reverse, 5-TGCCGTGCTCGATGGGGTACT-3). The resulting levels were then expressed as fold change over the parent UROtsa cell line.

Analysis of PCR results was performed by one-way analysis of variance (ANOVA) and Tukey or Dunnett's post-test. Data was represented as mean SEM of triplicate determinations with *$p<0.05$, **$p<0.01$, and ***$p<0.001$. GraphPad Prism 5 was used for all analyses.

Western Blot Analysis

Total protein was isolated from cell pellets and tumor tissue using 2% SDS 50 mM Tris-HCl, pH 6.8 with 1% protease inhibitor cocktail (Sigma-Aldrich). Tissue was frozen and ground to powder with liquid nitrogen before homogenizing in lysis buffer. Samples were boiled for 10 min followed by DNA shearing by sonication. Protein concentration was determined by BCA assay (Pierce). Samples were stored at -80 ^{o}C in 100 mM dithiothreitol.

Fifteen µg protein was separated by SDS-PAGE using the TGX AnyKd SDS polyacrylamide gel (BioRad). Samples were reduced in β-mercaptoethanol and boiled for 5 min prior to loading. Protein was transferred to a 0.2 µm PVDF membrane using the semi-dry technique followed by blocking in 5% nonfat dry milk in TBS-T for 90 min. Blots were incubated overnight at 4 ^{o}C in the primary antibodies N-cadherin (Invitrogen, cat# 333900, 1:1,000), E-cadherin (Santa Cruz, sc-7870, 1:1,000), β-actin (AbCam, ab8226, 1:1,000), eEF1A2 (Abnova, H00001917-A01, 1:1,000) and NT-3 (Santa Cruz,

sc-547, 1:200). Blots were probed with appropriate HRP-conjugated secondary antibodies (Cell Signaling) and visualized using Clarity Western ECL (BioRad).

Immunofluorescence

Parent UROtsa and transformed cells were cultured in 24-well plates containing 12 mm coverslips. Confluent cultures were fixed in ice-cold 100% methanol for 3-5 min at -20 ^{o}C. Cells were then incubated in rabbit α-human E-cadherin primary antibody (Santa Cruz, sc-7870) at 2 µg/ml followed by incubation with 2 µg/ml of goat α-rabbit Alexa Fluor 594-tagged secondary antibody (Invitrogen, A11012). Cells were then incubated with mouse α-human N-cadherin primary antibody at 10 µg/ml followed by 2 µg/ml goat α-mouse secondary antibody Alexa Fluor 488 (Invitrogen, A11001). All antibody incubations were done at 37 ^{o}C for 45 min each. Images were captured with a Leica DM5500 Q TCS SPE confocal system and Z-slices were imaged at the indicated optimal depth, stacked and processed using LAS-AF software and Adobe Photoshop.

Immunohistochemistry

Serial sections of subcutaneous and intraperitoneal tumors were cut at 3-5 µm for use in immunohistochemical protocols. The primary antibodies used were: polyclonal rabbit α-E-cadherin (Santa Cruz, 1:100), monoclonal mouse α-N-cadherin (Invitrogen, 1:100) and polyclonal rabbit α-Snail (Cell Signaling, 1:100). Immunohistochemical staining was performed on Leica Bond-Max Automated IHC Staining System (Leica, Bannockburn, IL). Paraffin sections were processed in the machine from deparaffinization until counterstaining by hematoxylin according to the manufacturer's recommended program with modification. Bond Polymer Refine Detection (Leica, DS9800) was used as the main reagents in the automatic staining process. Briefly, the

major steps includes deparaffinization, antigen retrieval in Bond Epitope Retrieval Solution 1 (Leica, Catalog No AR9961) for 20 min, peroxide block for 5 min, incubation with primary antibodies for 25 min at room temperature, incubation with Post Primary for 10 min, incubation with Polymer for 10 min, visualization with DAB for 10 min, and counterstaining with hematoxylin for 5 min. Slides were rinsed in distilled water, dehydrated in graded ethanol, cleared in xylene, and coverslipped. The presence and degree of immunoreactivity in the specimens was judged by two pathologists. The scale used was 0 to +3 with 0 indicating no staining, +1 staining of mild intensity, +2 staining of moderate intensity, and +3 staining of strong intensity.

Chromatin Immunoprecipitation

The ChIP-IT^{TM} Express kit from Active Motif was used for chromatin immunoprecipitation experiments. UROtsa parent cells were passaged five times in 1 µM cadmium chloride or sodium arsenite, followed by 48 hr exposure to MS-275 or 5-AZC. Cells were grown to confluency in 75 cm^2 flasks and fixed with 1% formaldehyde for 10 min. Cross linking was stopped with 0.125 M glycine stop solution and cells were scraped with 2 ml PBS containing Phenylmethylsulfonyl fluoride (PMSF). Cells were pelleted and resuspended in ice-cold lysis buffer, and homogenized using an ice-cold dounce homogenizer. Nuclei were pelleted and resuspended in digestion buffer containing PMSF and protease cocktail inhibitor. Chromatin was then sheared using enzymatic shearing cocktail at 37 ^oC for 5 min, resulting in chromatin fragments of 200-1,500 bp. Protein G-coated magnetic beads were incubated with 7 µg sheared chromatin and 3 µg antibody overnight at 4 ^oC. Antibodies for trimethylated Histone 3 Lysine 9 (Active Motif), trimethylated H3K27 (Active Motif), and anti-acetyl Histone 4

(Millipore). Samples were washed and the immune complex was then eluted. Crosslinking was reversed using crosslinking buffer, and DNA was analyzed by conventional PCR using the Gene Amp PCR core kit (Applied Biosystems). Primers were designed for two regions of the N-cadherin promoter. Region 1 targeted a 72 bp sequence using forward primer, 5- CGGCCCGCTATTTGTCATCAGCTC-3 and reverse, 5-CTCCCCACCCCCTTCTTCGC-3. An annealing temperature of 6 2^{o}C was used for Region 1. Region 2 targeted a 84 bp sequence using forward primer 5-ACGAGCCCGAAACCTCGCGTG-3 and reverse primer 5- ACCTTGGCCGGTGGAGGATGTGGA-3 with an annealing temperature of 61 ^{o}C. PCR products were run on gel electrophoresis and band optical density was quantified using Image Lab software (BioRad). Results were normalized to the amount of corresponding DNA sequence from the fragmented chromatin solution prior to precipitation.

Flow Cytometry

Cells were dissociated in 0.1% trypsin, 0.5mM $CaCl_2$ in PBS followed by 0.5 ml 10 mM EDTA. Non-specific staining was blocked using 1% bovine serum albumin (BSA) for 15 min on ice. Phycoerythrin (PE)-conjugated N-cadherin (mouse mAb clone 8C11, Biolegends cat # 350806) was added to cells at 1:10 and incubated at 4 ^{o}C in the dark for 30 min. Samples were washed two times in 0.1% BSA in PBS buffer before flow cytometry analysis. Cells were counted with a BD LSRII using FACSDiva software. Results were gated to exclude doublets and identify the singlet population

CHAPTER III

RESULTS

N-cadherin Induction in As^{3+}- and Cd^{2+}-transformed UROtsa Cells

To confirm the induction of N-cadherin observed by microarray, real time RT-PCR was performed in the As^{3+} and Cd^{2+} isolates. Expression was found to be significantly elevated compared to the non-malignant parent UROtsa cell line in the majority of isolates. N-cadherin was induced an average of 20-fold in As^{3+} transformants, and 5 to10-fold in Cd^{2+} isolates (Figure 3.1.A, B). Western blot analysis showed protein levels comparable to that of mRNA (Figure 3.1.C, D).

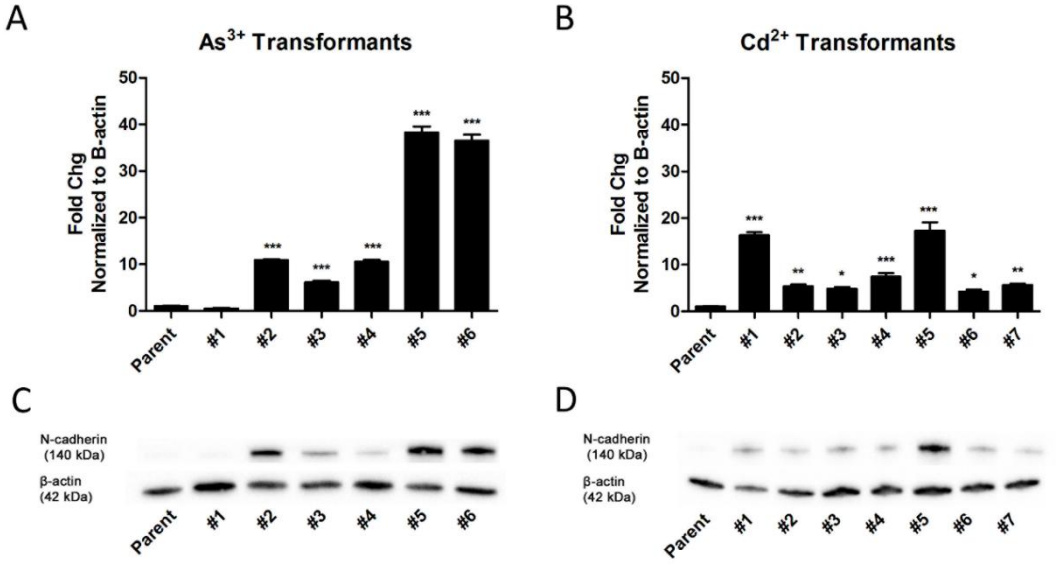

Figure 3.1 N-cadherin expression is elevated in As^{3+}- and Cd^{2+}-transformed UROtsa cells. Real time RT-PCR analysis of N-cadherin in parent UROtsa cell line and A) As^{3+} isolates, and B) Cd^{2+} isolates expressed as fold change normalized to β-actin. Western blot analysis of N-cadherin protein in A) As^{3+} isolates, and D) Cd^{2+} isolates. PCR results represent Mean ±SEM of triplicate determinations. *p<0.05, **p<0.01, ***p<0.001

Immunofluorescence experiments were performed using a subset of the As^{3+}- and Cd^{2+}-transformed isolates. Results showed that N-cadherin was localized to the plasma membrane (Figure 3.2), with the most staining observed in isolate As#6 (Figure 3.2.D). N-cadherin staining was only observed at regions of cell-cell contact (Figure 3.3). The parent UROtsa cell line showed positive staining in a very small percentage of cells (Figure 3.2.A), while no N-cadherin staining was observed in Cd^{2+} #7 (data not shown).

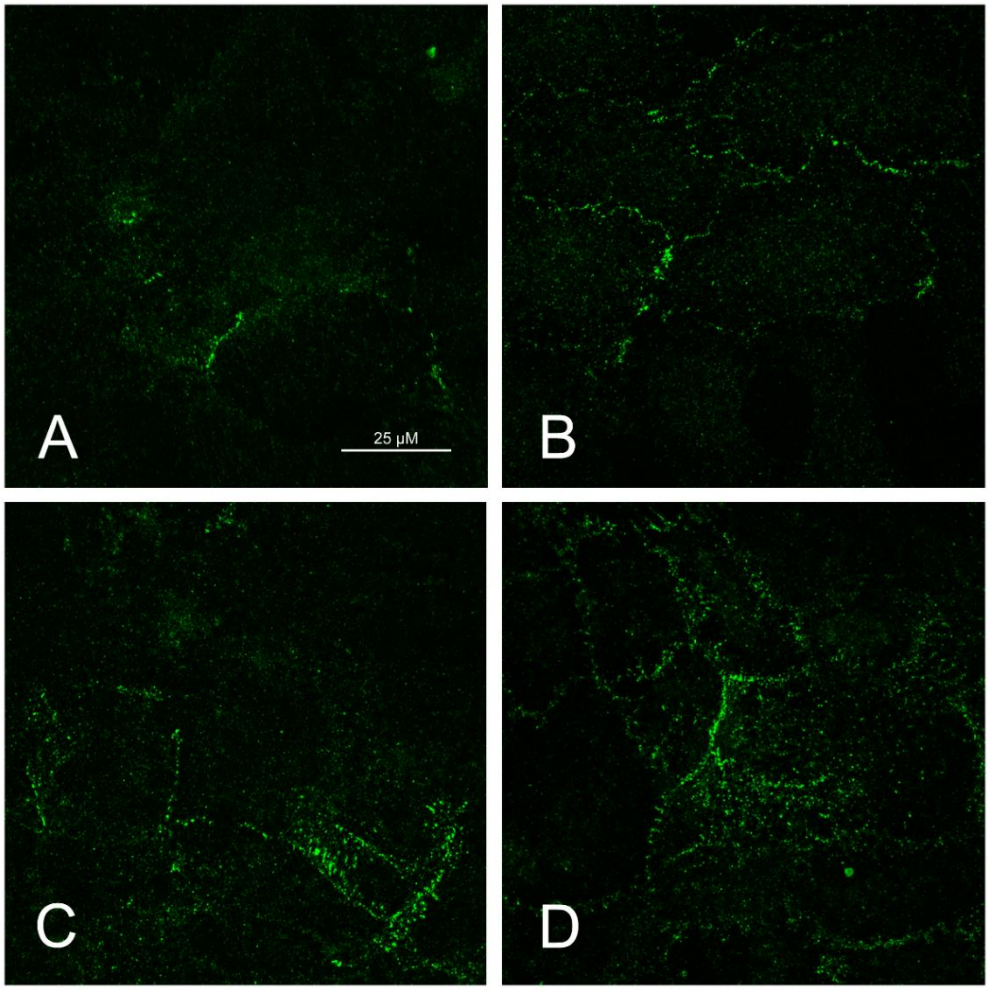

Figure 3.2 N-cadherin is highly expressed in As^{3+} isolate #6. N-cadherin expression is localized to the plasma membrane. Immunofluorescence staining for N-cadherin in A) parent UROtsa cells, B) Cd#1, C) As#3, and D) As#6. Cd#4 was also stained for N-cadherin, but showed no positive labeling. Bar= 25 µM.

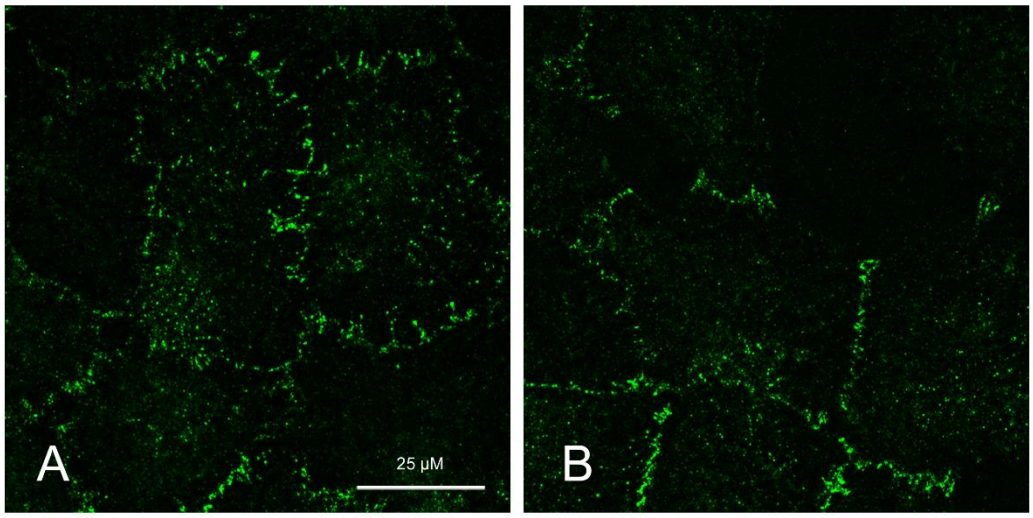

Figure 3.3 N-cadherin is expressed at cell-cell junctions. In N-cadherin-positive cells, the protein is localized to regions of cell-cell contact. Image A represents highly confluent As#6 cells with N-cadherin expression on all sides of the cell. Image B displays a region of less confluent As#6 cultures in which N-cadherin localization is evident only at regions of cell-cell contact.

Expression of N-cadherin was then measured in tumors formed by subcutaneous (SC) injection of transformed isolates into nude mice. Surprisingly, N-cadherin was not maintained in the subcutaneous heterotransplants at the mRNA or protein level (Figure 3.4). Immunohistochemical staining was also negative for N-cadherin in both As^{3+}- and Cd^{2+}-transformed tumors (Figure 3.5, 3.6). The tumor cells were negative for N-Cadherin, but the stromal cells showed focal weak staining of N-Cadherin. The staining of N-Cadherin in As#2 was a little stronger than other groups (Figure 3.5.B), while As#5 was almost negative (Figure 3.5.E). Some strongly positive structures are non-specific signal. N-cadherin was then investigated in tumors derived from intraperitoneal (IP) heterotransplants, in which positive focal staining was seen (Figure 3.7).

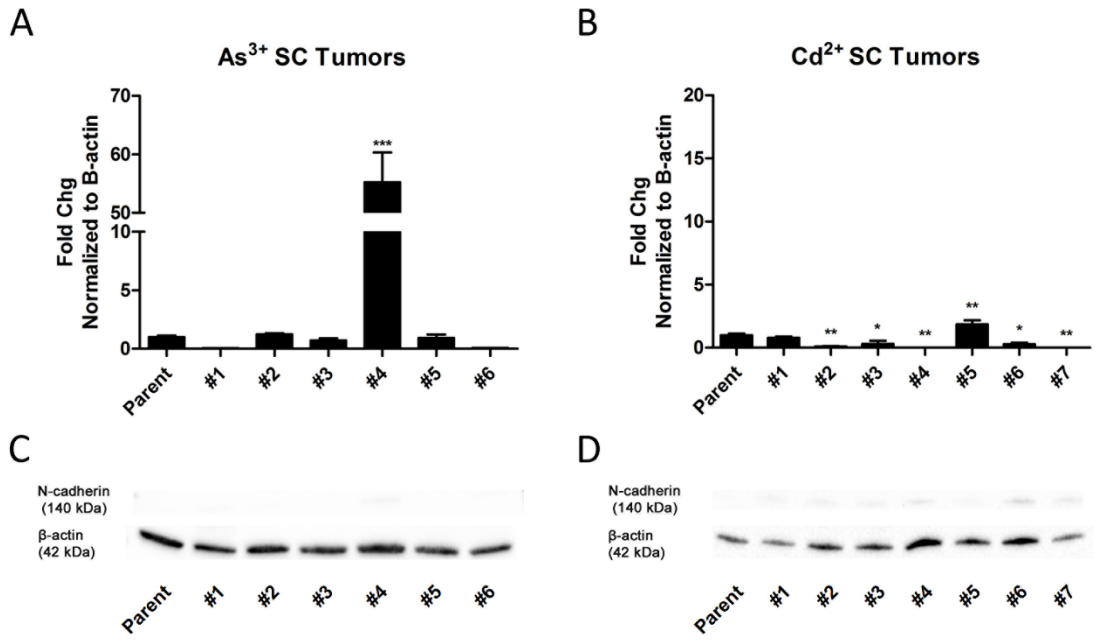

Figure 3.4 N-cadherin mRNA and protein levels are unchanged in subcutaneous heterotransplant tumors derived from As^{3+}- and Cd^{2+}-transformed isolates. A) Real time RT-PCR analysis of N-cadherin in A) parent UROtsa cell line and As^{3+} isolates, and B) parent UROtsa cell line and Cd^{2+} isolates expressed as fold change normalized to β-actin. C) Western blot analysis of N-cadherin protein in C) As^{3+} isolates, and D) Cd^{2+} isolates. PCR results represent Mean ±SEM of triplicate determinations. *$p<0.05$, **$p<0.01$, ***$p<0.001$

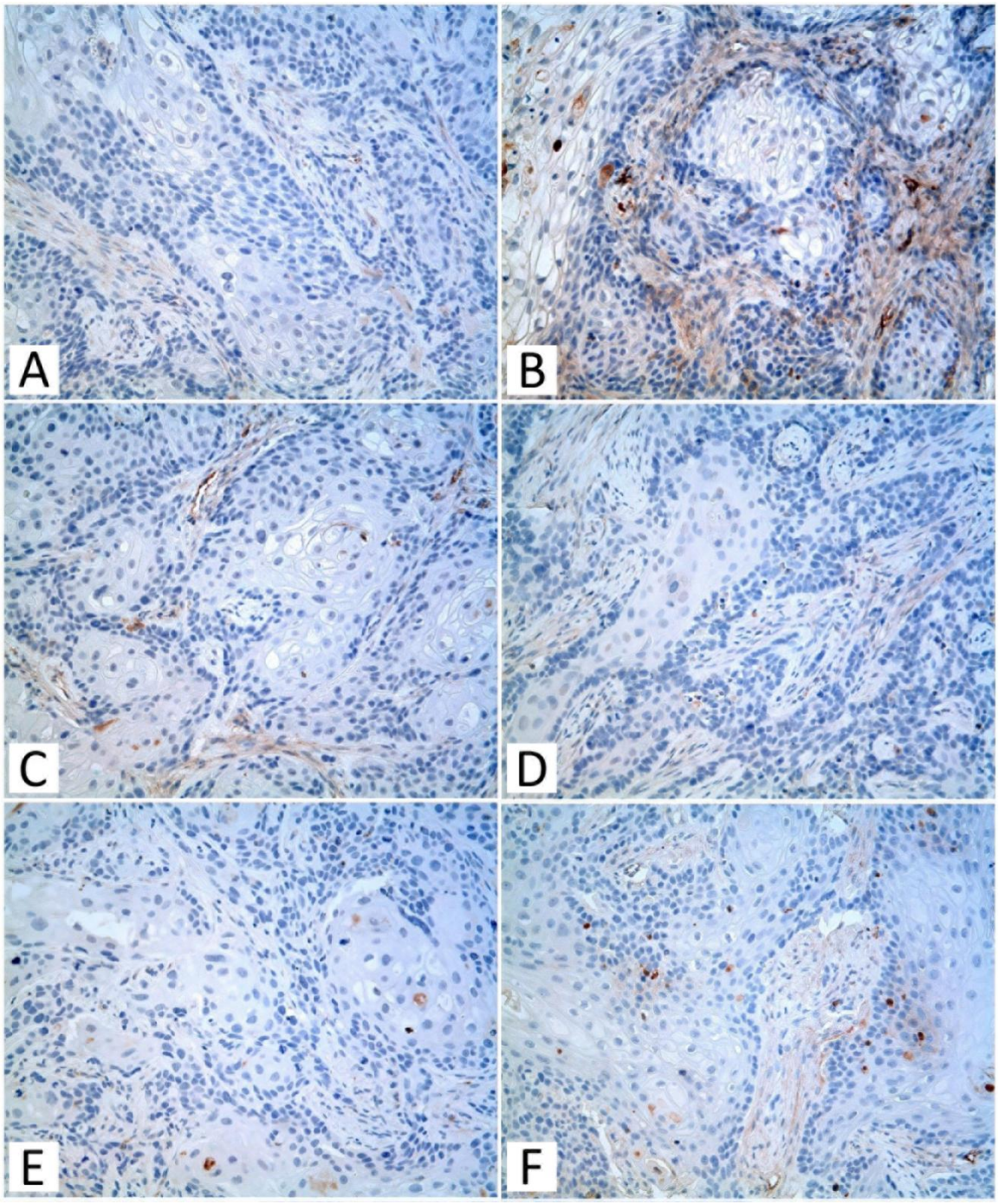

Figure 3.5 Immunohistochemical analysis demonstrates negative staining in subcutaneous heterotransplant tumors derived from As^{3+}-transformed isolates. The tumor cells are negative for N-Cadherin, but the stromal cells show focal weak staining of N-Cadherin. The staining of N-Cadherin in As #2 is a little stronger than other groups, and As#5 is almost negative. Some strongly positive structures are non-specific signal. A) As#1, B) As#2, C) As#3, D) As#4, E) As#5, F) As#6. Magnification 200X.

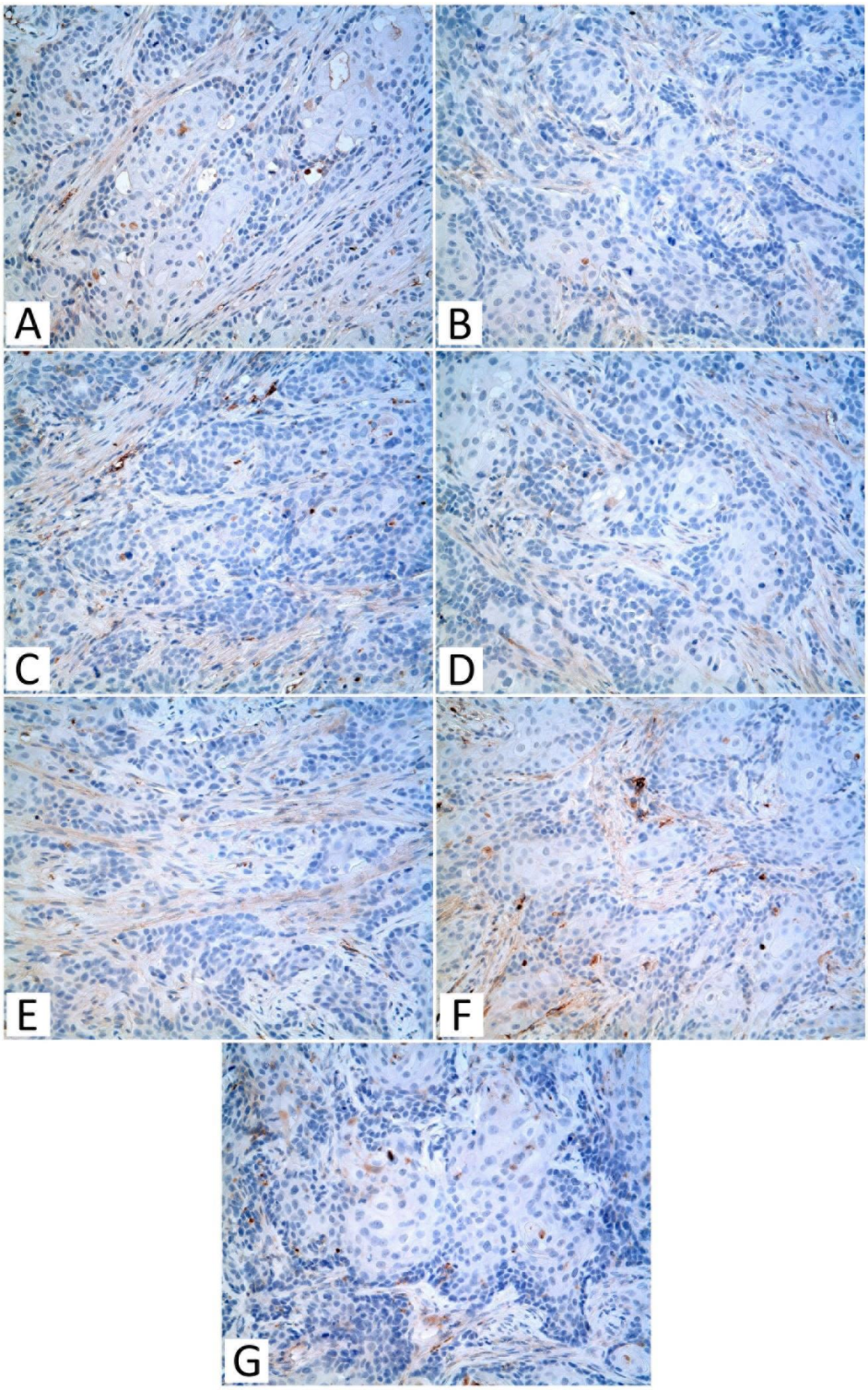

Figure 3.6 Immunohistochemical analysis demonstrates negative staining in subcutaneous heterotransplant tumors derived from Cd^{2+}- transformed isolates. The tumor cells in Cd^{2+} tumors are negative for N-Cadherin, but the stromal cells show focal weak staining of N-Cadherin. Some strongly positive structures are non-specific signal. A) Cd#1, B) Cd#2, C) Cd#3, D) Cd#4, E) Cd#5, F) Cd#6, G) Cd#7. Magnification 200X.

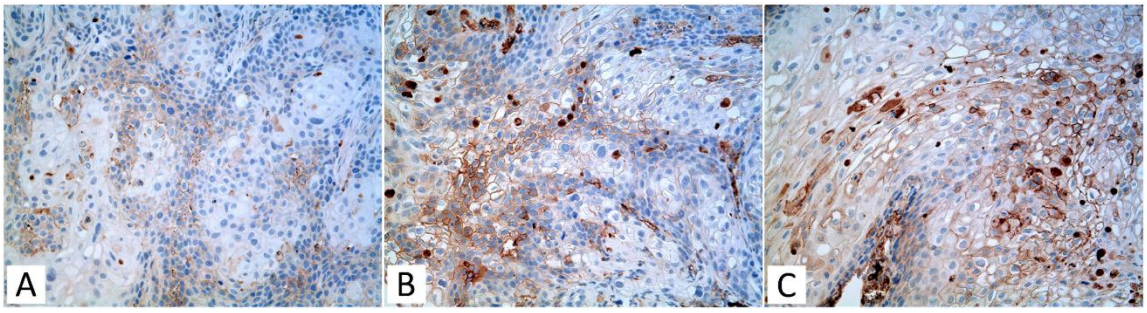

Figure 3.7 N-cadherin is focally expressed in intraperitoneal tumors. In contrast to subcutaneous tumors, the all 3 IP tumors show focal weak staining of N-Cadherin. The strongly N-Cadherin positive round structures are non-specific staining. A) As#1, B) As#3, C) Cd#1. Magnification 200X

Cell population heterogeneity may be a cause of the inconsistent results for N-cadherin expression *in vivo*. During transformation, numerous phases of massive die-off followed by regrowth of surviving colonies occurred, allowing the opportunity for some heterogeneity in the population to arise. To investigate whether the lack of a clonal population played a part in tumor phenotype, flow cytometry was performed for N-cadherin among isolates with varying N-cadherin expression as observed by PCR and Western blot. The As^{3+} isolates #1, #3, and #6 were chosen for their low, moderate, and high expression of N-cadherin protein, respectively (Figure 3.1.C). The Cd^{2+}-transformed isolates #4, #1, and #5 similarly demonstrated low, medium, and high N-cadherin protein relative to parent UROtsa cells in previous experiments (Figure 3.1.D). Flow cytometric analysis using PE-conjugated N-cadherin antibody indicated a dramatic increase in the percent of cells positive for N-cadherin in As^{3+} isolate #6 alone (Figure 3.8, Table 3.1), with 98.5% of cells positive for N-cadherin in isolate #6 compared to 1.31% in the parent UROtsa cell line. For the remaining isolates, less than 2% were positive for N-cadherin.

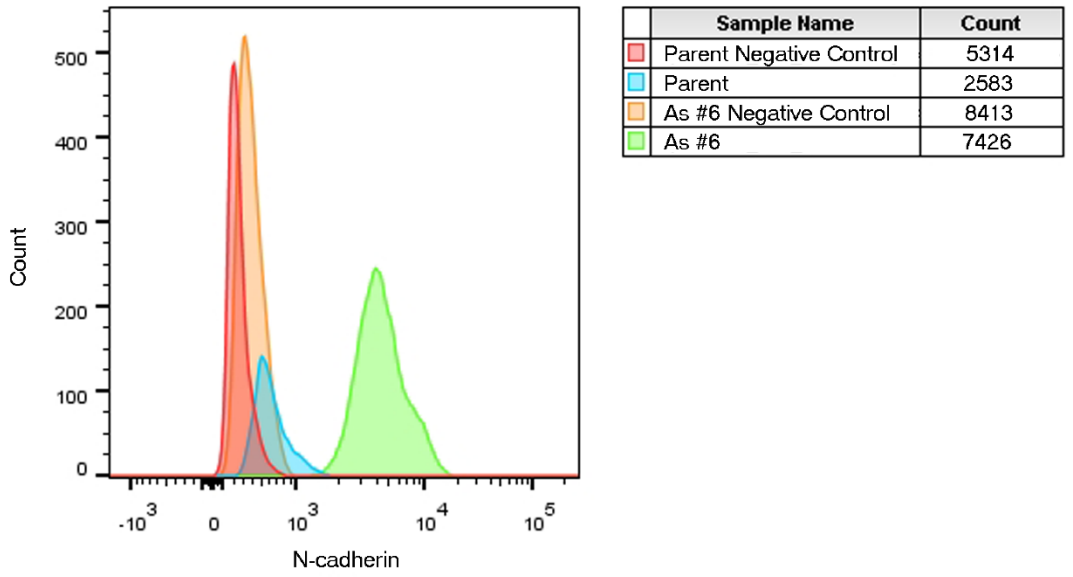

Figure 3.8 The As^{3+} isolate #6 has dramatically increased numbers of N-cadherin-positive cells. Flow cytometry analysis for N-cadherin indicated by PE fluorescence in parent and As^{3+} #6. Negative samples are no antibody controls.

Isolate	Cells (Number)	Low N-cadherin (Number)	Low N-cadherin (Percent)	Moderate N-cadherin (Number)	Moderate N-cadherin (Percent)	High N-cadherin (Number)	High N-cadherin (Percent)
As #1	7896	6257	79.2	994	12.6	65	0.82
As #3	7317	3840	52.5	2982	40.8	117	1.6
As #6	7536	2	0.027	9	0.12	7426	98.5
Cd #1	7140	3325	46.6	3207	44.9	101	1.41
Cd #4	8072	5725	70.9	1736	21.5	77	0.95
Cd #5	6868	1866	27.2	4354	63.4	60	0.87
Parent	4437	1677	37.8	2583	58.2	58	1.31

Table 3.1 As^{3+} isolate #6 has the highest percentage of N-cadherin-positive cells. Table indicates number and percent of cells positive for low, medium, and high intensity PE-conjugated N-cadherin. Negative samples indicate no antibody controls.

The fact that all isolates formed tumors lacking N-cadherin, independent of its expression *in vitro*, suggested that a unique subset of cells negative for N-cadherin existed within the cell population, and that this subset was responsible for tumor

formation. The potential for tumor-initiating cells, or cancer stem cells, was then investigated. Indeed, microspheres were derived from transformants by seeding at low density on low-adherence flasks, a typical protocol for initial cancer stem cell isolation. Further, the individual cells were able to regenerate microspheres following repeated dissociation, confirming their self-renewal capability. Upon IP injection into nude mice, the microspheres were also able to initiate tumor formation, further indicating their cancer stem cell-like characteristics. PCR analysis for cancer stem cell markers was performed, revealing that the microspheres expressed increased levels of ALDH1A1, though CD44 expression was reduced relative to the corresponding isolates (Figure 3.9.A, B). Upon investigation of N-cadherin in the microspheres, mRNA levels were compared to their corresponding transformed isolates, indicating that this putative cancer stem cell population does not express N-cadherin (Figure 3.9.C).

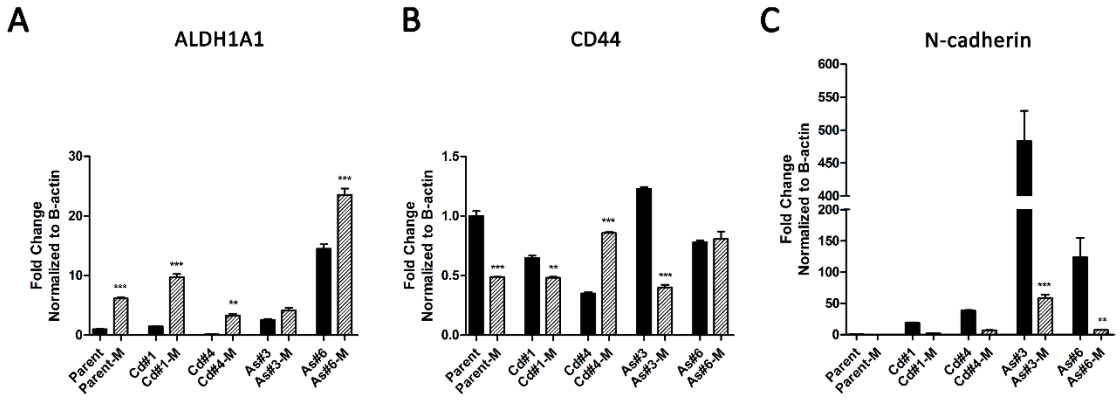

Figure 3.9 Microspheres originating from As^{3+}- and Cd^{2+}-transformed isolates express cancer stem cell marker ALDH1A1, but low levels of N-cadherin. A) Real time RT-PCR analysis of A) ALDH1A1 in parent UROtsa cells, As^{3+} and Cd^{2+} transformants and corresponding microspheres, B) CD44, and C) N-cadherin in parent UROtsa cells, As^{3+} and Cd^{2+} transformants and corresponding microspheres expressed as fold change normalized to β-actin. PCR results represent Mean ±SEM of triplicate determinations. *p<0.05, **p<0.01, ***p<0.001

The transcriptional regulation of N-cadherin is largely unknown. While a number of transcription factors have been implicated in various tissues, no studies are available on the regulation of N-cadherin in bladder cancer progression through EMT. To determine whether N-cadherin expression is a participant in cancer initiated specifically by As^{3+} or Cd^{2+}, rather than a change occurring downstream of carcinogenesis, non-malignant parent UROtsa cells were exposed to 1 μM $CdCl_2$ or $NaAsO_2$. Sodium arsenite failed to induce N-cadherin expression (Figure 3.10.A), while mRNA and protein levels were induced beginning at 15 days of cadmium exposure (Figure 3.10.B, C).

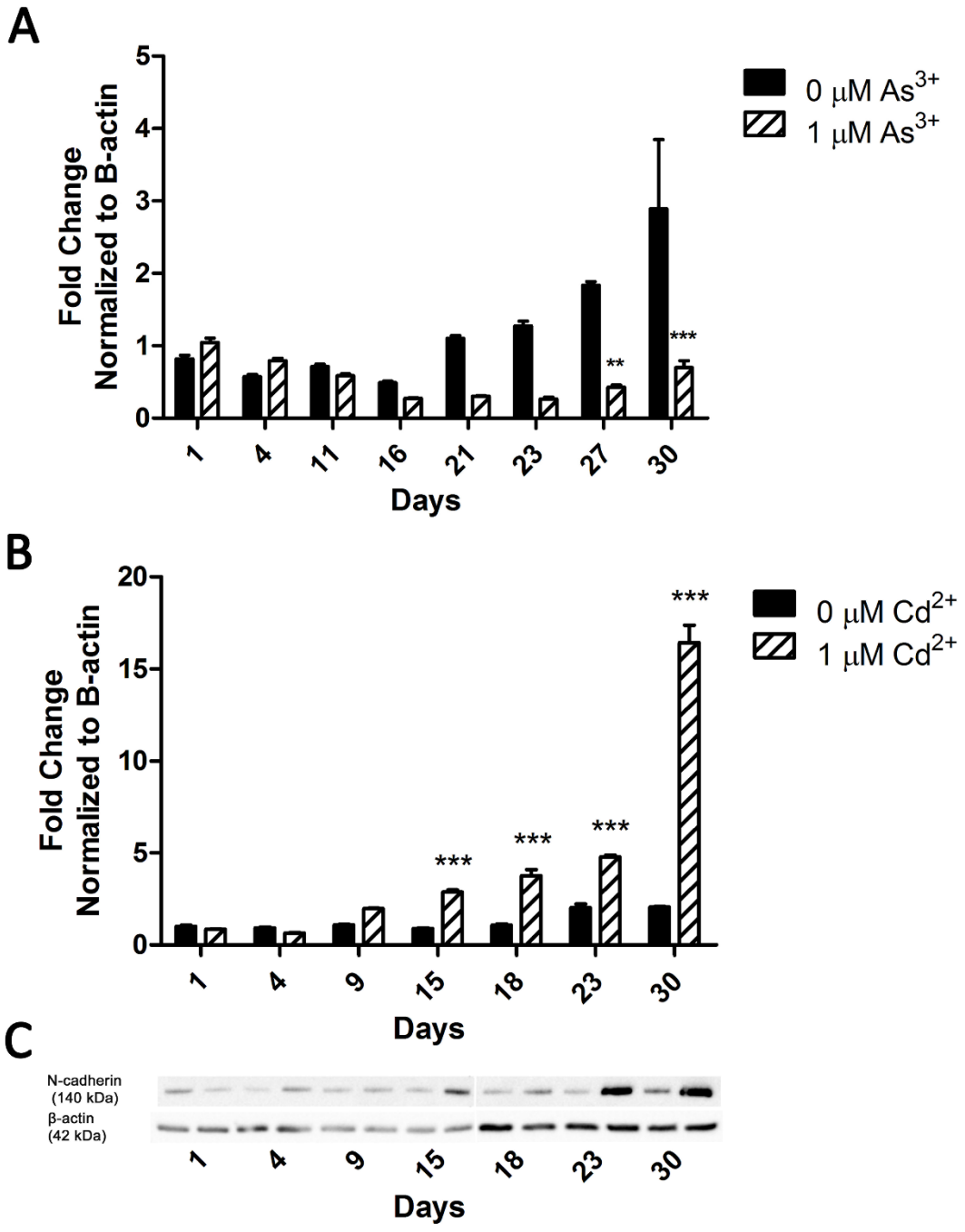

Figure 3.10 N-cadherin expression is induced in parent UROtsa cells exposed to 1 μM $CdCl_2$ over 30 days. A) Real time RT-PCR analysis of N-cadherin over 30 days exposure to 1 μM sodium arsenite expressed as fold change normalized to β-actin. B) Real time RT-PCR analysis of N-cadherin over 30 days exposure to 1 μM cadmium chloride expressed as fold change normalized to β-actin. C) Western blot analysis of N-cadherin protein over 30 days exposure to 1 μM cadmium chloride. PCR results represent Mean ±SEM of triplicate determinations. *p<0.05, **p<0.01, ***p<0.001

Interestingly, the expression of N-cadherin is maintained in As^{3+}- and Cd^{2+}-transformed cells after removal of the heavy metals, indicating that permanent changes in gene regulation have taken place. To determine whether epigenetic modifications may play a role in N-cadherin expression, parent UROtsa cells were treated with the histone deacetylase inhibitor MS-275 and the DNA methyltransferase inhibitor 5'-azacytidine (5-AZC). Expression of N-cadherin mRNA was induced in a dose-dependent manner upon MS-275 exposure (Figure 3.11.A), whereas very little change was seen after exposure to 5-AZC (Figure 3.11.B), indicating that histone acetylation state may regulate expression of N-cadherin in UROtsa cells.

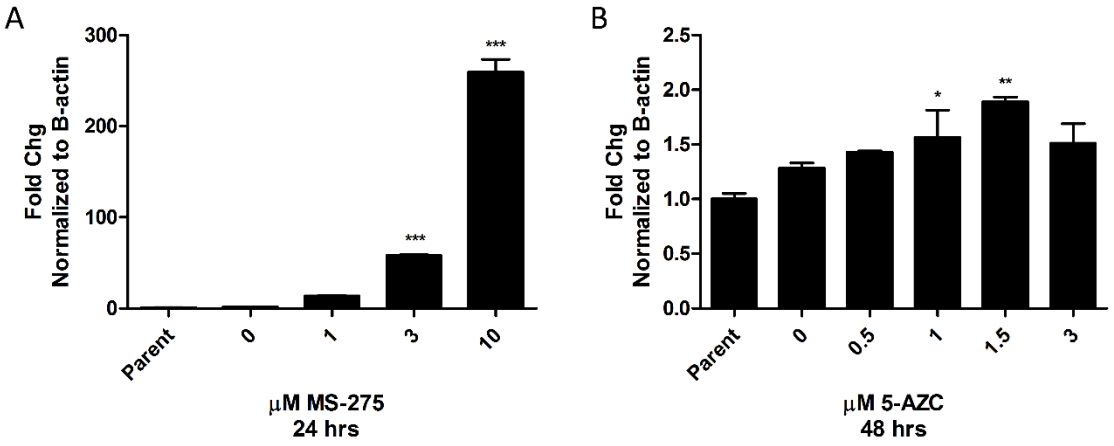

Figure 3.11 N-cadherin expression is altered by MS-275 exposure, while relatively unchanged following 5'-AZC. A) Real time RT-PCR analysis of N-cadherin following 24 hr treatment with 0, 1, 3, and 10 μM MS-275. Expressed as fold change normalized to β-actin. B) Real time RT-PCR analysis of N-cadherin following 48 hr treatment with 0, 0.5, 1, 1.5, and 3 μM 5'-AZC. Expressed as fold change normalized to β-actin. PCR results represent Mean ±SEM of triplicate determinations. *$p<0.05$, **$p<0.01$, ***$p<0.001$

To further investigate the role of histone modification on N-cadherin transcription, chromatin immunoprecipitation (ChIP) was performed for histone 4 total acetylation and histone 3 lysine 9 trimethylation at two regions within 2,000 bp upstream

of the N-cadherin transcription start site (Figure 3.12). Exposure to cadmium and arsenite did not alter H3K9Me3 at Region 1. In addition, MS-275 treatment did not change H3K9Me3 levels at this region (Figure 3.13). At Region 2, parent UROtsa cell exposure to sodium arsenite for five passages led to increased H4Ac levels (Figure 3.14). Cadmium chloride treatment induced H4Ac after 48 hrs, though the increased levels were not maintained long-term. However, treatment with histone deacetylase MS-275 dramatically induced H4Ac in all treatment groups (Figure 3.14).

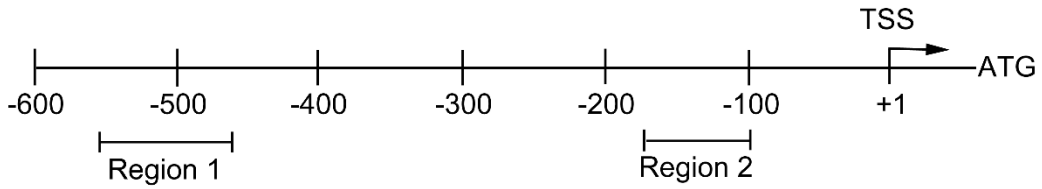

Figure 3.12 Schematic illustration of the N-cadherin promoter.

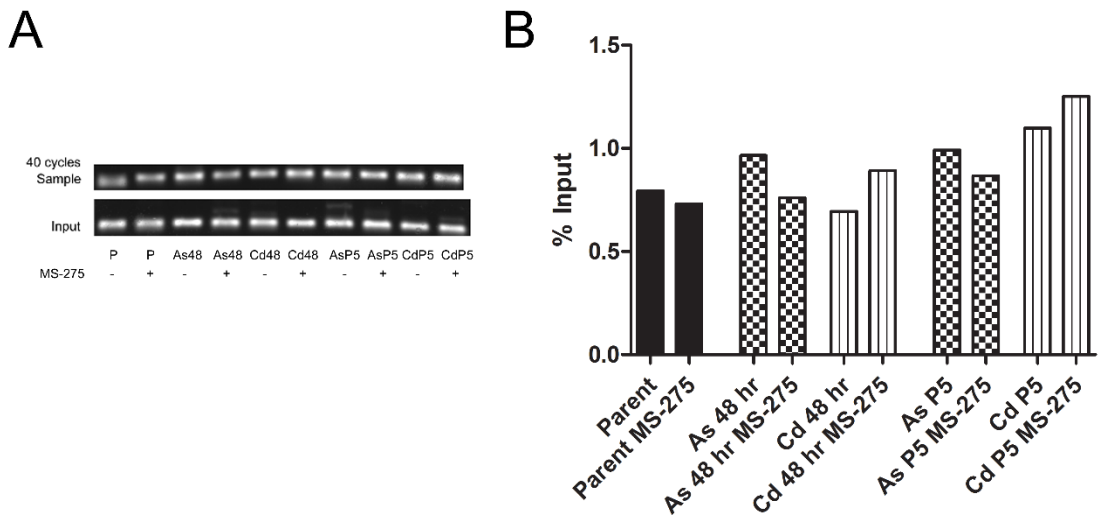

Figure 3.13 Histone 3 lysine 9 trimethylation is unchanged at Region 1 of the N-cadherin promoter following MS-275, As^{3+}, or Cd^{2+} exposure. A) Ethidium bromide-stained gel showing amplification of H3K9Me3 using semiquantitative PCR. B) Quantified results of H3K9Me3 normalized to percentage of input.

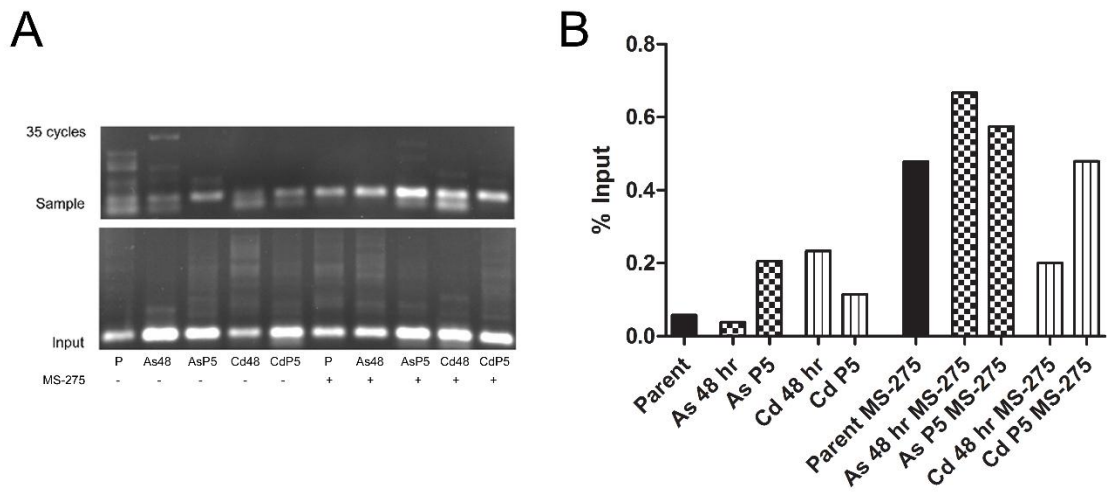

Figure 3.14 Arsenite exposure and MS-275 increase total histone 4 acetylation at Region 2 of the N-cadherin promoter. A) Ethidium bromide-stained gel showing amplification of H4Ac using semiquantitative PCR. B) Quantified results of H4Ac normalized to percentage of input. P5 indicates exposure through five passages of cell culture.

EMT Progression in As^{3+}- and Cd^{2+}-transformed UROtsa Cells

The levels of E-cadherin were determined both *in vitro* and in heterotransplants originating from As^{3+} and Cd^{2+} isolates. E-cadherin was unchanged at the mRNA level in both As^{3+}- and Cd^{2+}-transformed UROtsa cells (Figure 3.15.A), and no alterations were seen in protein as determined by Western blot analysis (Figure 3.15.B). Immunofluorescent staining for E-cadherin demonstrated localization of the protein at the cell membrane at regions of cell to cell contact. E-cadherin was consistently labeled in all isolates examined (Figure 3.16). Co-immunofluroescence for N-and E-cadherin indicated that N-cadherin did not replace E-cadherin localization at the membrane in any of the transformed isolates (Figures 3.17, 3.18).

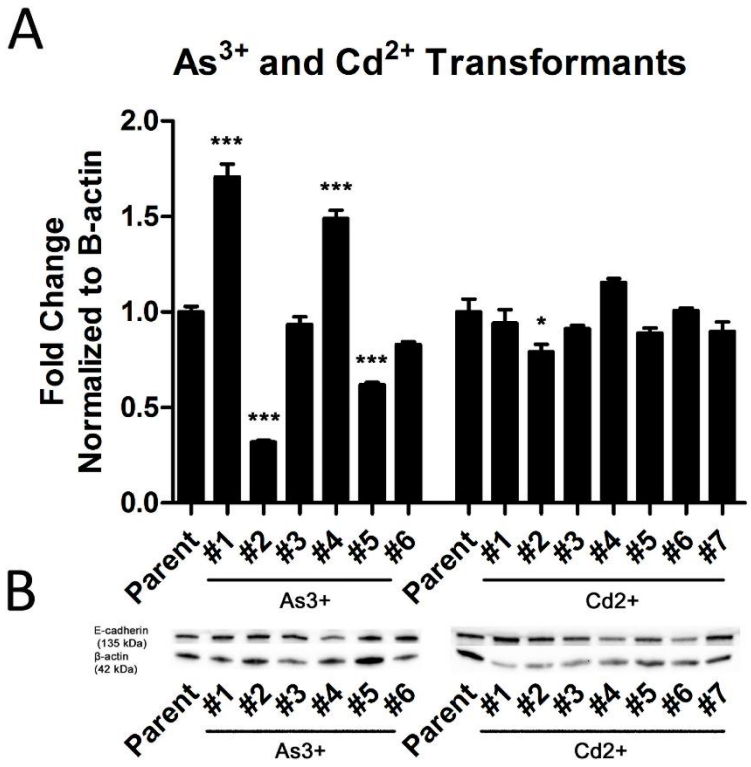

Figure 3.15 E-cadherin is unchanged in As^{3+} and Cd^{2+} transformants. A) Real time RT-PCR analysis of E-cadherin in parent UROtsa cell line and As^{3+} and Cd^{2+} isolates expressed as fold change normalized to β-actin. B) Western blot analysis of E-cadherin protein in As^{3+} and Cd^{2+} isolates. PCR results represent Mean ±SEM of triplicate determinations.

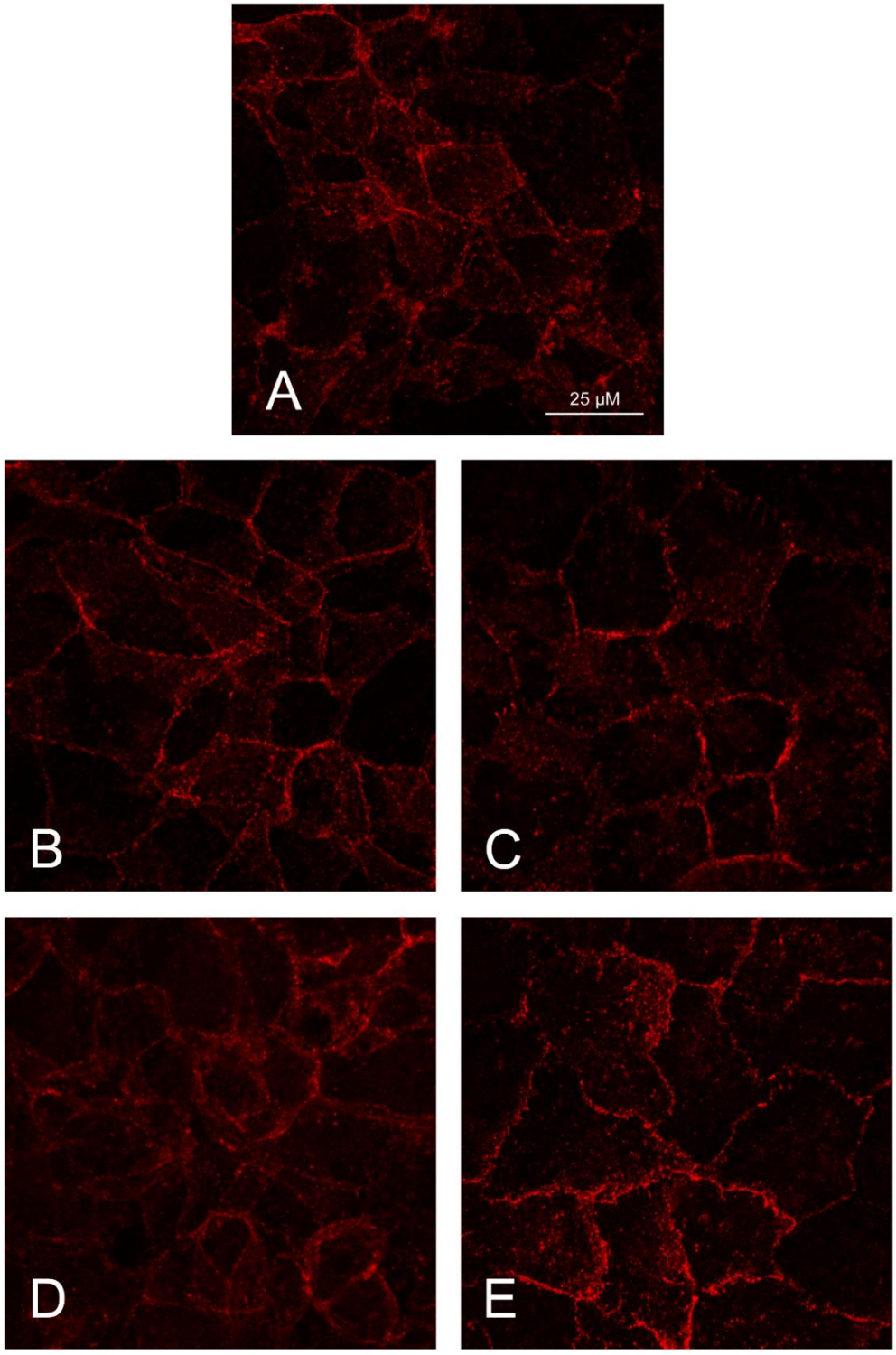

Figure 3.16 E-cadherin is consistently expressed at the cell membrane in As^{3+}- and Cd^{2+}-transformed UROtsa cells. A) Parent UROtsa cell line, B) As#3, C) As#6, D) Cd#1, E) Cd#4. Bar= 25 µM.

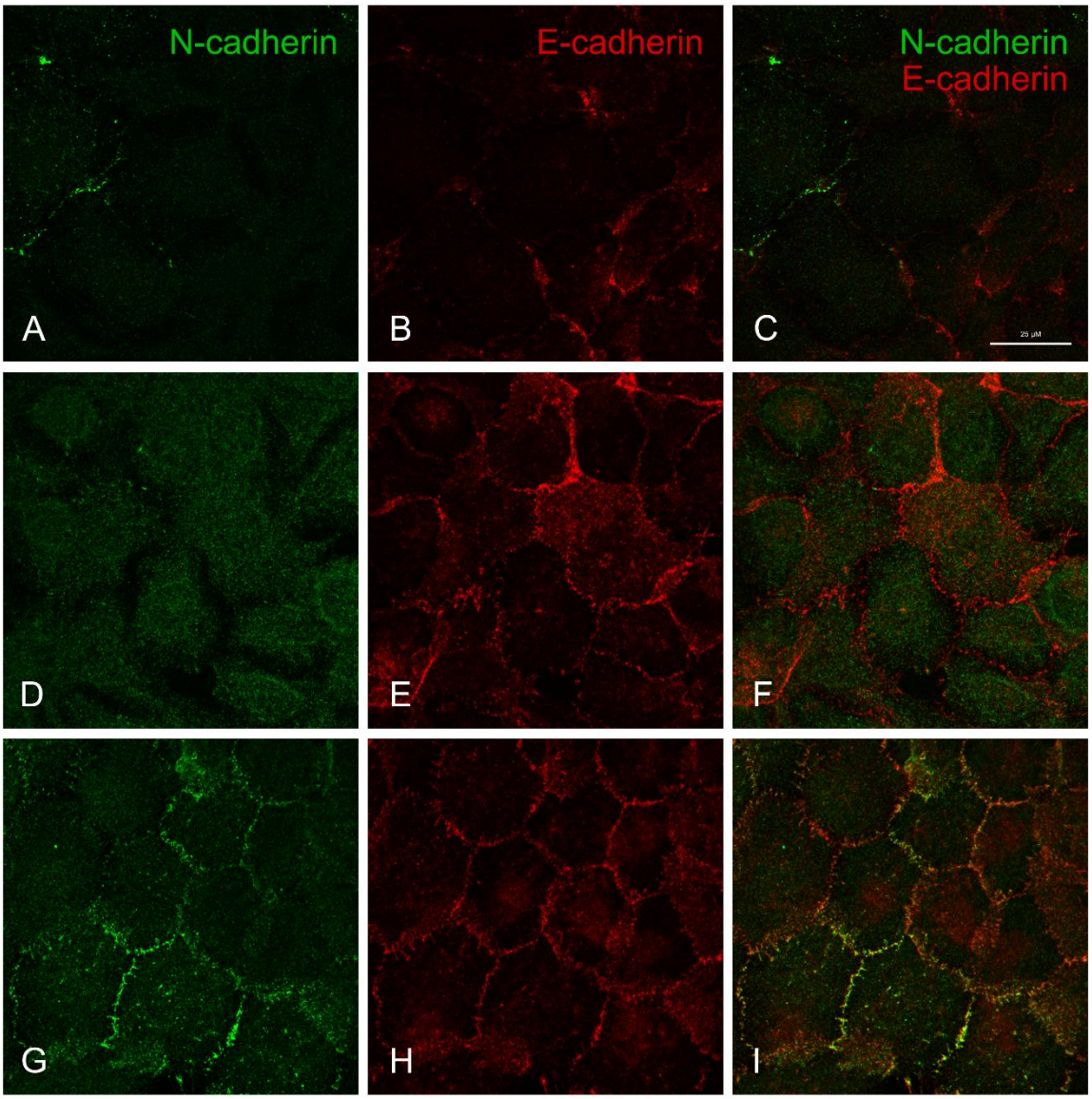

Figure 3.17 N-cadherin and E-cadherin are co-expressed at the cell membrane in As^{3+}-transformed UROtsa cells. N-cadherin staining in A) parent UROtsa cell line, D) As#3, and G) As#6. E-cadherin staining in B) parent UROtsa cell line, E) As#3, and H) As#6. N-cadherin and E-cadherin co-immunofluorescence in C) parent UROtsa cell line, F) As#3, and I) As#6.

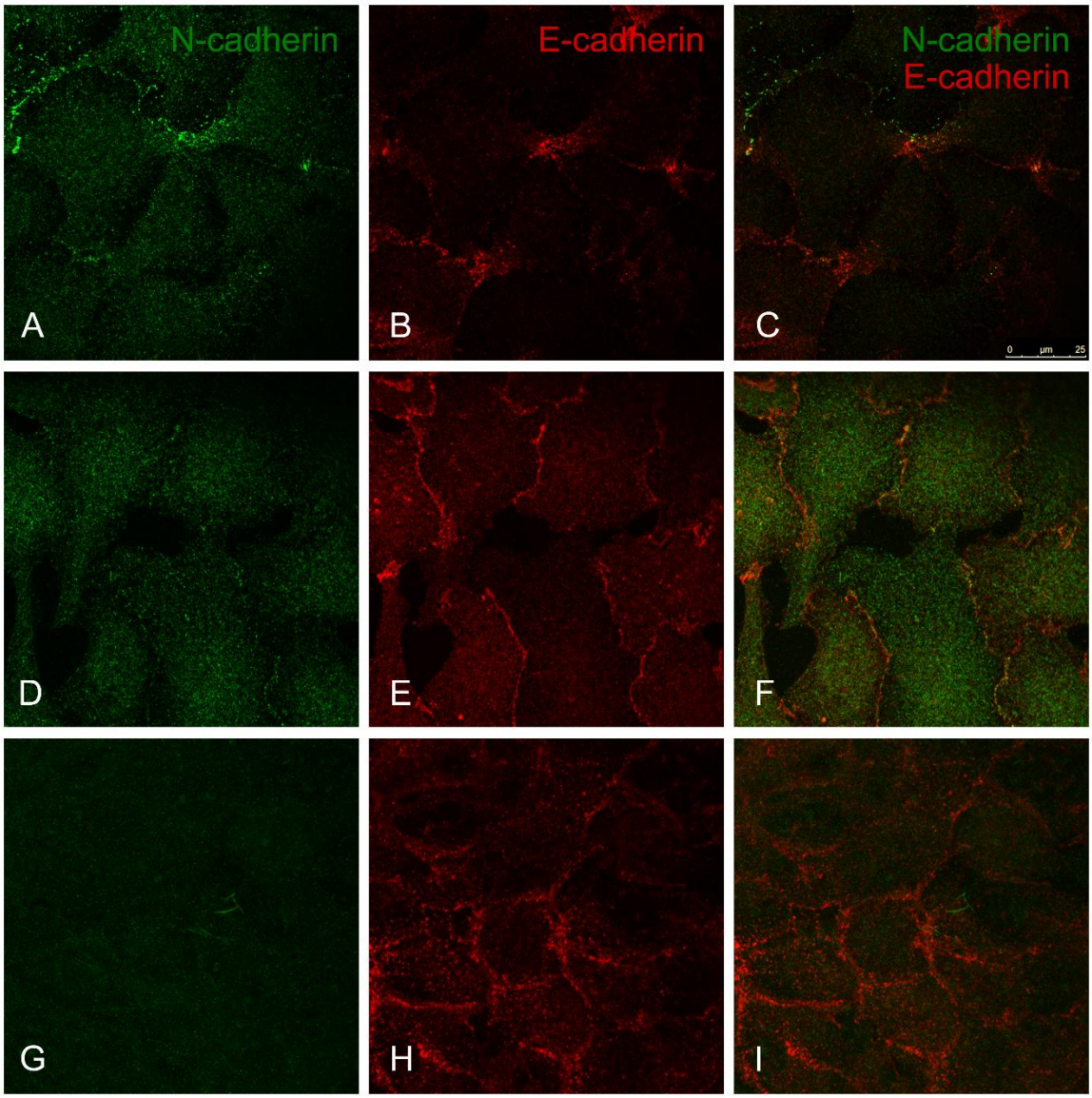

Figure 3.18 N-cadherin and E-cadherin are co-expressed at the cell membrane in Cd^{2+}-transformed UROtsa cells. N-cadherin staining in A) parent UROtsa cell line, D) #1, and G) Cd#4. E-cadherin staining in B) parent UROtsa cell line, E) Cd#1, and H) Cd#4. N-cadherin and E-cadherin co-immunofluorescence in C) parent UROtsa cell line, F) Cd#1, and I) Cd#4.

Investigation of E-cadherin in subcutaneous heterotransplant tumors yielded similar results, with no change observed in As^{3+} or Cd^{2+} tumors (Figure 3.19). While some induction was seen at the mRNA level in the As^{3+} isolates (Figure 3.19.A), a corresponding increase in E-cadherin protein was not found (Figure 3.19.B). Tumor immunohistochemistry showed SC tumors strongly positive at the plasma membrane for

E-cadherin in both As^{3+}- and Cd^{2+}-derived tumors (Figures 3.20 and 3.21). Levels were similarly strong in the IP heterotransplant tumors (Figure 3.22).

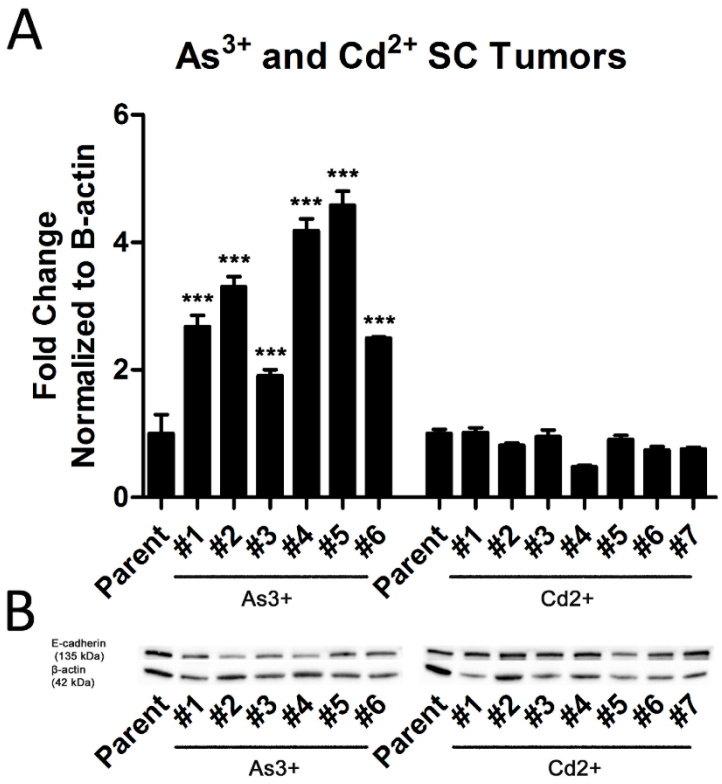

Figure 3.19 E-cadherin is unchanged in subcutaneous heterotransplants. A) Real time RT-PCR analysis of E-cadherin in parent UROtsa cells and SC tumors derived from As^{3+} and Cd^{2+} isolates expressed as fold change normalized to β-actin. B) Western blot analysis of E-cadherin protein in SC tumors originating from As^{3+} and Cd^{2+} isolates. PCR results represent Mean ±SEM of triplicate determinations.

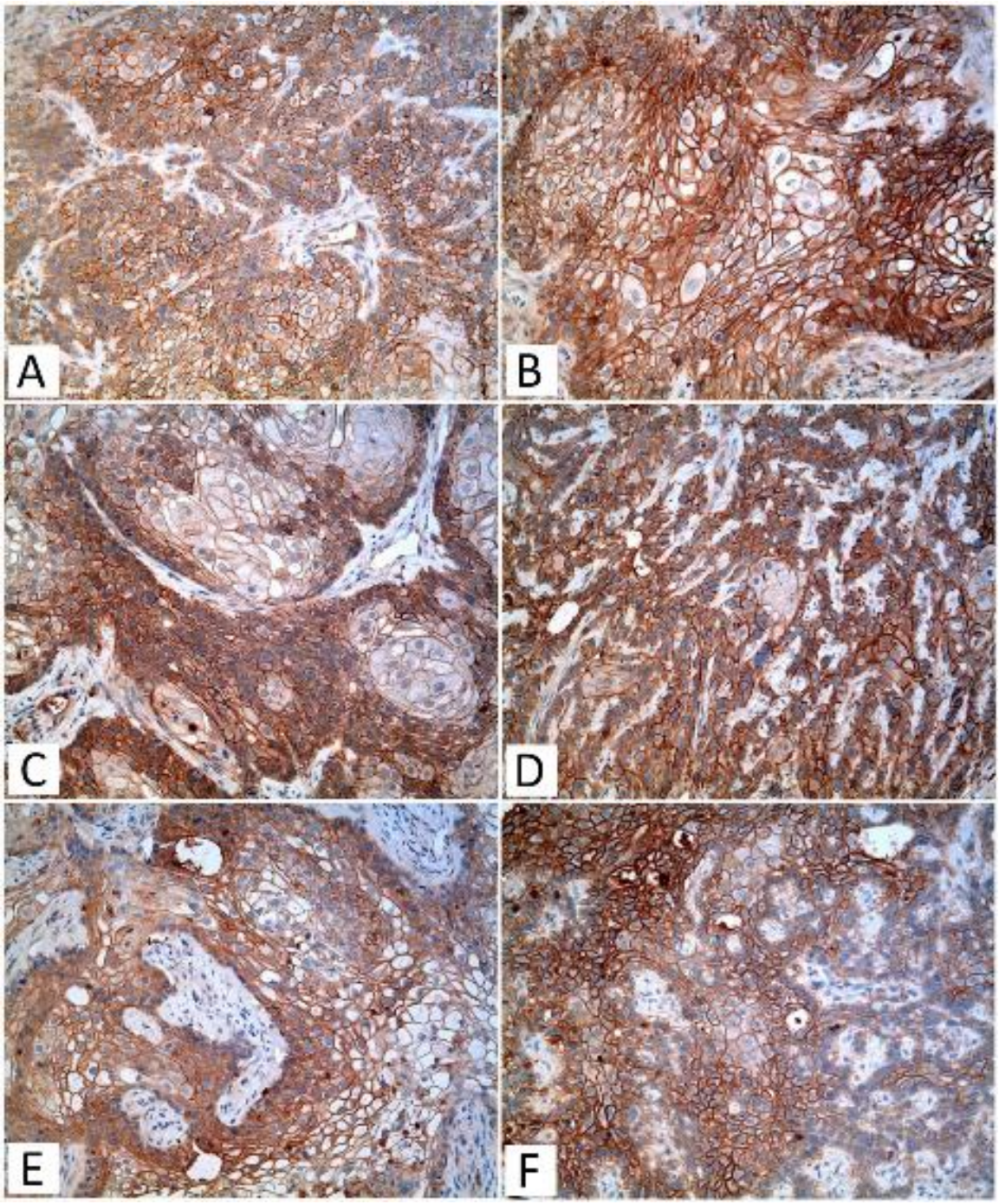

Figure 3.20 Immunohistochemical analysis demonstrates strong E-cadherin staining in subcutaneous heterotransplant tumors derived from As^{3+}- transformed isolates. E-cadherin is strongly positive in As^{3+} heterotransplant tumors. The staining is stronger in the peripheral cells than the cells in the center of tumor nests. Magnification 200X A) As#1, B) As#2, C) As#3, D) As#4, E) As#5, F) As#6.

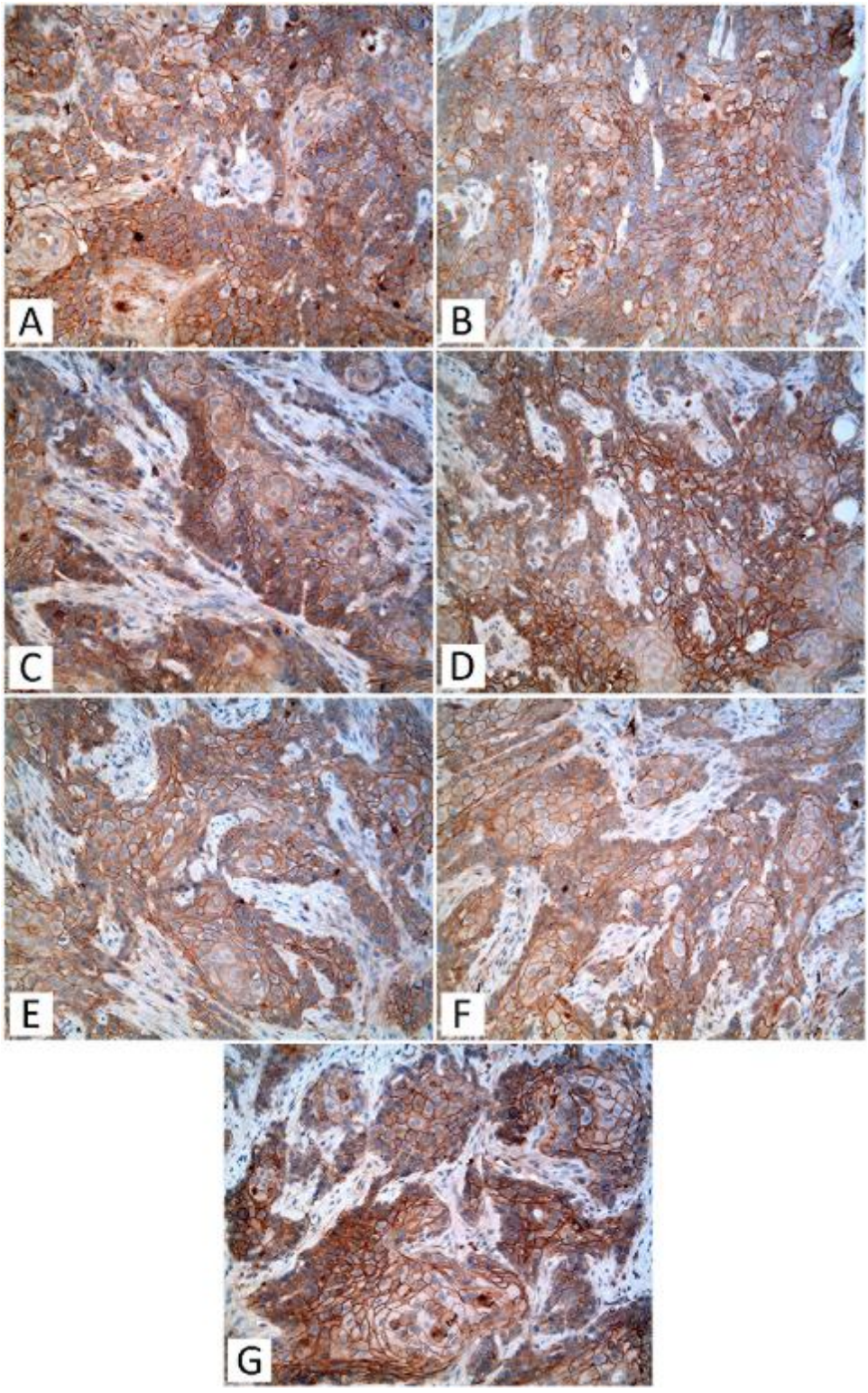

Figure 3.21 Immunohistochemical analysis demonstrates strong E-cadherin staining in subcutaneous heterotransplant tumors derived from Cd^{2+}- transformed isolates. E-cadherin is strongly positive in heterotransplant tumor formed from all Cd^{2+} isolates. The staining is stronger in the peripheral cells than the cells in the center of tumor nests. Magnification 200X. A) Cd#1, B) Cd#2, C) Cd#3, D) Cd#4, E) Cd#5, F) Cd#6, G) Cd#7.

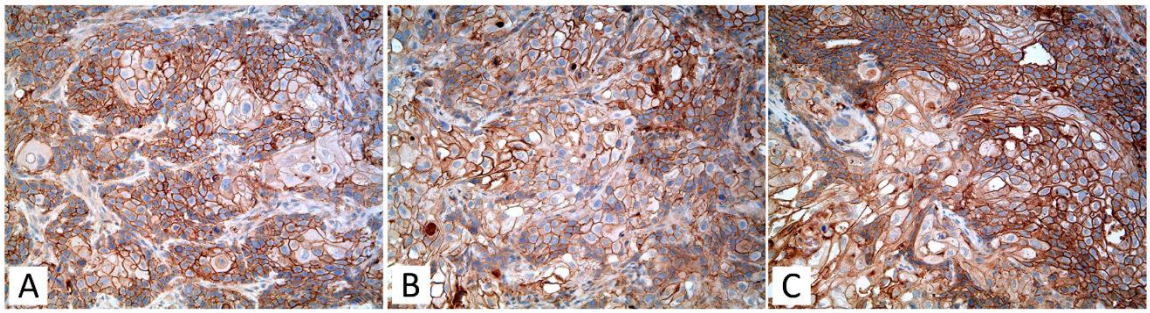

Figure 3.22 E-cadherin is strongly positive in IP heterotransplant tumors. A) As#1, B) As#3, C) Cd#1. E-Cadherin is strongly positive in the tumor cells from all 3 IP tumors, with staining pattern similar to its subcutaneous counterparts. Magnification 200X.

The levels of N-cadherin mRNA were then compared to the human bladder cancer cell lines J82 and TCCSUP, which have been previously characterized as mesenchymal, and the epithelial bladder cancer RT4 (Figure 3.23). The UROtsa isolates As#6 and Cd#5 highly expressing N-cadherin displayed levels of N-cadherin comparable to the cell lines J82 and TCCSUP. In fact, As#6 demonstrated higher N-cadherin expression than the human bladder cancer cell lines. However, RT-PCR with a different set of primers which detect all splice variants of N-cadherin found that the cell lines J82 and TCCSUP contain higher levels of total N-cadherin mRNA in comparison to the UROtsa isolates As#6 and Cd#5 (Appendix, Figure 5.1), suggesting that the human bladder cancer cell lines utilize alternative splice variants to a greater extent.

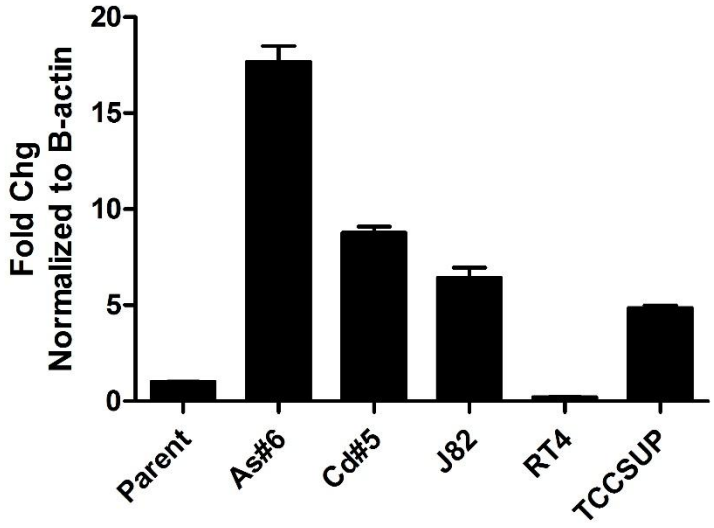

Figure 3.23 N-cadherin mRNA is expressed in the transformed UROtsa isolates Cd#5 and As#6 at similar or higher levels than the mesenchymal-like bladder cancer cell lines J82 and TCCSUP. PCR analysis of N-cadherin expressed as fold change normalized to β-actin. PCR results represent Mean ±SEM of triplicate determinations.

To further characterize the EMT state of As^{3+}- and Cd^{2+}-transformed UROtsa cells, the expression of the pro-EMT transcription factors Twist, Snail, Slug, Zeb1, and Zeb2 were measured at the mRNA level *in vitro*. Expression of Twist was significantly increased five to 15-fold in both the As^{3+} and Cd^{2+} isolates compared to parent UROtsa cells (Figure 3.24). Snail mRNA was significantly induced in As^{3+}-transformed isolates relative to parent, with the exception of isolate #4, which was dramatically increased (Figure 3.25.A). Induction was also seen at a similar level in the Cd^{2+}-transformed UROtsa cells (Figure 3.25B).

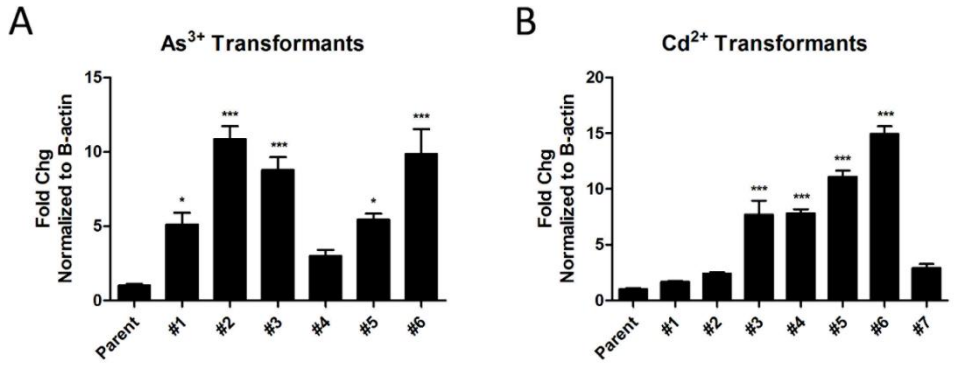

Figure 3.24 Twist expression is induced in As^{3+} and Cd^{2+} isolates. A) Real time RT-PCR analysis of Twist in parent UROtsa cells and A) As^{3+} isolates, and B) Cd^{2+} isolates expressed as fold change normalized to β-actin. PCR results represent Mean ±SEM of triplicate determinations. *p<0.05, **p<0.01, ***p<0.001

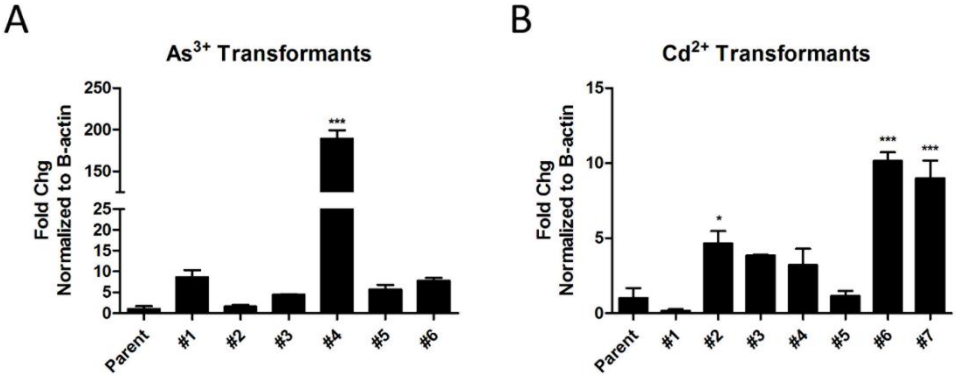

Figure 3.25 Snail expression is induced in As^{3+} and Cd^{2+} isolates. A) Real time RT-PCR analysis of Twist in parent UROtsa cells and A) As^{3+} isolates and B) Cd^{2+} isolates expressed as fold change normalized to β-actin. PCR results represent Mean ±SEM of triplicate determinations. *p<0.05, **p<0.01, ***p<0.001

Immunohistochemistry was performed for Snail on heterotransplant tumors originating from the transformed isolates injected IP (Figure 3.26). The tumors deep within the abdominal cavity (retroperitoneum or around kidney) from all 3 mice showed moderate or moderate to strong staining of Snail (Figure 3.26.B, D, F), while the staining of Snail is weaker in the superficial tumor in peritoneum from the same mice (Figure 3.26.A, C, E). Snail staining was strongest at the center of the tumor nests in the more differentiated cells, while weaker at the periphery.

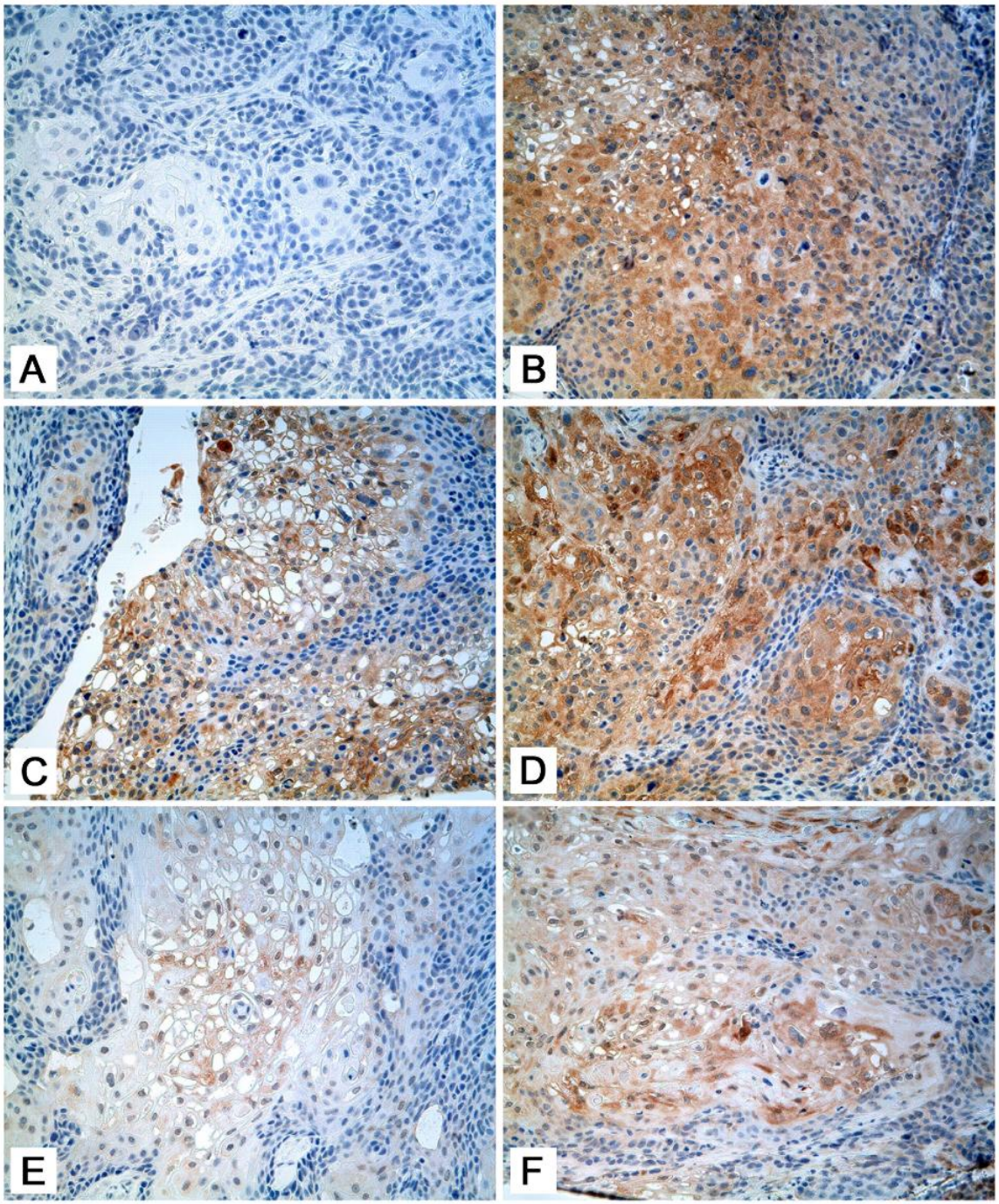

Figure 3.26 Immunostaining for Snail is positive in IP tumors derived from As^{3+} and Cd^{2+} isolates. As#1 tumor located A) at peritoneum, B) deep in abdominal cavity near kidney. As#3 tumor located C) at peritoneum, D) deep in abdominal cavity. Cd#1 tumor located E) at peritoneum, F) deep in abdominal cavity. The positive staining of Snail is mainly located in the center of the tumor nests, the cells that are relatively well differentiated with more cytoplasm. The less differentiated cells at the periphery are almost negative for Snail or only show very weak staining. Magnification 200X.

Vimentin expression was then considered, as it is a common marker for mesenchymal cells. The majority of As^{3+} isolates showed unchanged levels of Vimentin mRNA, with the exception of a significant decrease in As#1, and significantly increased expression in As#5 (Figure 3.27.A). In Cd^{2+}-transformed UROtsa cells, Vimentin was significantly reduced in most isolates (Figure 3.27.B). Analysis of the pro-EMT transcription factors Slug, Zeb1, and Zeb2 was also performed at the mRNA level, though no expression was detected.

Transcription factor 4 (TCF4), is an E2-2 protein recently associated with EMT (Sobrado et al., 2009). Interestingly, expression of TCF4 mRNA was significantly enhanced in most As^{3+} isolates about 10 to 50-fold compared to parent UROtsa cells(Figure 3.28.A). TCF4 was similarly induced in the Cd^{2+} transformants, to a slightly lesser extent (Figure 3.28.B).

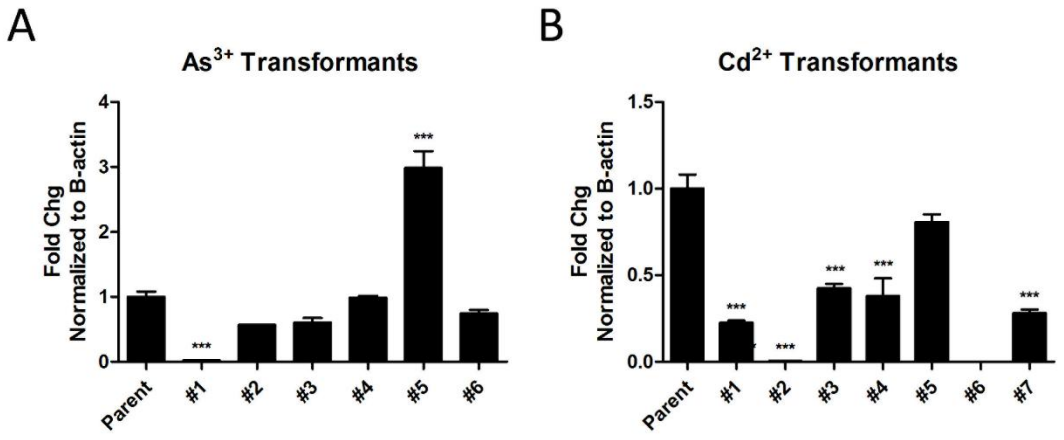

Figure 3.27 Vimentin expression is unaltered in As^{3+}-transformed UROtsa cells, while induced in Cd^{2+} isolates. A) Real time RT-PCR analysis of Vimentin in parent UROtsa cells and As^{3+} isolates expressed as fold change normalized to β-actin. B) Real time RT-PCR analysis of Vimentin in parent UROtsa cells and Cd^{2+} isolates expressed as fold change normalized to β-actin. PCR results represent Mean ±SEM of triplicate determinations. *p<0.05, **p<0.01, ***p<0.001

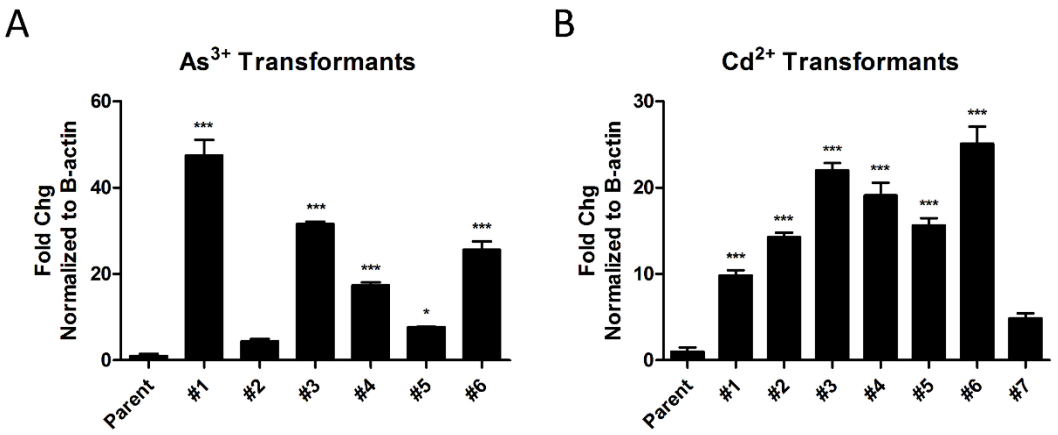

Figure 3.28 TCF4 expression is induced in As^{3+} and Cd^{2+} isolates. A) Real time RT-PCR analysis of TCF-4 in parent UROtsa cells and As^{3+} isolates expressed as fold change normalized to β-actin. B) Real time RT-PCR analysis of TCF-4 in parent UROtsa cells and Cd^{2+} isolates expressed as fold change normalized to β-actin. PCR results represent Mean ±SEM of triplicate determinations. *p<0.05, **p<0.01, ***p<0.001

Other EMT-associated genes were evaluated at the mRNA level. STEAP1, or six transmembrane epithelial antigen of the prostate 1, expression was induced in Cd^{2+}-transformed UROtsa cells *in vitro* and in a number of SC tumors (Figure 3.29.B and D). STEAP1 was less consistently induced in the As^{3+} transformants, though it was elevated in a number of isolates *in vitro* and *in vivo* (Figure 3.29.A and C). STEAP1 is considered to increase during EMT, though further experimental evidence is required to confirm its role in EMT. Occludin (OCLN), a component of tight junctions, is typically decreased during EMT (Ikenouchi, Matsuda, Furuse, & Tsukita, 2003). However, in As^{3+}- and Cd^{2+}-transformed UROtsa cells, occludin was increased in many isolates *in vitro* and in SC tumors (Figure 3.30). Interleukin 1 receptor antagonist, or IL1RN, is another gene downregulated during EMT, though its expression was unchanged in As^{3+}-transformed UROtsa cells and significantly decreased in Cd^{2+} transformants (Figure 3.31).

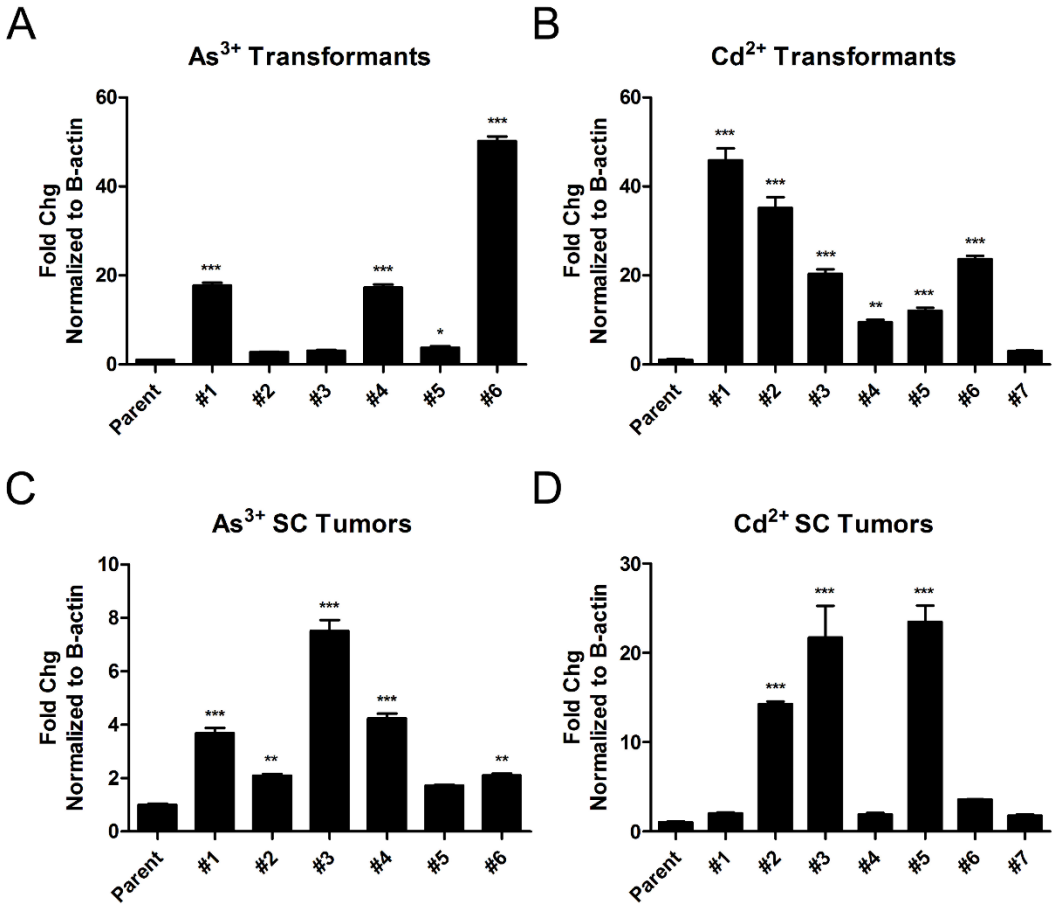

Figure 3.29 STEAP1 is consistently induced in Cd^{2+}-transformed UROtsa cells *in vitro* and maintained in some subcutaneous tumors. Real time RT-PCR analysis expressed as fold change over parent normalized to β-actin in A) As^{3+}-transformed UROtsa cells, B) Cd^{2+}-transformed UROtsa cells, C) SC tumors derived from As^{3+} transformants and D) SC tumors derived from Cd^{2+} transformants. Results represent Mean ±SEM of triplicate determinations. *p<0.05, **p<0.01, ***p<0.001

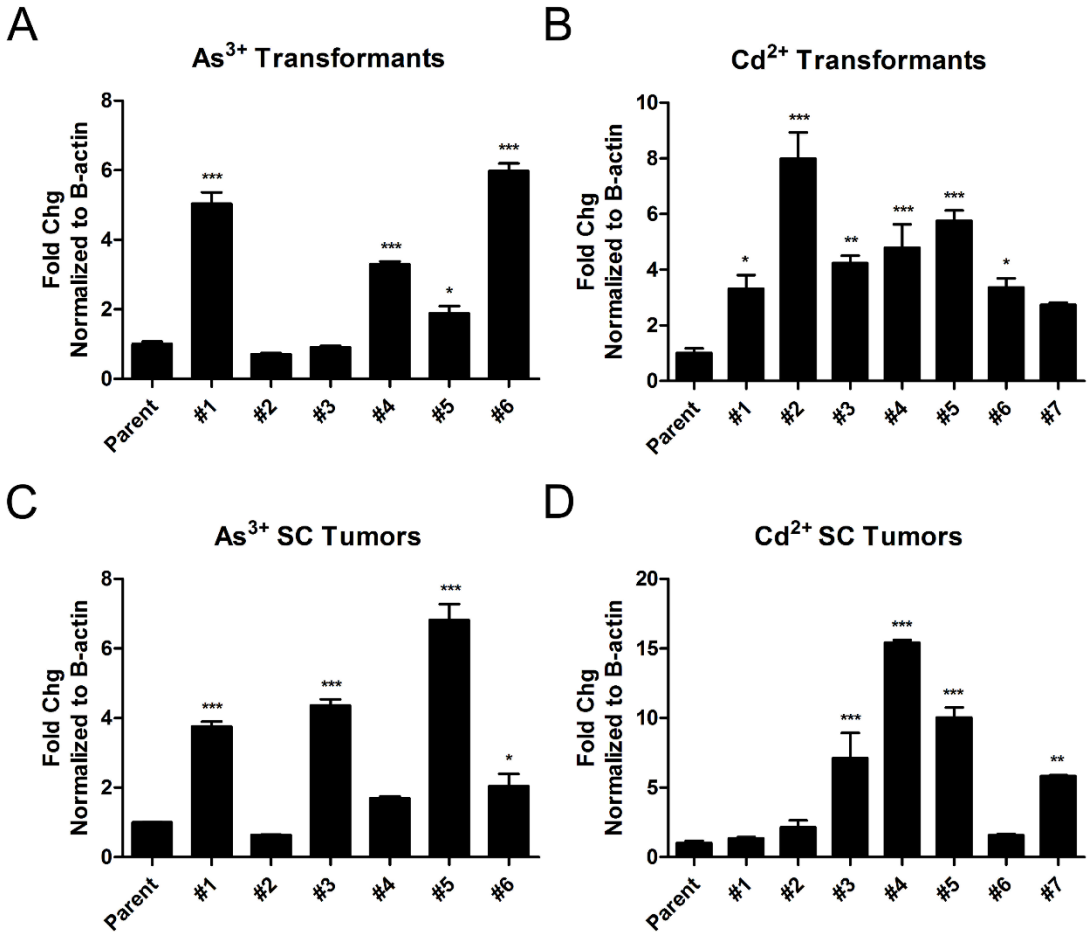

Figure 3.30 OCLN is consistently induced in Cd^{2+}-transformed UROtsa cells *in vitro* and maintained in select subcutaneous tumors. Real time RT-PCR analysis expressed as fold change over parent normalized to B-actin in A) As^{3+}-transformed UROtsa , B) Cd^{2+}-transformed UROtsa cells, C) SC tumors derived from As^{3+} transformants and D) SC tumors derived from Cd^{2+} transformants. Results represent Mean ±SEM of triplicate determinations. *p<0.05, **p<0.01, ***p<0.001

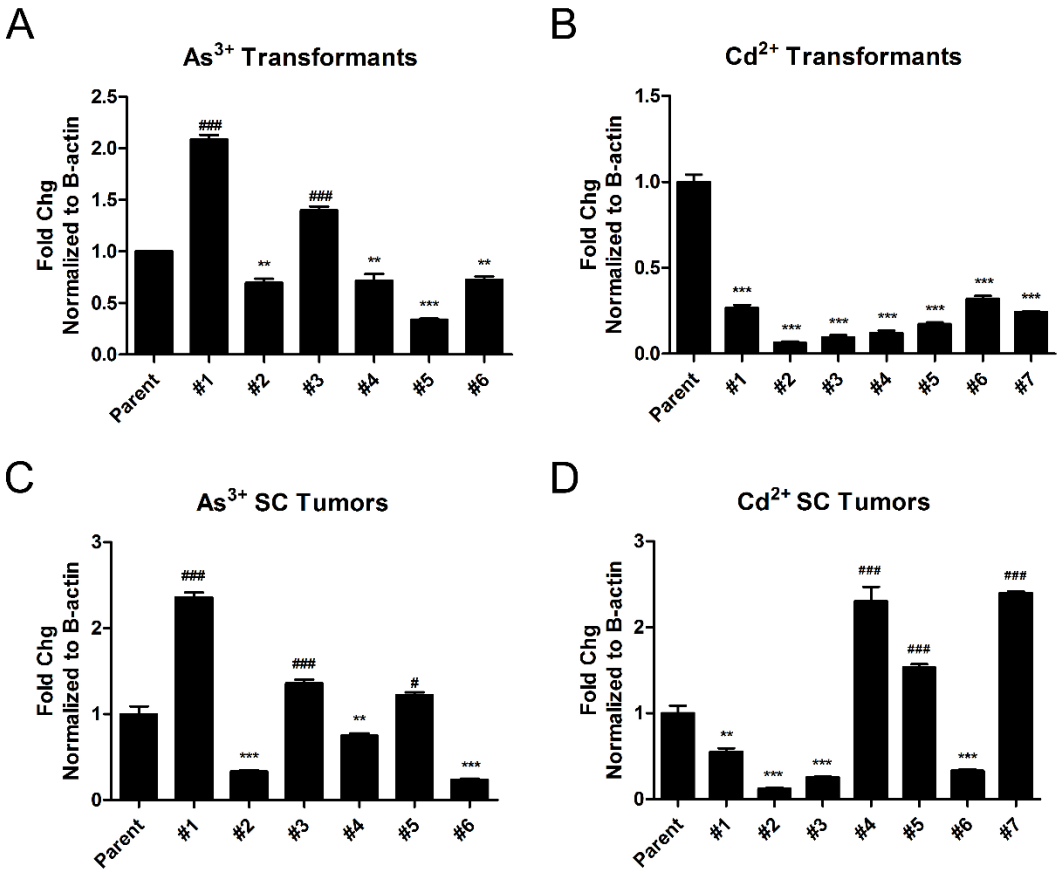

Figure 3.31 IL1RN is varied in Cd^{2+}-transformed UROtsa cells *in vitro* and *in vivo*. Real time RT-PCR analysis expressed as fold change over parent normalized to B-actin in A) As^{3+}-transformed UROtsa cells, B) Cd^{2+}-transformed UROtsa cells, C) SC tumors derived from As^{3+} transformants and D) SC tumors derived from Cd^{2+} transformants. Results represent Mean ±SEM of triplicate determinations. *p<0.05, **p<0.01, ***p<0.001 # indicates significantly induced $^{\#}p<0.05$, $^{\#\#}p<0.01$, $^{\#\#\#}p<0.001$.

CHAPTER IV

DISCUSSION

Model Systems of Bladder Cancer *in vivo*

The fact that N-cadherin expression is maintained in IP, but not SC heterotransplants suggests that tumor microenvironment may play a role in regulation of N-cadherin and in tumor development in general. While expression of N-cadherin is highly induced *in vitro* in As^{3+}- and Cd^{2+}-transformed UROtsa cells, the cell lines may not have maintained their molecular characteristics upon subcutaneous injection due to the lack of a supportive environment for progression through EMT. When injected IP, however, the environment more closely replicates that of bladder cancer cells progressing through EMT and metastasis, which promotes the maintenance of N-cadherin expression in transformed UROtsa cells. Animal models for bladder cancer are scarce in comparison to those of other cancers (Kobayashi, Owczarek, McKiernan, & Abate-Shen, 2015).

The compatibility of *in vitro* and animal models is an issue that is overlooked in a number of cancers. Subcutaneous xenografts are a popular system due to the ease of cell transplant and observation of tumor formation and growth. However, numerous clinical trials for cancer therapeutics based on testing in SC tumor models have proven unsuccessful (Suggitt & Bibby, 2005). In a study of colon cancer, subcutaneous tumors demonstrate sensitivity to doxorubicin, while lung metastases developed by tail vein injection of cancer cells are resistant. Further, expression of the genes MDR1 and p-glycoprotein is enhanced in the resistant metastases compared to the subcutaneous tumors (Dong et al., 1994). Human tumor xenografts of ovarian carcinoma also display site-specific sensitivity to the anti-cancer drug flavone acetic acid. Intraperitoneal tumors fail

to respond to treatment, while subcutaneous tumors show growth inhibition (Pratesi, Manzotti, Tortoreto, Audisio, & Zunino, 1991). Interestingly, the majority of studies involving tumor heterotransplants only observe the effects of drug treatment on tumor formation and growth, and do not investigate whether the compounds targeted by the drug in *in vitro* studies are present or altered in the animal model. Further, while some studies compare xenograft and original tumor histology and general appearance, molecular characterization rarely occurs. The xenograft lines UCRU-BL-12 and UCRU-BL-14 are an example in which the original SC tumors were histologically similar, but following serial implantations, differing DNA profiles developed with the emergence of aneuploid populations (Russell et al., 1986). In an orthotopic model of bladder cancer, expression of various integrins and MMPs is altered compared to *in vitro* levels in RT4 cells (Imao et al., 1999). Proper pairing between *in vitro* cell lines and animal models may result in higher success rates at clinical trials and the development of biomarkers of better predictive value for a number of cancers in addition to bladder cancer.

Some success has been found in other heterotransplant models. While subcutaneous injection of cancer cells encapsulates the tumor and reduces the potential for metastasis (Ahlering, Dubeau, & Jones, 1987; Kubota, 1994), injection of cells into the peritoneum is considered to more closely replicate the environment into which bladder, prostate, ovarian, and gastric cancers initially metastasize (Garson, Shaw, Clark, Yao, & Vanderhyden, 2005). In fact, the bladder cancer cell line RT4 and endometrial carcinoma line EJ shows little metastatic potential when transplanted subcutaneously. However, when the same lines are injected via tail vein, metastatic sites develop. When injected orthotopically to the bladder lumen, the cells develop tumors similar in histology

and behavior to their tumors of origin (C. Zhang, Awasthi, Schwarz, & Schwarz, 2013). The development of a renal capsule model of bladder cancer using As^{3+}- and Cd^{2+}-transformed UROtsa cells is currently in development.

Bladder Cancer Stem Cells

Heterogeneity among cells within the transformed isolates may also contribute to dissimilar N-cadherin expression in tumor heterotransplants versus *in vitro* cultures. The UROtsa cell line and its transformants are not clonal populations. During transformation with sodium arsenite and cadmium chloride, the cells experienced numerous phases of massive cell death followed by regrowth from surviving cells, in which the surviving clones were not isolated for clonal expansion. Examination of cellular heterogeneity within each isolate had not been performed previously.

To quantitatively determine the number of cells positive for N-cadherin, flow cytometry was performed on As^{3+} and Cd^{2+} isolates expressing low, medium, and high N-cadherin as indicated by Western blot. Results of the flow cytometry experiments found that N-cadherin was only detected on the highest expressing isolate, As#6, and that 98.5% of the cells were positive for the protein. This is contrary to the findings from Western blot analysis, suggesting that the levels initially observed included both intracellular and membrane-bound N-cadherin, while the flow cytometry only detected membrane-bound protein. Additionally, Western blot analysis with the antibody used for flow cytometry demonstrated lower sensitivity, indicating that antibody did not detect the N-cadherin on the the moderately-expressing isolates As#3 and Cd#1.

To further investigate the hypothesis that population heterogeneity was at play in the As^{3+}- and Cd^{2+}-transformed UROtsa, the presence of tumor-initiating cells, or cancer

stem cells, was investigated were identified within As^{3+}- and Cd^{2+}-transformed UROtsa cells, suggesting that a unique subpopulation of cells *in vitro* are responsible for tumor formation *in vivo* which may then display different molecular characterization than observed in culture.

Microspheres were isolated by cell culture in serum-free media at low density on low-adherence substrates. Following microsphere, or urosphere, formation, self-renewal was confirmed by the ability to reform colonies following multiple rounds of dissociation (data not shown). The microspheres were able to form tumors following IP injection into nude mice, further validating their stem cell-like characteristics (data not shown).

Interestingly, the putative stem cells display significantly reduced N-cadherin expression compared to their counterparts grown in serum-free media as evaluated by RT-PCR, even in As^{3+} isolate #6, which shows the most dramatic increase in N-cadherin compared to the parent UROtsa cell line, with 98.5% of cells positive for N-cadherin by flow cytometry analysis. This suggests that a small subset of N-cadherin-negative cells act as tumor-initiating cells to develop tumors *in vivo*, resulting in the lack of N-cadherin expression observed.

Bladder cancer stem cells were first isolated as side populations from primary cultures of low-grade papillary urothelial carcinoma. Side population (SP) is defined by the ability to efflux the DNA-binding dye Hoescht 33342, and has been further characterized as a functional marker for stem cells in numerous normal and cancerous tissues. Another marker for bladder cancer stem cells is $EMA^{-}CD44v6^{+}$, which was initially identified in primary cultures of low-grade papillary carcinoma. This cell population possesses the ability for anchorage-independent colony formation, self-

renewal, and proliferation *in vitro* (Y. M. Yang & Chang, 2008). Cancer stem cells demonstrate an enhanced ability to form tumors *in vivo* that replicate the original tumor. In a study by Chan et al., $CD44^+$ cells isolated from patient tumors display increased ability to form tumors following SC injection into nude mice compared to $CD44^-$ cancer cells. Further, the $CD44^+$ cells are able to be serially transplanted for three additional passages (Chan et al., 2009).

Cancer stem cells have been isolated from immortalized bladder cancer lines, as well. Side populations were identified in the bladder cancer cell lines SW780, UM-UC-6, UM-UC-6dox, 253J-BV, and HT-1197 (Jun, Peng, Zi, Wei, & Xiang, 2008). The cells demonstrate higher colony-forming efficiency in soft agar than non-SP cells, as well as tumor formation in subcutaneous xenografts. Expression of the ABC transporters ABCG2 and MDR1 is significantly increased in SP cells, supporting their enhanced efflux capability. Further, the stem cell genes Oct-4 and Bmi-1 are also elevated in the SP cells. Stem-like cells have also been identified in SP cells from the transitional cell carcinoma cell line T24. The side populations display increased cell growth and elevated expression of ABCG2 expression, a marker of stem cells (Ning et al., 2009). Stem cell-like compartments have been identified in heterotransplant models of bladder cancer. Human SW780 urothelial carcinoma xenografts derived from high-grade invasive carcinoma demonstrate basal-like $CK17^+$ staining in cells at the tumor-stroma interface and CK20 expression within the interior of tumor nodules which resembles staining seen in superficial cells of the normal urothelium (X. He et al., 2009).

Aldehyde dehydrogenase 1 expression has also emerged as a marker for bladder cancer stem cells. $ALDH1A1^+$ cells isolated from the bladder cancer cell lines RT4,

HTB-9, and HTB-4 display significantly higher colony forming efficiency which is reversed upon ALDH1A1 knockdown. Further, anchorage-independent growth is impaired in cells with reduced ALDH1A1. $ALDH1A1^{+}$ cells demonstrat increased *in vivo* tumorigenicity when compared with $ALDH1A1^{-}$ cells, and the tumors are able to be regenerated for at least three cycles. In human bladder cancer specimens, ALDH1A1 is not observed in normal urothelium, though it is colocalized with tumor cells positive for the stem cell marker CD44. In addition, ALDH1A1 status is significantly correlated with grade and stage of bladder carcinoma, incidence of recurrence, progression, and inversely associated with survival (Y. Su et al., 2010).

There is no consensus on bladder cancer stem cell markers (van der Horst, Bos, & van der Pluijm, 2012). Other stem cell markers that have been utilized include VEGFR2, CD133, Sox2, Nanog, and 67LR (Goodwin Jinesh, Willis, & Kamat, 2014; van der Horst et al., 2012). For the purpose of identifying stem cell-like populations with the UROtsa cell line and its transformants, the markers ALDH1A1 and CD44 were used. RT-PCR analysis demonstrated increased expression of ALDH1A1 mRNA, though not CD44 in urospheres compared to the transformants grown in serum-free media.

In light of the theory that N-cadherin-negative stem cells are forming subcutaneous tumors lacking N-cadherin expression, why might these same cells create tumors in the peritoneum that regain N-cadherin? Once again, tumor microenvironment appears to play a role. In small cell lung cancer, tumor specimens serially propagated *in vivo* lose expression of tumor-specific genes when transitioned to cell culture conditions. This change in gene expression is not reversed upon regraftment into mice, implicating permanent changes in cell phenotype dependent upon tumor environment (Daniel et al.,

2009). The progression of cells through EMT to metastasis specifically is also regulated by environment (Polyak & Weinberg, 2009). A study inducing EMT in hamster cheek pouch carcinoma-1 cells by TGF-β found that both mesenchymal-like and epithelial-like cells establish tumors upon subcutaneous injection. Only cells induced to undergo EMT invade adjacent tissue, and neither cell type metastasizes to the lung. However, upon intravenous injection only the epithelial cells develop lung metastases. Subcutaneous injection of a mixture of both epithelial and EMT-induced cells allows invasion and lung metastasis of epithelial cells (T. Tsuji et al., 2008). In another study utilizing prostate and bladder cancer cell lines, tumor-initiating cells demonstrating epithelial characteristics are able to metastasize and colonize distant sites, while cells with a mesenchymal phenotype do not have this ability. Instead, the mesenchymal-like tumor-initiating cells show enhanced local invasiveness when compared to the epithelial cells (Celià-Terrassa et al., 2012). This suggests that the tumor microenvironment plays a role in cancer progression to metastasis, and that both epithelial and mesenchymal stem cells promote cancer progression (Polyak & Weinberg, 2009). Lastly, cancer stem cells in particular are dependent upon their surrounding conditions for maintenance of the tumor-initiating phenotype. Heterogeneity has been identified in stem-like populations isolated from human bladder transitional cell carcinoma. These cells are positive for the stem cell markers CD133, Oct-3/4, and nestin, and display increased proliferation and self-renewal. However, upon continued culture the cells gradually loset their proliferative and morphological characteristics and are unable to induce xenograft tumors *in vivo* (Bentivegna et al., 2010). These studies suggest that N-cadherin expression in tumor

heterotransplants requires an environment supportive of EMT, and that tumor stem cells are also vulnerable to changes in microenvironment.

The origins of cancer stem cells remain unclear. They may arise from normal stem or progenitor cells (Feng Li, Tiede, Massagué, & Kang, 2007), or may be derived from differentiated cells that undergo a series of oncogenic hits to acquire self-renewal ability and immortality (Clarke et al., 2006). However, numerous studies have found that heavy metals can cause normal stem cells to develop a cancer stem cell-like phenotype. Normal stem cells from human prostate acquire cancer stem cell-like characteristics when co-cultured with transformed malignant epithelial cells. However, the phenotype is only adapted when stem cells are cultured with arsenic-transformed, but not *N*-methyl-*N*-nitrosourea-transformed epithelial cells (Yuanyuan Xu et al., 2013). In human keratinocyte HaCaT cells, transformation by low dose exposure to sodium arsenite occurrs via EMT, followed by the acquisition of a malignant cancer stem cell-like phenotype (R. Jiang et al., 2013). Human pancreatic ductal epithelial cells exposed to chronic cadmium induce non-adherent spheroid formation and expression of the stem cell markers OCT4 and CD44, as well as a cancer phenotype indicated by enhanced invasion and expression of the pancreatic cancer marker S100P (Qu, Tokar, Kim, Bell, & Waalkes, 2012). Arsenic induces EMT and malignant transformation in human bronchial epithelial cells, as well as cancer stem cell-like characteristics, which are directly regulated by HIF-2α (Yuan Xu et al., 2012).

Human prostate stem cells show enhanced resistance to arsenite-induced cytotoxicity compared to the mature parental cell line, and possess hyper-adaptability to arsenic. Further, experiments by Tokar et al. indicate that exposure to arsenic induces

greater numbers of free-floating spheres in the parental prostate cell line than cadmium or *N*-methyl-*N*-nitrosourea (Tokar, Qu, et al., 2010). Additional studies prove that arsenite exposure transforms normal prostate stem cells to a malignant cancer stem cell-like phenotype with high invasion capacity and loss of contact inhibition. The cells are also able to form tumors when heterotransplanted that were highly aggressive, containing immature epithelial- and mesenchymal-like cells (Tokar, Diwan, & Waalkes, 2010). As previously mentioned, during As^{3+}- and Cd^{2+}-induced transformation in UROtsa cells, a small percentage of cells survived numerous rounds of cytotoxicity. It would prove quite interesting to isolate those cells and determine whether they contain cancer stem cell markers, as well as the changes that occur with each round of toxicity.

Future experiments using flow cytometry to determine the expression of cancer stem cells including ALDH1A1, CD44, and CD133 will be necessary to establish that the microspheres indeed contain cancer stem cells. Additional studies to determine the expression E-cadherin and N-cadherin in the cancer stem cell population are also required, as it may be that an epithelial tumor-initiating cell population establishes IP tumors, while an N-cadherin-expressing population develops tumors subcutaneously.

In order to address the role of microenvironment on N-cadherin expression, the renal capsule model will be utilized. Grafting cells in the renal capsule is more efficient than subcutaneous injections and has good predictive value of clinical response (Baiocchi, Biffoni, Ricci-Vitiani, Pilozzi, & De Maria, 2010; Suggitt & Bibby, 2005). Further, normal urothelial cells injected into the renal capsule are able to establish and grow, providing an *in vivo* control for comparison with tumors derived from As^{3+}- and Cd^{2+}-transformed UROtsa cells (Oottamasathien et al., 2006).

Characterization of EMT in UROtsa Transformants

Since N-cadherin induction is a common sign of the epithelial-to-mesenchymal transition, the As^{3+}- and Cd^{2+}-transformed UROtsa cells where characterized for additional markers of EMT. No changes in E-cadherin were seen at the mRNA or protein level in the transformed UROtsa cells. Further, E-cadherin did not appear to replace N-cadherin at the plasma membrane, but instead was co-expressed. While E-cadherin is typically replaced by N-cadherin during EMT in the bladder, there are cases in which N- and E-cadherin are co-expressed, and that when this occurs, the functional properties of N-cadherin dominate over E-cadherin. In a study by Rieger-Christ and colleagues of a panel of bladder cancer cell lines, bladder cancers expressing high levels of E-cadherin with no N-cadherin display little invasive capacity, and those with high N-cadherin and reduced E-cadherin demonstrate high levels of invasiveness. Interestingly, when N- and E-cadherin are co-expressed, invasive capacity is elevated in comparison with N-cadherin-negative cell lines, though not to the extent of cell lines with high N-cadherin and low E-cadherin (Kimberly M Rieger-Christ et al., 2004). This implies that the pro-migratory property of N-cadherin overcomes the pro-epithelial effects of E-cadherin when co-expressed, allowing EMT progression with enhanced motility and invasion. This has also been observed in breast cancer, in which exogenous induction of N-cadherin in the MCF-7 cell line induces higher migration rates and increased invasion in Matrigel. When injected into nude mice, the cells co-expressing N- and E-cadherin are able to form metastatic tumors expressing both cadherins (Hazan, Phillips, Qiao, Norton, & Aaronson, 2000).

The pattern of progression through EMT, that is, the timing of various markers and changes in behavior, has not been well-characterized in cancer. It is often dependent upon the cell type observed and the agent inducing the transition. N-cadherin induction has been correlated with tumor invasiveness, suggesting that it is upregulated late in EMT. When compared to the epithelial human bladder cancer cell line RT4, N-cadherin induction in As^{3+}- and Cd^{2+}-transformed UROtsa cells was elevated. However, the level of induction relative to mesenchymal bladder cancers J82 and TCCSUP depended upon the inclusion of N-cadherin splice variants, in which the human bladder cancer cell lines appear to utilize alternative splicing. Analysis of protein expression will ultimately determine whether N-cadherin levels in the UROtsa transformants are indeed at the extent of that seen in J82 and TCCSUP. Elevated Vimentin expression is often associated with late stage EMT; however in the UROtsa transformants it was not induced. Further, transformed UROtsa cells maintained an epithelial appearance (Sens et al., 2004). Interestingly, whereas N-cadherin demonstrates an important role for cell motility in a study of TGF-β1-induced EMT in mammary epithelial cells, it does not affect the morphological changes that accompany EMT. siRNA-mediated inhibition of N-cadherin expression does not alter cell morphology, while motility is decreased, as seen in wound-healing and transwell motility assays (M. Maeda, Johnson, & Wheelock, 2005). However, in the case of As^{3+}- and Cd^{2+} transformed UROtsa cells, only a few isolates demonstrate increased migration which do not correlate to N-cadherin expression and the transformed cells do not have increased invasive ability (J Larson, 2012). This suggests that while N-cadherin, Twist, and Snail are significantly elevated in transformed UROtsa cells, the cells are in the initial states of EMT. There are no models of this type for

bladder cancer, suggesting that the As^{3+}- and Cd^{2+}-transformed UROtsa cells will be of benefit for further characterization of the patterns of gene expression and behavioral changes in bladder cancer-associated EMT. While arsenite exposure did not induce N-cadherin expression in parent UROtsa cells, expression was elevated with increased duration of cadmium exposure, providing a model system for the progression of EMT in bladder. Future experiments could include analysis of other EMT markers throughout this exposure period. The miR-200 family should also be explored in this system, as its expression has been associated with early stages of EMT in bladder cancer.

Other markers of EMT were investigated in As^{3+}- and Cd^{2+}-transformed UROtsa cells at the mRNA level, as well. The pro-mesenchymal transcription factor Twist was significantly induced in both As^{3+} and Cd^{2+} transformants. Interestingly, phosphorylated Twist activates transcription of TGF-β2 (Xue et al., 2012), an EMT-inducer that was upregulated on the As^{3+} array and to a lesser extent on the microarray for Cd^{2+} transformants (Gao, Zhu, Nilsson, & Sundfeldt, 2014; Garrett et al., 2014; Medici, Hay, & Olsen, 2008). Snail, another transcription factor promoting EMT, was also significantly elevated. Vimentin expression was mostly unchanged in As^{3+}-transformants, though reduced in the majority of Cd^{2+} isolates. Transcription factor 4, or TCF4, was significantly induced in As^{3+}- and Cd^{2+}-transformed UROtsa cells. This class 1 bHLH factor E2-2 protein is not to be confused with T-cell-specific transcription factor 4 (TCF7L2), a factor associated with the Wnt signaling pathway. This transcription factor is relatively unexplored in EMT, though studies have proven that it is a potent inducer of EMT in MDCK cells (Sobrado et al., 2009). Additional transcription factors Zeb1 and

Zeb2 were measured, though expression was undetectable or unchanged (data not shown).

Other genes associated with EMT that were investigated included STEAP1, OCLN, and IL1RN. STEAP1, or six-transmembrane epithelial antigen of the prostate 1, is normally expressed at the membrane in low levels in bladder, but it is significantly upregulated in a number of bladder cancer cell lines, including UM-UC03, TCCSUP, and J82 (Hubert et al., 1999). In Cd^{2+}-transformed UROtsa cells, STEAP1 was significantly induced *in vitro*, and numerous isolates demonstrated elevated expression in SC tumors. STEAP1 was less consistently induced in As^{3+} transformants *in vitro* and *in vivo*. STEAP1 appears to play a role in tumor growth and intercellular communication, as knockdown in prostate cancer and oral squamous cell carcinoma xenografts significantly reduces tumor volume and inhibited intercellular communication *in vitro* (T. Yamamoto et al., 2013). Further study of STEAP1 expression in bladder cancer is needed, as meta-analysis of gene expression data from 40 human tumor types revealed that STEAP1 is significantly induced in 11 cancers, but bladder cancer is not one of them (Moreaux, Kassambara, Hose, & Klein, 2012). STEAP1 is induced during progression through EMT, though further evidence is required to confirm this association.

Occludin downregulation is observed in the epithelial-to-mesenchymal transition. Occludin is an integral membrane protein localized at tight junctions. In a Snail-induced model of EMT in mouse epithelial cells, Snail directly regulates occludin to decrease its expression (Ikenouchi et al., 2003). However, occludin was not reduced in As^{3+} and Cd^{2+} transformants. In fact, expression was significantly upregulated in Cd^{2+}-transformed UROtsa cells *in vitro*, and numerous SC tumors overexpressed occludin. Evaluation of

occludin expression at the protein level, as well as other tight junction proteins, may indicate whether loss of tight junction functionality is occurring in this bladder cancer model.

Interleukin 1 receptor antagonist (IL1RN) is also considered to decrease during EMT, though evidence is limited. In Cd^{2+}-transformed UROtsa cells, IL1RN expression was significantly reduced, though results were varied in SC tumors. In As^{3+}-transformants, IL1RN was relatively unchanged. Interestingly, IL1RN gene polymorphism is associated with increased risk of bladder cancer (Ahirwar, Agrahari, Mandhani, & Mittal, 2009; Bid, Manchanda, & Mittal, 2006; Bozdoğan et al., 2014). Further, reduced IL1RN expression is significantly correlated with aggressive bladder cancer (Worst et al., 2014).

Other groups have determined the EMT state of numerous bladder cancer cell lines. The TCCSUP, RT4, and J82 cell lines have been reviewed here (Table 4.1). The J82 cell line, also known as HTB-1, is derived from a poorly differentiated invasive transitional cell carcinoma of Stage T3 (O'Toole, Price, Ohnuki, & Unsgaard, 1978). It is the most mesenchymal of the three lines, with strong N-cadherin expression, low levels of E-cadherin, induced Vimentin and increased levels of the transcription factors Twist, Snail, Slug, Zeb1, and Zeb2. TCCSUP, or HTB-5, originates from Stage 4 transitional cell carcinoma and also contains mesenchymal characteristics with increased N-cadherin and pro-mesenchymal transcription factors, but without loss of E-cadherin, and does not display elevated Vimentin. RT4, or HTB-2, is the most epithelial of the three cell lines, and was derived from transitional cell papilloma. The cell line shows little induction of N-cadherin, strong E-cadherin, no Vimentin expression, and varied levels of pro-

mesenchymal transcription factors (Baumgart et al., 2007). While further experiments are required to fully compare the As^{3+}- and Cd^{2+}-transformed UROtsa cells to these cell lines, they appear to be most similar to the TCCSUP cell line. Differences include the expression of Zeb1, Zeb2, Slug, and P-cadherin. Zeb1, Zeb2, and Slug were expressed at barely detectable levels which were unchanged in the As^{3+}- and Cd^{2+}-transformed UROtsa cells (data not shown). P-cadherin was expressed, through changes in expression were variable in the transformed cells (Appendix 5.1).

By characterizing the early and late events of EMT in bladder tumors, biomarkers may be discovered which could earlier predict cancers with metastatic potential. It may be that As^{3+}- and Cd^{2+}-induced EMT utilizes a different pathway to induce EMT, or that TCCSUP represent a later stage. Analysis of human bladder cancer tumors from arsenic-endemic regions may further establish the role of N-cadherin as a marker specific for heavy metal-induced bladder carcinogenesis and the initial stages of EMT.

	TCCSUP	RT4	J82	UROtsa	As^{3+} UROtsa	Cd^{2+} UROtsa	Reference
N-cadherin				-	+	+	Sandquist et al. 2015
	++	-					Hänze et al. 2013
		++	+				Hao et al. 2012
	++		+++				Wallerand et al. 2010
		-	++				Sayan et al. 2009
		-	+++				Wu et al. 2013
	+++	-	+++				Baumgart et al. 2007
E-cadherin				+	+	+	Sandquist et al. 2015
	-	+++					Hänze et al. 2013
			+				Yang et al. 2014
		+++	+				Cheng et al. 2013
	+++		-				Wallerand et al. 2010
		+++	+				Hao et al. 2012
	++	+++	+				Tran et al. 2012
		+++	-				Sayan et al. 2009
		++					Choi et al. 2012
		+++	-				Wu et al. 2013
	-	+++	-				Baumgart et al. 2007
Vimentin				+	+	-	Sandquist et al. 2015
	-	-					Hänze et al. 2013
		+	+++				Cheng et al. 2013
		-					Choi et al. 2012
		-	++				Wu et al. 2013
			+++				Yang et al. 2014
	-	-	+++				Baumgart et al. 2007
Snail				+	++	++	Sandquist et al. 2015
			++				Yang et al. 2014
	++	-	-				Matsui et al. 2012
Zeb1				-	-	-	Sandquist et al. 2015
		-					Cheng et al. 2013
	+++	+	+++				Tran et al. 2012
		-	+++				Sayan et al. 2009
			+				Yang et al. 2014
		-					Choi et al. 2012
Zeb2				-	-	-	Sandquist et al. 2015
	+++	+	+++				Tran et al. 2012
		+	+				Sayan et al. 2009
		-					Choi et al. 2012
Twist				+	++	++	Sandquist et al. 2015
			+++				Yang et al. 2014
		+					Zhang et al. 2007
	+++						Shiota et al. 2010
Slug	-	-	-				Sandquist et al. 2015
		+	+				Cheng et al. 2013
	++	++	+				Matsui et al. 2012
		+	+++				Wu et al. 2013
P-cadherin				+	+	+	Sandquist et al. 2015
	+	+					Mialhe et al. 2000
		+	-				Sayan et al. 2009

Table 4.1 EMT characterization of transformed UROtsa cells with the human bladder cancer cell lines TCCSUP, RT4, and J82. +++ high, ++ moderate, + low, and – no expression.

Regulation of N-cadherin

While the importance of N-cadherin in the epithelial-to-mesenchymal transition has been well established, its regulation is relatively unknown. The transcription factor Twist regulate N-cadherin promoter activity by binding at an E-box within the first intron in prostate cancer cells (Alexander et al., 2006). Further, Twist was a top induced gene in As^{3+}-transformed UROtsa cells and significantly upregulated in Cd^{2+}-transformed isolates as indicated by microarray analysis (Garrett et al., 2014). Twist is a well-known repressor of E-cadherin that participates in EMT; therefore, dual functionality of Twist as both a repressor and inducer of E-cadherin and N-cadherin, respectively, is an attractive possibility that should be explored in a wider variety of cancers.

The potential regulation of Twist by arsenite exposure has not been fully studied. In human bronchial epithelial cells transformed by arsenite, the exposure inducs EMT, including the expression of Twist. Further, Twist upregulation is increased in nonmalignant cells depending upon duration of arsenite exposure, indicating metal-dependent expression. However, cancer cells treated with arsenite show a different response. Arsenic trioxide is an effective treatment for some cancers, including hepatocellular carcinoma. In this cancer, arsenic trioxide reduces cell migration and invasiveness and inhibits EMT by suppressing Twist (G. Z. Wang et al., 2014). In non-small-cell lung cancer, arsenic trioxide-induced cell death is enhanced by inhibition of Twist (Seo et al., 2014). As such, further studies are needed to explore the divergent mechanisms of Twist regulation by arsenite in normal and cancerous cell types. There is less evidence for regulation of Twist by cadmium exposure. In cadmium-treated mice, fibrotic kidney EMT is induced, accompanied by elevated Twist expression (Chakraborty

et al., 2010). It would also be worthwhile to investigate whether Twist is regulating N-cadherin in As^{3+}- and Cd^{2+}-transformed UROtsa cells, considering the fact that E-cadherin expression was unaltered by heavy metal transformation. It may be the case that Twist is acting solely as an inducer of N-cadherin expression, or that other regulatory factors are at play.

N-cadherin expression was altered by treatment with the histone deacetylase inhibitor MS-275, suggesting that acetylation contributes to the regulation of N-cadherin transcription. Exposure to sodium arsenite over 5 passages in the parent UROtsa cell line appeared to induce total levels of histone 4 acetylation at Region 2 of the N-cadherin promoter. Further, histone acetylation state was modified at Region 2 following exposure to MS-275, indicating that this may be a region of regulatory activity for N-cadherin transcription. However, numerous studies have indicated that arsenic reduces histone acetylation globally. Chu *et al.* found that exposure to arsenic reduces global histone acetylation (Chu et al., 2011) and another demonstrated that As(III) and MMA(III) reduce H4K16 acetylation in a time- and dose-dependent manner (Ge et al., 2013; Jo et al., 2009). Experiments with UROtsa cells exposed to longer durations of sodium arsenite and in transformed cells will confirm whether the increase in H4 acetylation at the N-cadherin promoter is a gene-specific change, or if longer exposures to arsenic are needed to elevate histone acetylation at this region.

This work has demonstrated that N-cadherin is induced in As^{3+}- and Cd^{2+}-transformed UROtsa cells, and that a unique early EMT signature may have potential to act as a biomarker of bladder cancer induced by arsenic and cadmium. These studies revealed important findings on the transcriptional regulation of N-cadherin, as well as

histone acetylation at the promoter. N-cadherin induction was recapitulated in an intraperitoneal animal model, though expression was not detected in tumors derived from subcutaneous heterotransplants. Additionally, putative bladder cancer stem cells did not express N-cadherin at high levels. These findings have broad implications in the field of biomarker and cancer research, in which the results of *in vitro* studies are not successful in clinical studies. By incorporating the factors of tumor microenvironment and cell population in the use of animal models, a greater number of cancer biomarkers and therapies may be successfully validated for clinical use.

APPENDIX

Expression of N-cadherin Splice Variants

When all splice variants of N-cadherin mRNA were targeted, N-cadherin expression in UROtsa isolates As#5 and Cd#5 was not to the level of the bladder cancer cell lines J82 and TCCSUP, though expression was elevated compared with the RT4 cell line. The primers here are from Bio-Rad (qHsaCID00015189) and target splice variants ENST00000269141, ENST00000399380, ENST00000418492, ENST00000430882, and ENST00000413878. The splice variants detected by the Qiagen primers used for Figure 3.23 only include NM_001792, XM_005258181, and XM_005258182.

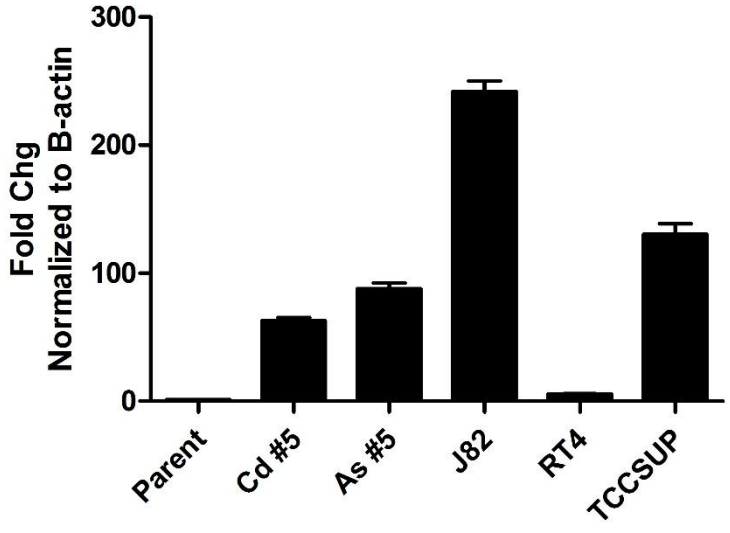

Figure 5.1 Expression of total N-cadherin splice variants in As^{3+}- and Cd^{2+}-transformed UROtsa is lower than that of J82 and RT4 cell lines. RT-PCR analysis of N-cadherin expression in the highest N-cadherin-expressing transformed isolates and three human bladder cancer cell lines. Data expressed as fold change normalized to β-actin. PCR results represent Mean ±SEM of triplicate determinations.

P-cadherin Expression

P-cadherin is typically expressed in low amounts at the basal cell layer of the urothelium with aberrant expression investigated as a bladder cancer biomarker. Further, the expression of P-cadherin has been recently proposed as a bladder cancer stem cell marker (Bryan, 2014).

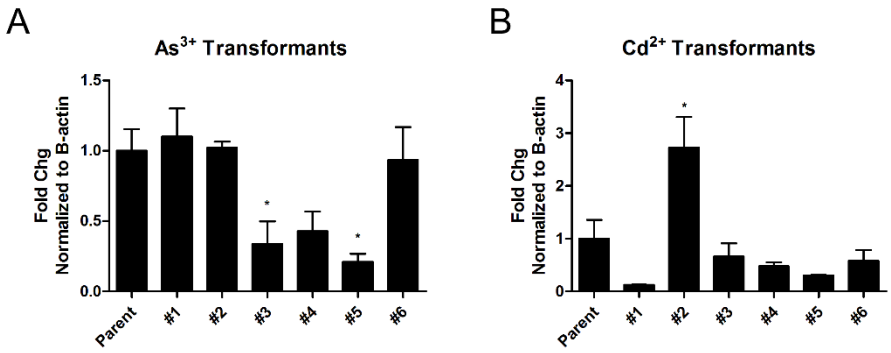

Figure 5.2 P-cadherin expression is variable in As^{3+}- and Cd^{2+}-transformed UROtsa cells. Real time RT-PCR analysis expressed as fold change over parent normalized to β-actin in A) As^{3+} isolates and B) Cd^{2+} isolates. Results represent Mean ±SEM of triplicate determinations. *p<0.05, **p<0.01, ***p<0.001.

Eukaryotic Elongation Factor 1A2 Expression

Eukaryotic elongation factor 1A2, or eEF1A2, is a subunit of the elongation factor 1 complex that promotes translation elongation. eEF1A2 is a proto-oncogene, with overexpression observed in a number of cancers including prostate, ovarian, and colon cancer. Translation elongation factors have been associated with cadmium carcinogenesis (Joseph, 2009). Commercial antibodies for eEF1A2 are not specific and also target eEF1A2, though the Scaggiante group has developed specific antibodies (Scaggiante et al., 2012).

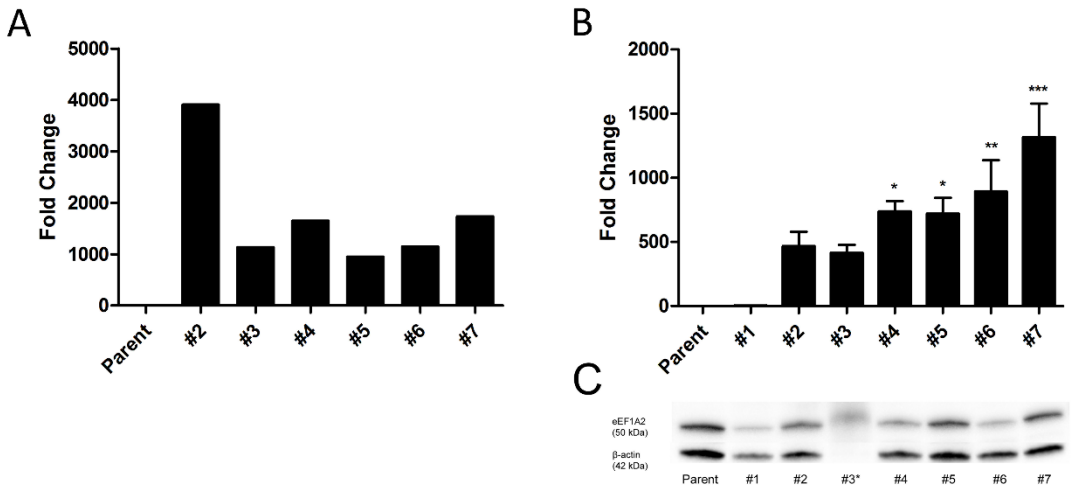

Figure 5.3 eEF1A2 is induced in Cd^{2+} transformants *in vitro*. A) PCR array validation results for eukaryotic elongation factor 1A2 in Cd^{2+}-transformed UROtsa cells. Isolate #1 was not included in array. B) Real time RT-PCR analysis expressed as fold change over parent confirms significant induction, though trends among isolates differ from the initial PCR array. Annealing temperature was optimized to 66^{o}. C) Western blot analysis for eEF1A2 protein in Cd^{2+}-transformed UROtsa and parent cells. *Isolate #3 is SC heterotransplant protein. Results represent Mean ±SEM of triplicate determinations. *$p<0.05$, **$p<0.01$, ***$p<0.001$

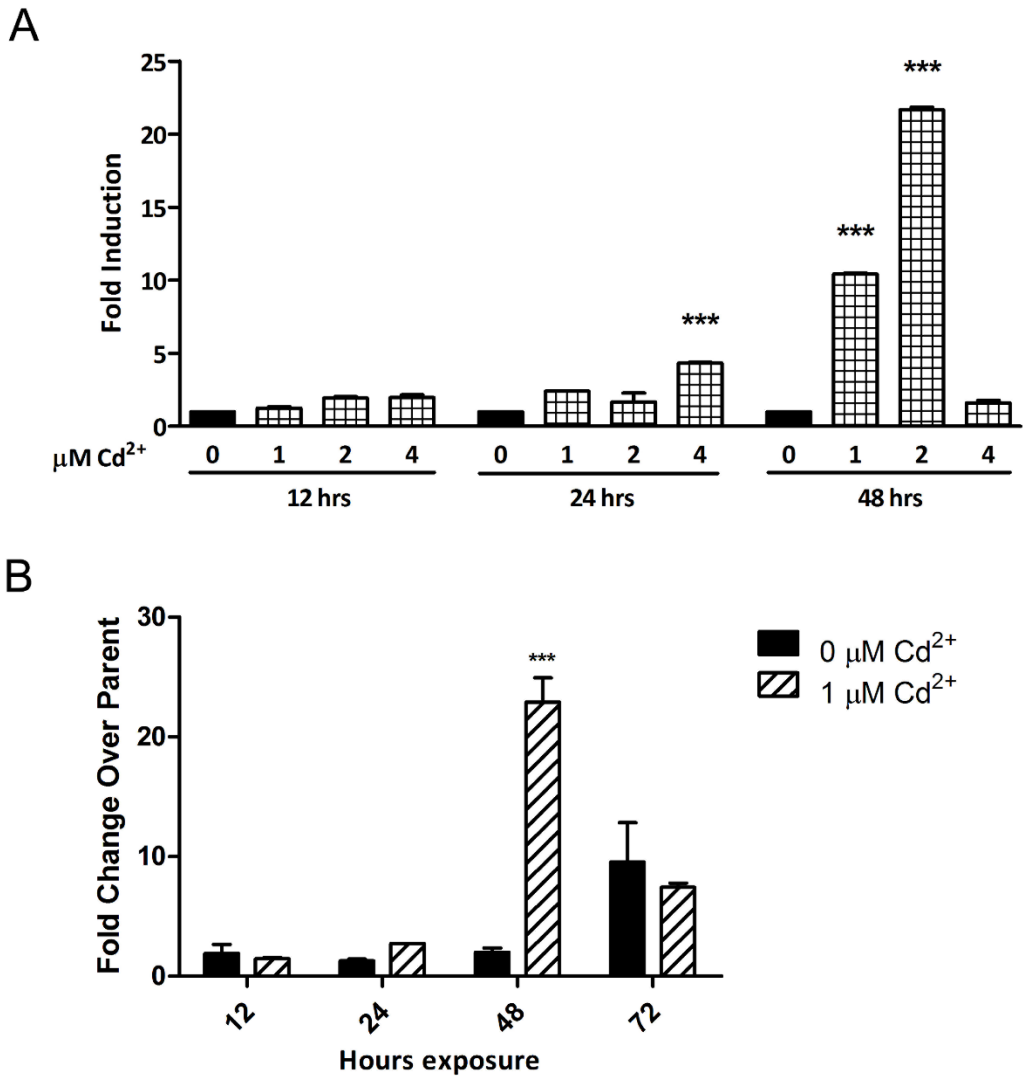

Figure 5.4 eEF12 expression is dependent upon Cd^{2+} exposure in non-malignant UROtsa cells. Real time RT-PCR analysis of eEF1A2 in parent UROtsa cells and Cd^{2+}-exposed isolates *in vitro*. eEF1A2 mRNA is elevated following 48 hrs 1 μM Cd^{2+} exposure to parent UROtsa cells. Induction was most apparent at 48 hrs. A) UROtsa cells exposed to 0, 1, 2, and 4 μM cadmium chloride for 12, 48, and 72 hrs expressed as fold change over time-matched non-treated control. B) Selected results from 1 μM exposure at all time points. Data represented as fold change over parent UROtsa cells at 0 hrs exposure. Results represent Mean ±SEM of triplicate determinations. *p<0.05, **p<0.01, ***p<0.001

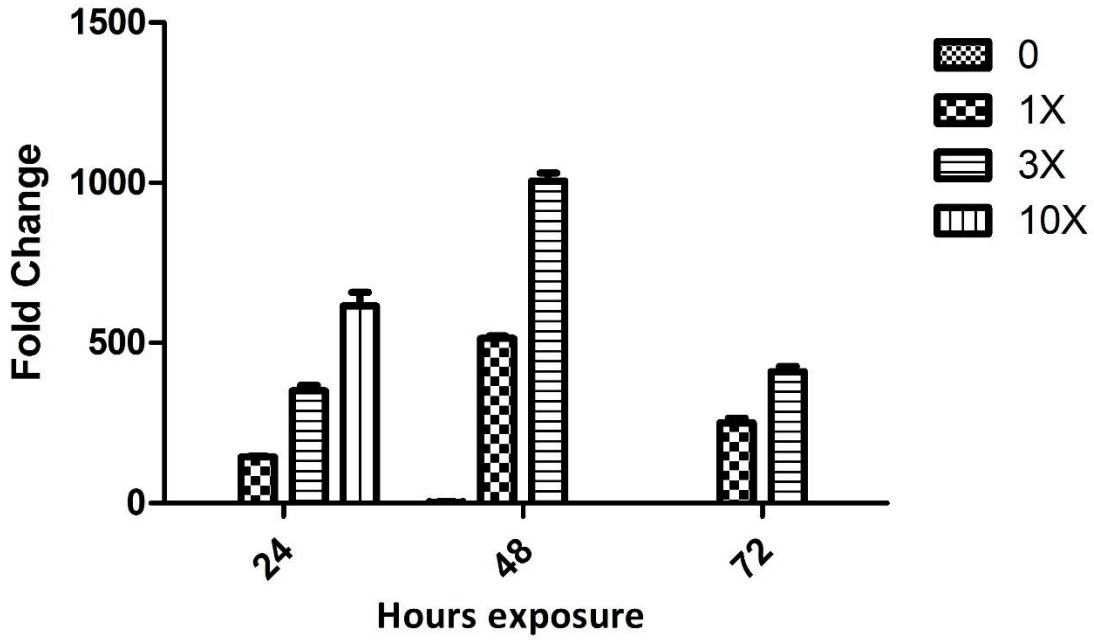

Figure 5.5 eEF1A2 expression is regulated by histone acetylation state. eEF1A2 mRNA expression is induced in a dose-dependent manner following 24, 48, and 72 hr exposure to the histone deacetylase inhibitor MS-275 in parent UROtsa cells. UROtsa cells were only exposed to 10X MS-275 at the 24 hr time point. Expression increases with duration of exposure between 24 and 48 hrs, followed by a decrease at 72 hrs, while dose-dependent expression is maintained.

NR2F1 and NR2F2 Induction in As^{3+}- and Cd^{2+}-transformed UROtsa Cells

Nuclear receptor subfamily 2, group F, member 1 (NRF2F1) and member 2 (NRF2F2) experiments were performed by undergraduate Andrew Millbridge. Previously, RT-PCR analysis of 39 transitional cell carcinomas demonstrated a significant decrease in NR2F1 expression relative to normal tissue from the same patients (Ham, Lee, Yu, & Choi, 2008). In the bladder cancer cell line J82, retinoic acid-induced growth inhibition and apoptosis is promoted by NR2F1 (B. Lin, Chen, Xiao, & Kumar, 2000). NR2F1 and NR2F2 have almost completely identical DNA binding domains, though the N-terminal regions of the two proteins significantly differ (Tsai & Tsai, 1997).

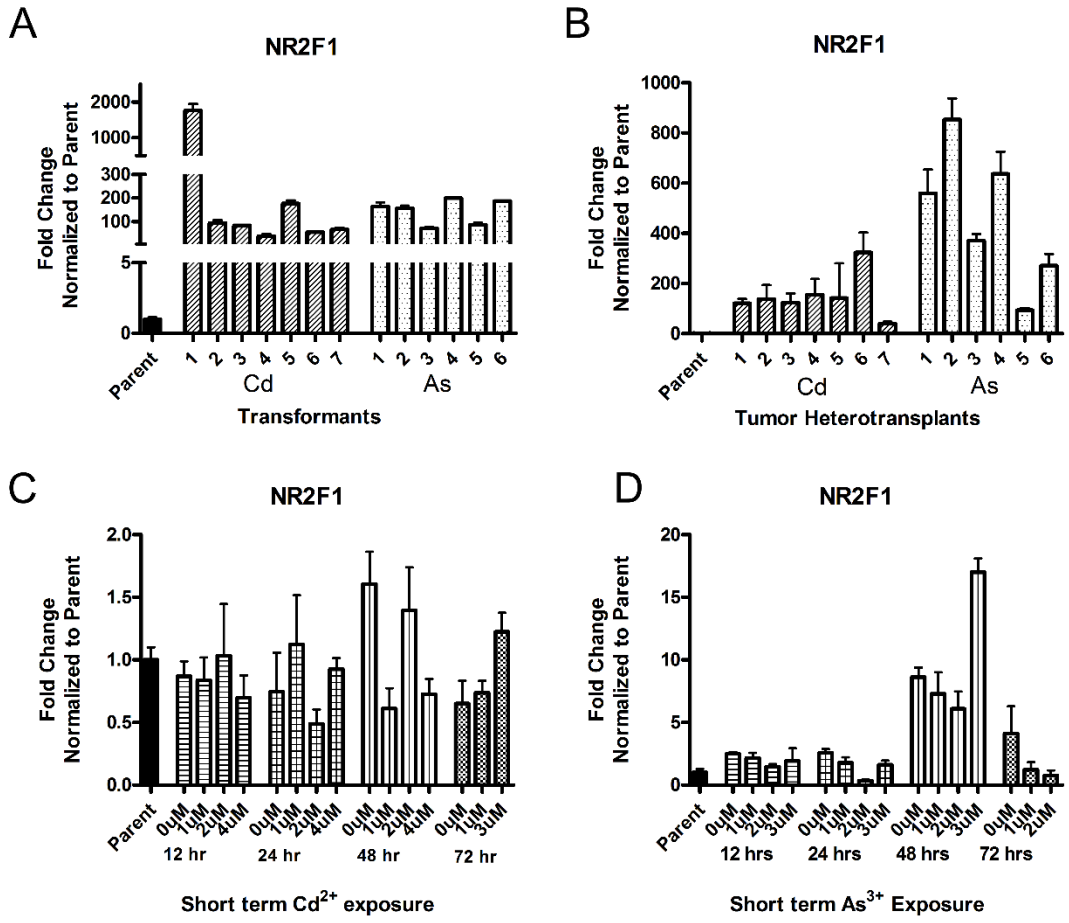

Figure 5.6 NR2F1 is induced in As^{3+}- and Cd^{2+}-transformed isolates and corresponding subcutaneous heterotransplants. A) Real time RT-PCR analysis of NR2F1 in parent UROtsa cells and As^{3+} and Cd^{2+} isolates *in vitro*. B) Real time RT-PCR analysis of NR2F1 in parent UROtsa cells and As^{3+} and Cd^{2+} SC heterotransplants. C) NR2F1 expression with 0, 1, 2, and 4 µM Cd^{2+} exposure for 12, 24, 48, and 72 hrs. D) NR2F1 expression after 0, 1, 2, and 3 µM As^{3+} exposure for 12, 24, 48, and 72 hrs. Data expressed as fold change relative to parent UROtsa cell line. PCR results represent Mean ±SEM of triplicate determinations.

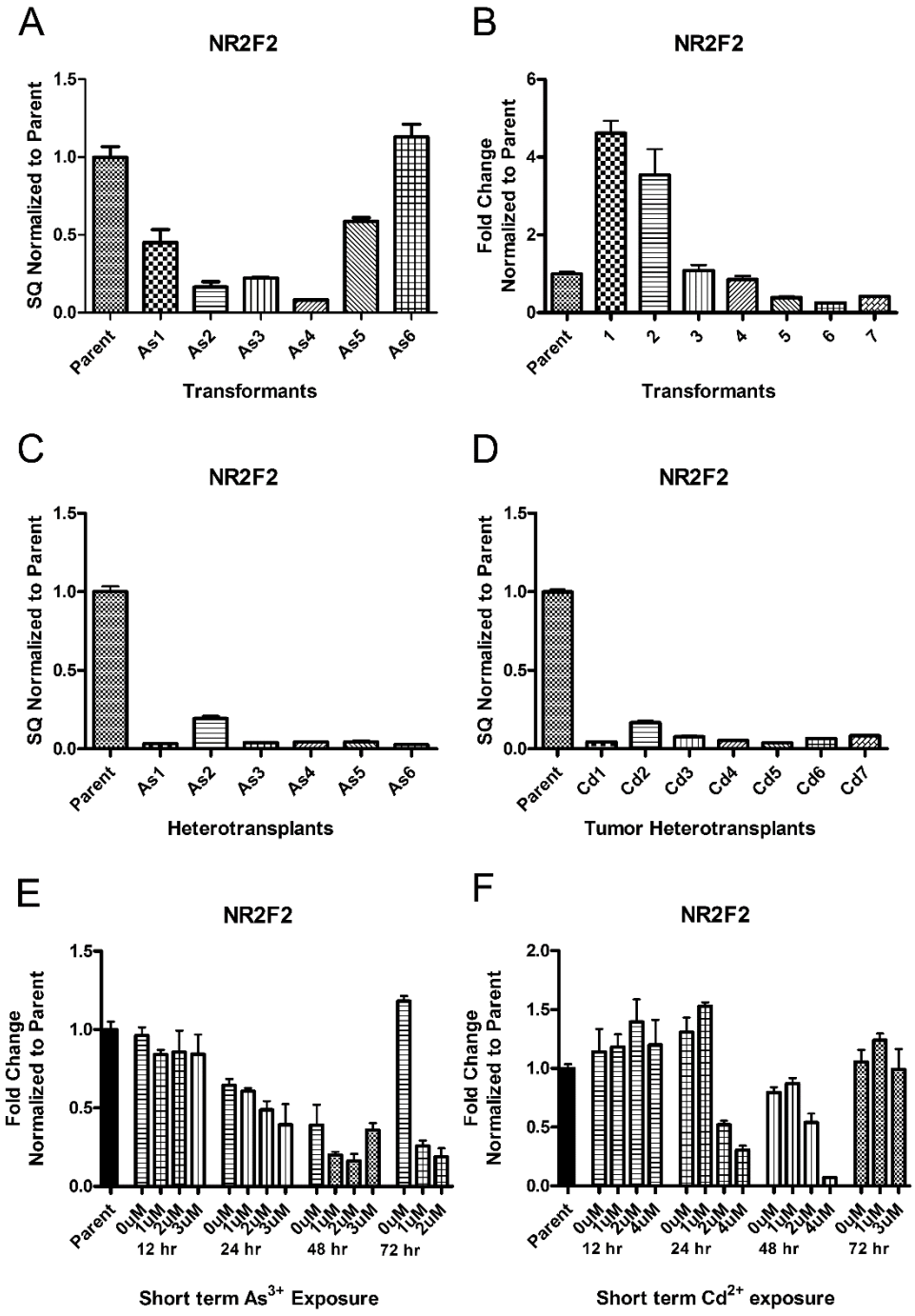

Figure 5.7 NR2F2 remains mostly unchanged in As^{3+}- and Cd^{2+}-transformed isolates *in vitro*, but is reduced in subcutaneous tumors. Real time RT-PCR analysis of NR2F1 in A) As^{3+} transformants and B) Cd^{2+} isolates *in vitro*. C) As^{3+} SC tumors and D) Cd^{2+} SC tumors. E) Short-term As^{3+} exposure to parent UROtsa cells. F) Short-term Cd^{2+} exposure to parent UROtsa cells. Data is expressed as fold change over parent. PCR results represent Mean ±SEM of triplicate determinations.

Microarray Validation by Short-term As^{3+} Exposure

To determine genes of interest from those differentially expressed in As^{3+}-transformed UROtsa, the top five-induced genes from the microarray were selected and changes in gene expression following short-term arsenic exposure were measured. The genes include UDP glycosyltransferase 8 (UGT8), latrophilin 2 (LPHN2), LIM and calponin homology domains 1 (LIMCH1), carboxypeptidase 6 (CPA6), and eukaryotic elongation factor 1 alpha 2 (eEF1A2). eEF1A2 was the only gene significantly altered by arsenic exposure, with results listed in a separate figure.

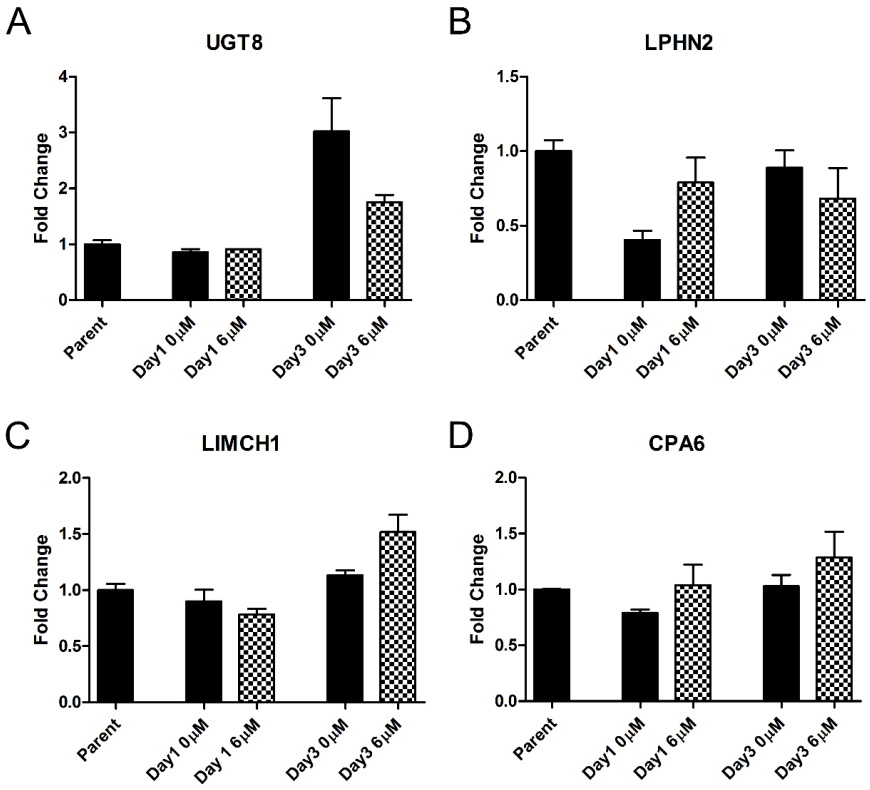

Figure 5.8 Microarray validation by analysis of short-term As^{3+} exposure. Selected genes were the top-most induced on the As^{3+} array, and significantly increased on the array of Cd^{2+}-transformed UROtsa cells. A) UGT8, B), LPHN2, C) LIMCH1, and D) CPA6 revealed no alteration in expression following one or three days with 6 μM sodium arsenite. Data is expressed as fold change over parent. PCR results represent Mean ±SEM of triplicate determinations.

Neurotrophin-3 Expression in As^{3+}- and Cd^{2+}-transformed UROtsa Cells

Neurotrophin-3 (NTF3 or NT3) experiments were performed by undergraduate Tyler Titcomb. A review of scientific literature and omics signatures for muscl-invasive bladder cancer revealed that the neurotrophin signaling pathway was significantly associated with the disease (Bhat et al., 2015).

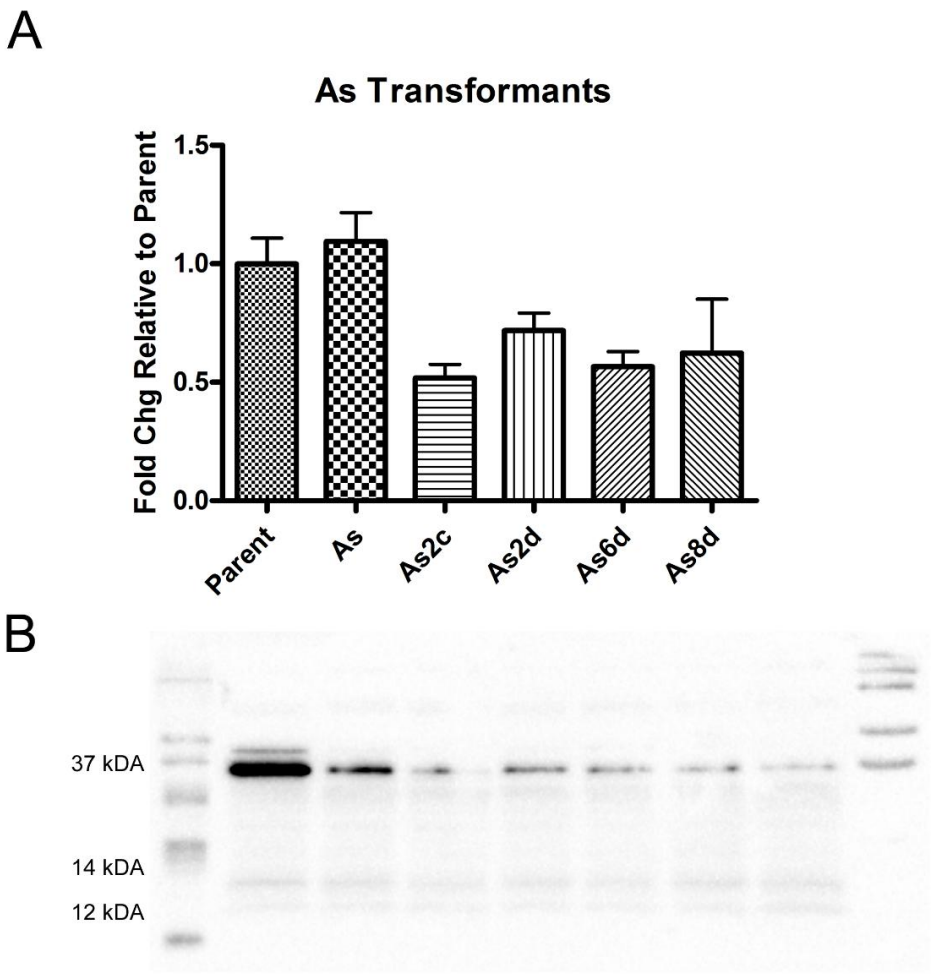

Figure 5.9 NTF3 is reduced in As^{3+}-transformed UROtsa cells at the mRNA and protein level. A) Real time RT-PCR for neurotrophin-3 in parent and As^{3+} transformants expressed as fold change over parent. PCR results represent Mean ±SEM of triplicate determinations. B) Western blot analysis for NTF3 at 35 kDa.

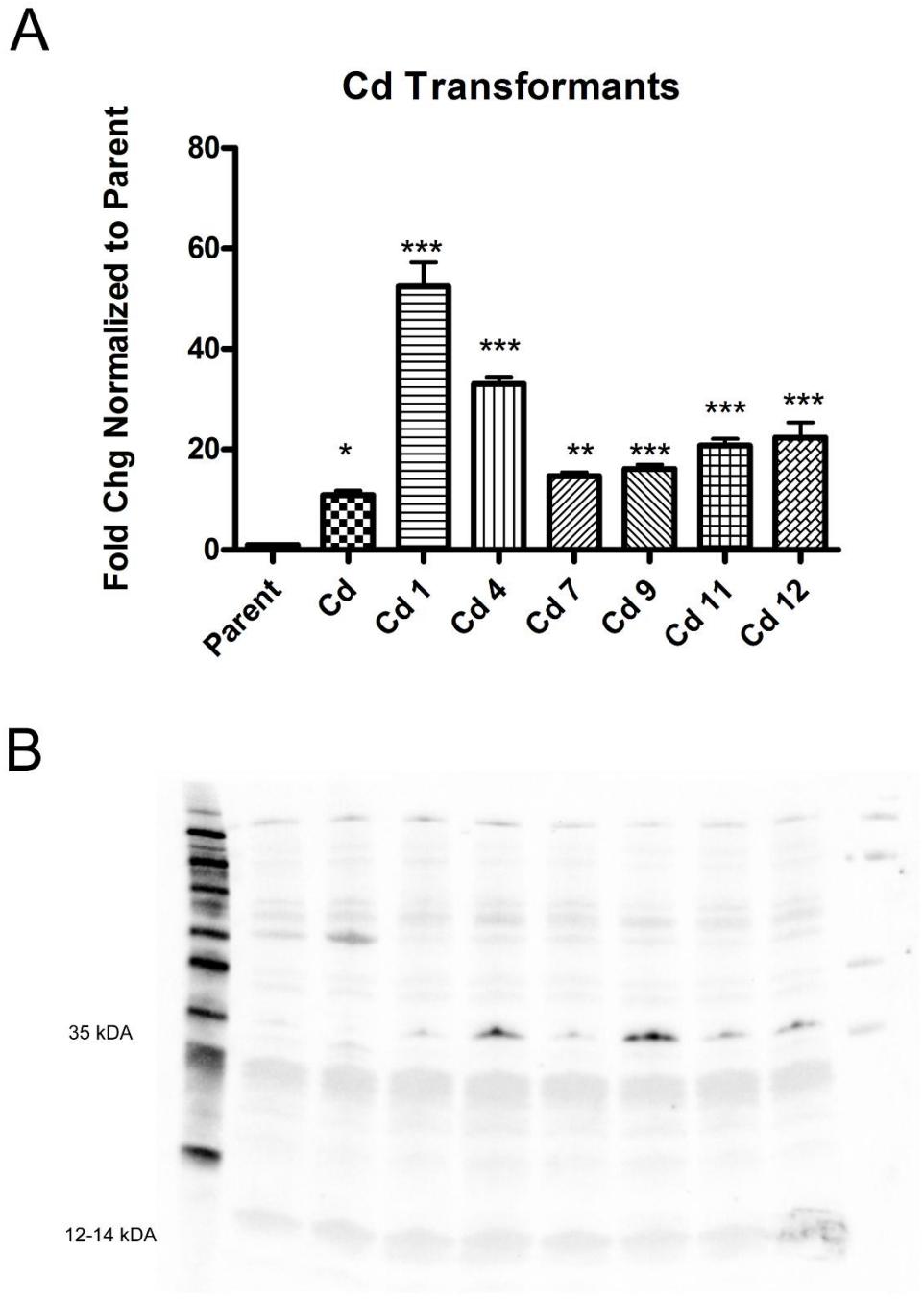

Figure 5.10 NTF3 is induced in Cd^{2+}-transformed UROtsa cells. A) Real time RT-PCR analysis for NTF3 expressed as fold change over parent. PCR results represent Mean ±SEM of triplicate determinations. B) Western blot analysis for NTF3 at 35 kDa. *p<0.05, **p<0.01, ***p<0.001

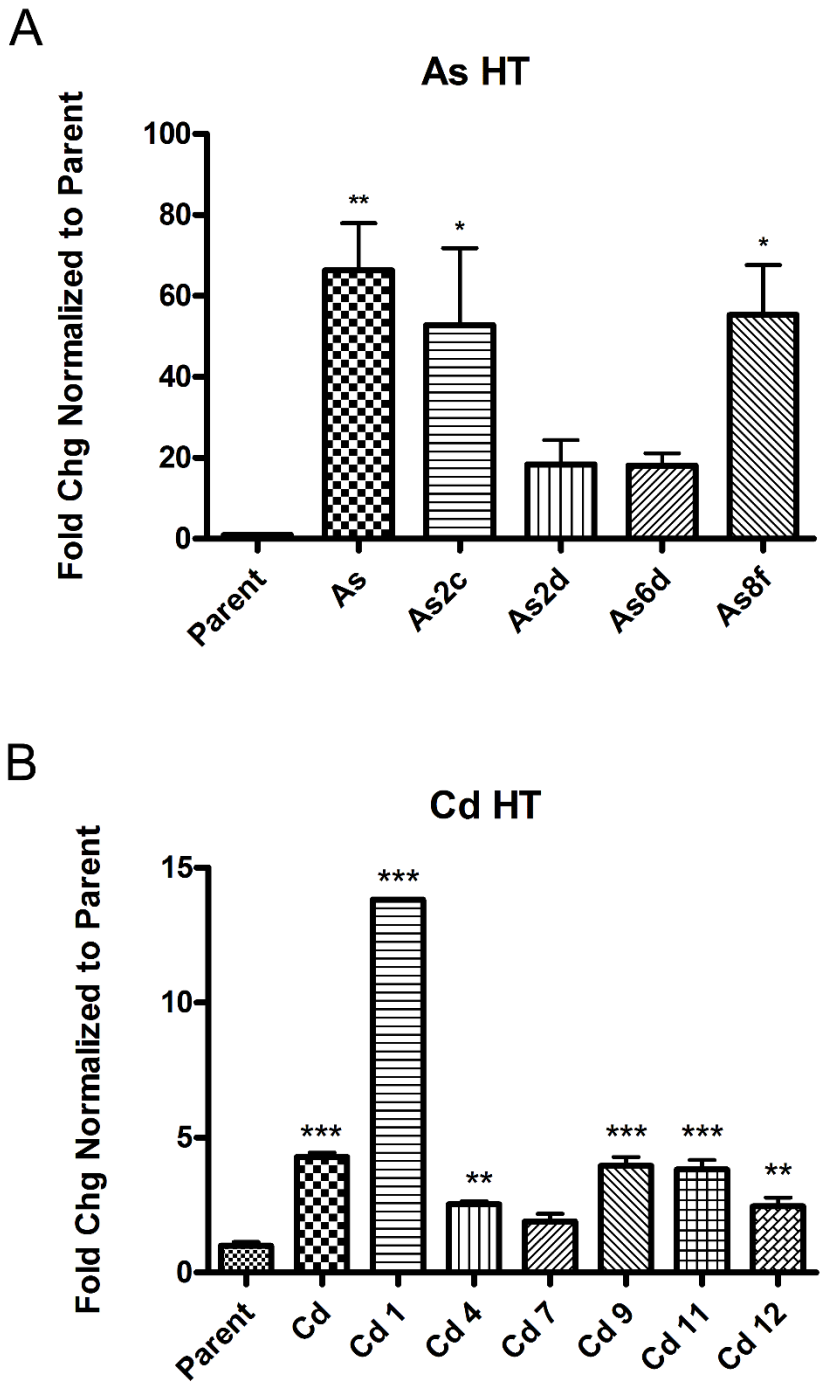

Figure 5.11 Neurotrophin-3 expression is increased in As^{3+} and $Cd2^{+}$ subcutaneous tumors. Real time RT-PCR analysis for NTF-3 in A) As^{3+} SC tumors and B) Cd^{2+} SC tumors expressed as fold change over parent. PCR results represent Mean ±SEM of triplicate determinations. *p<0.05, **p<0.01, ***p<0.001

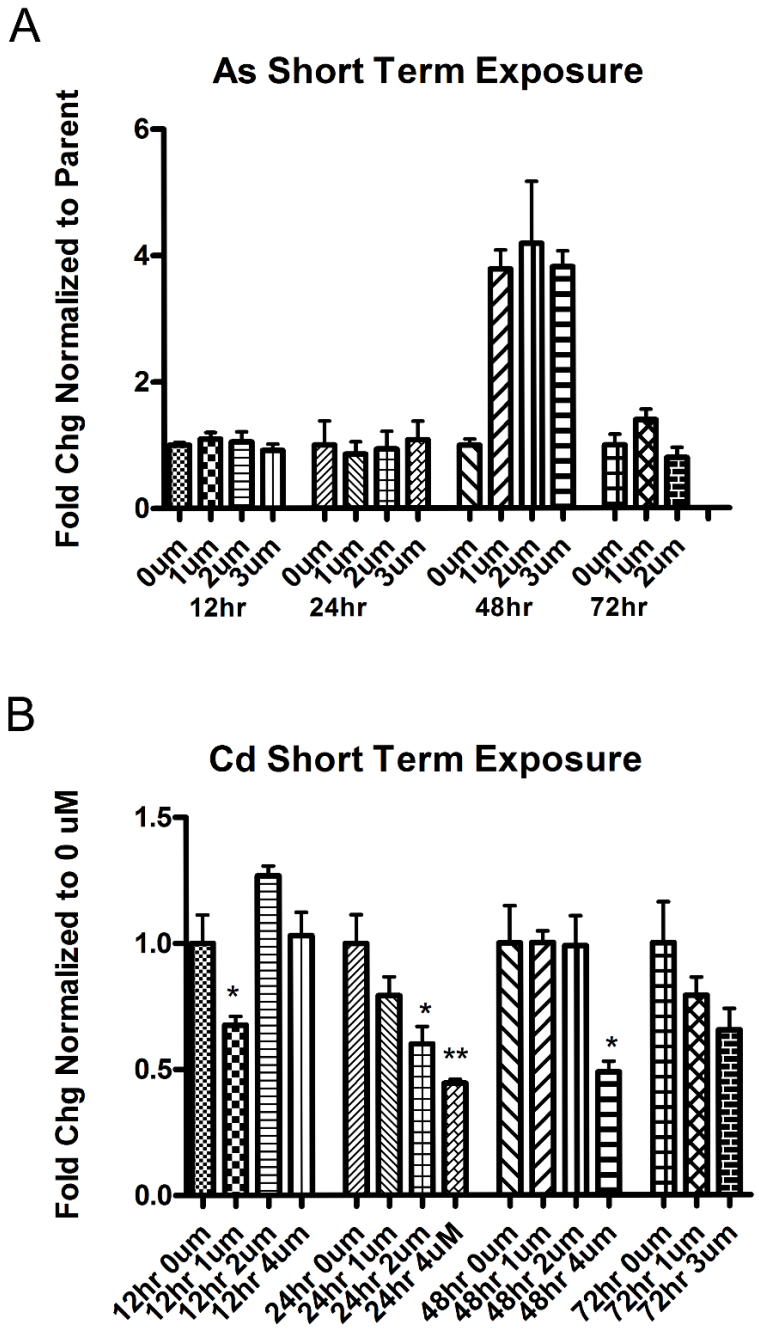

Figure 5.12 Neurotrophin-3 expression is unchanged following short-term As^{3+} and Cd^{2+} exposure. A) Real time RT-PCR for short-term sodium arsenite exposed parent UROtsa cells. The 48 hr time point samples were likely misquantified. B) RT-PCR analysis for short-term cadmium chloride exposure. Data expressed as fold change over parent. PCR results represent Mean ±SEM of triplicate determinations. *p<0.05, **p<0.01, ***p<0.001

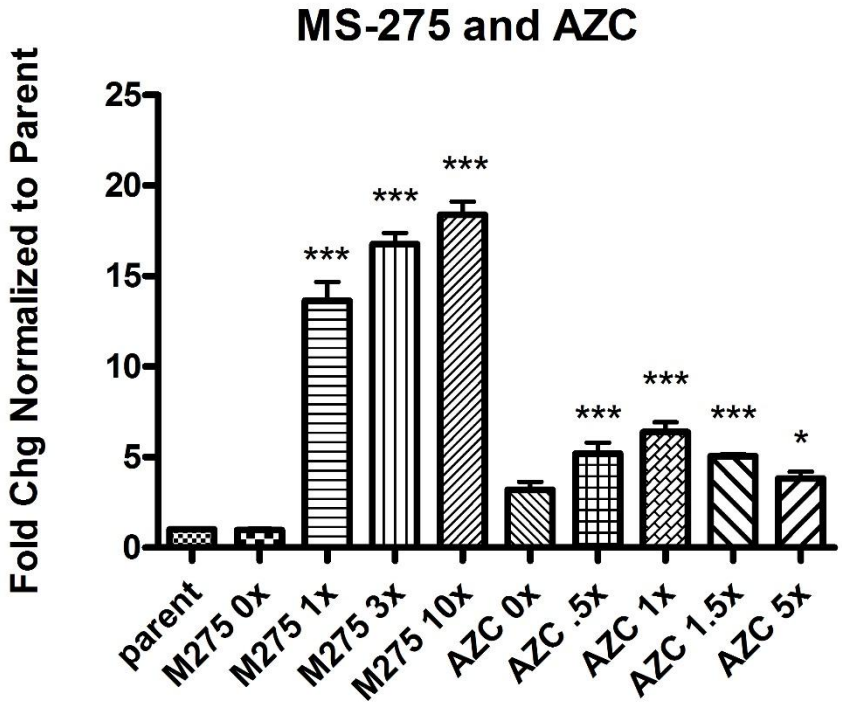

Figure 5.13 Neurotrophin-3 expression is altered by histone deacetylase inhibitor and DNA methyltransferase inhibitor treatment. parent UROtsa cells were treated with MS-275 for 24 hrs and 5'-azacytidine for 48 hrs. Real time RT-PCR results expressed as fold change over parent. PCR results represent Mean ±SEM of triplicate determinations. *p<0.05, **p<0.01, ***p<0.001

Ephrin Receptor A4 Induction in As^{3+}- and Cd^{2+}-transformed UROtsa Cells

Ephrin receptor A4 (EPHA4) research was performed by undergraduate Tyler Titcomb. EPHA4 promotes motility and invasion in pancreatic and prostate cancer (Batson, Maccarthy-Morrogh, Archer, Tanton, & Nobes, 2014; C. Liu, Huang, Wang, Kong, & Zhang, 2014) and is correlated with gastric cancer recurrence (Oki et al., 2008).

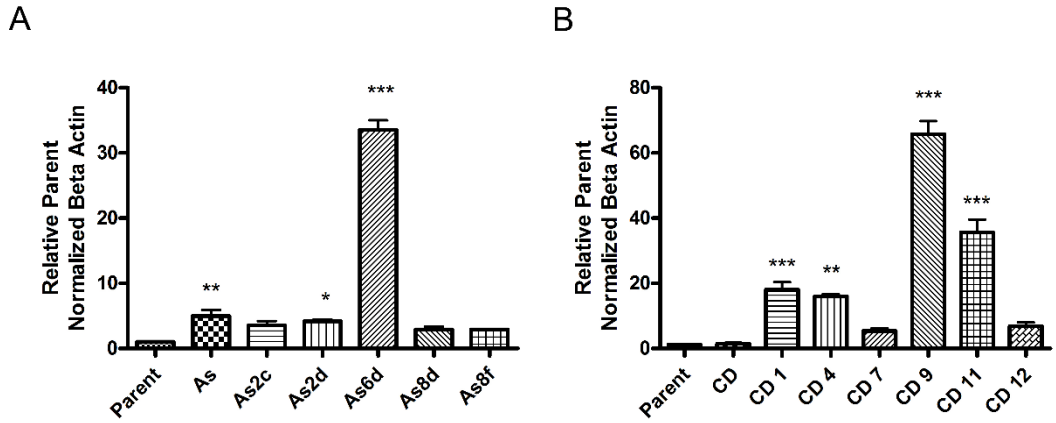

Figure 5.14 Ephrin Receptor A4 expression is increased in As^{3+} and Cd^{2+} transformants. Real time RT-PCR analysis in A) As^{3+}-transformed and B) Cd^{2+}-transformed UROtsa cells expressed as fold change over parent. PCR results represent Mean ±SEM of triplicate determinations. *p<0.05, **p<0.01, ***p<0.001

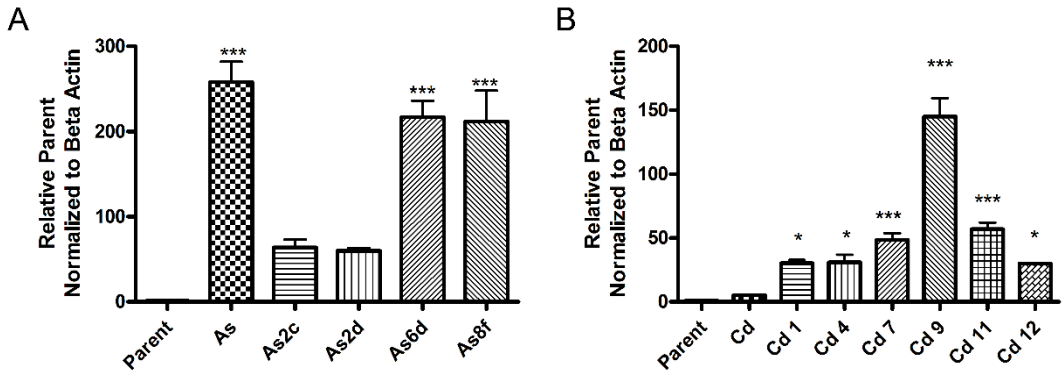

Figure 5.15 EPHA4 expression is elevated in As^{3+} and Cd^{2+} subcutaneous tumors. Real time RT-PCR analysis of A) As^{3+} SC tumors and B) Cd^{2+} SC tumors expressed as fold change over parent. PCR results represent Mean ±SEM of triplicate determinations. *p<0.05, **p<0.01, ***p<0.001

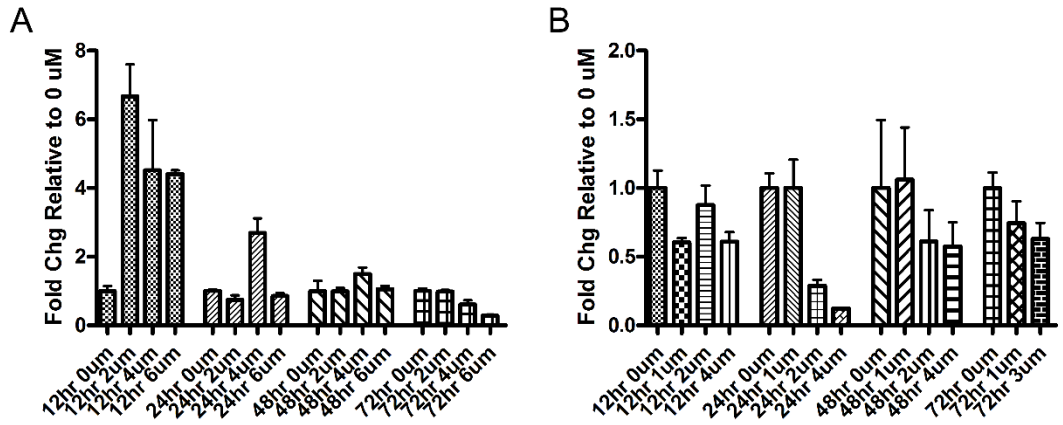

Figure 5.16 EPHA4 expression is induced after 12 hrs As^{3+} exposure. A) Real time RT-PCR analysis of parent UROtsa cells exposed to sodium arsenite. B) RT-PCR analysis of short-term cadmium chloride. PCR results represent Mean ±SEM of triplicate determinations.

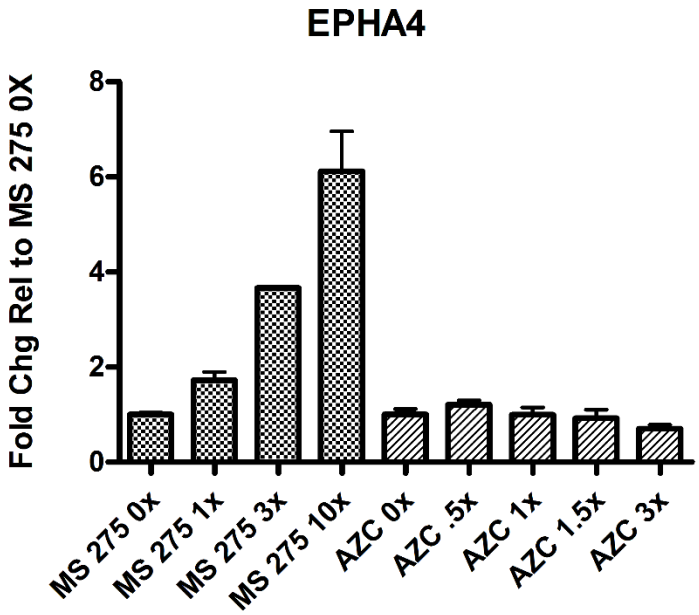

Figure 5.17 EPHA4 is induced by MS-275, but not 5'-AZC treatment. Parent UROtsa cells treated with 24 hrs MS-275 and 48 hrs 5'-azacytidine. Real time RT-PCR analysis expressed as Mean ±SEM of triplicate determinations.

Ets Variant 7 Induction in As^{3+}- and Cd^{2+}-transformed UROtsa Cells

Ets variant 7 (ETV7) is also known as telomere length regulation protein (Tel2). Experiments evaluating the expression of this gene were performed by undergraduate Andrew Millbridge. ETV7 functions as a protein to mediate Hsp90 regulation of phosphatidylinositol-3 kinase-like kinases (PIKKs), proteins involved in DNA repair, cell cycle control, regulation of cell growth, degradation of mRNA, and control of gene expression (Takai, Wang, Takai, Yang, & de Lange, 2007). Hsp90 activates PIKKs via the R2TP complex and ETV7, in which ETV7 mediates the interaction between PIKKs and the R2TP complex. ETV7 stabilizes PIKK enzymes including mTOR, SMG1, and ATM (Horejsí et al., 2010; Kaizuka et al., 2010). Further, ETV7 mediates the recruitment of ATM1/Tel1 kinase to the site of double stranded DNA breaks for repair (Anderson et al., 2008). ETV7 can also act as a transcription factor (Gu et al., 2001). Expression of ETV7 in cancers has been little studied. ETV7 expression is elevated in breast cancer (J. He et al., 2007) and is considered a hematopoietic oncogene (Carella et al., 2006), and increased ETV7 protein is observed in hepatocellular carcinoma (Matos, Witzmann, Cummings, & Schmidt, 2009). However, ETV7 is reduced in drug-resistant gastric cancer (O. Maeda et al., 2014).

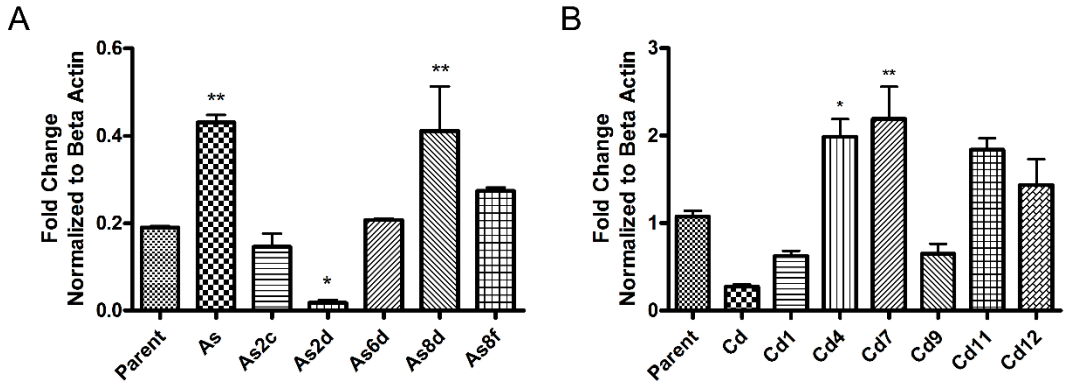

Figure 5.18 Ets variant 1 expression is induced in As^{3+} and Cd^{2+} transformants. Real time RT-PCR analysis of ETV7 in A) As^{3+}-transformed UROtsa cells and B) Cd^{2+}-transformed UROtsa cells expressed as fold change normalized to β-actin. PCR results represent Mean ±SEM of triplicate determinations. *p<0.05, **p<0.01, ***p<0.001

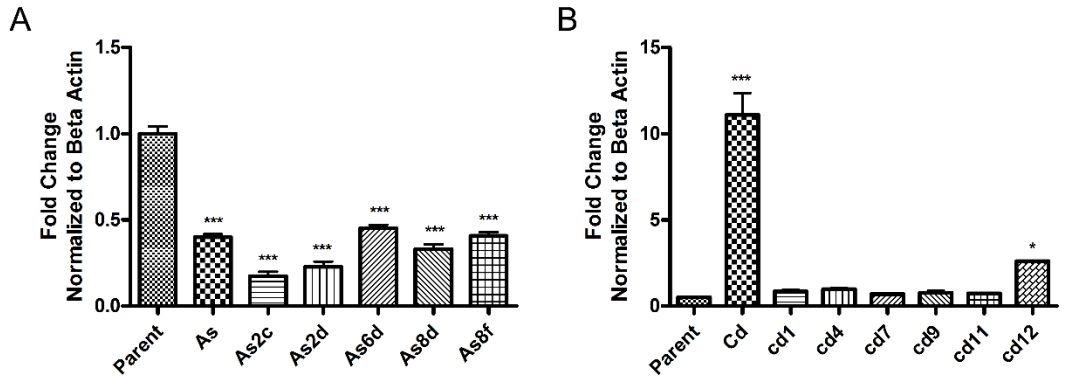

Figure 5.19 ETV7 is reduced in As^{3+} subcutaneous tumors, and relatively unchanged in Cd^{2+} tumors. Real time RT-PCR analysis of ETV7 in A) As^{3+} SC tumors and B) Cd^{2+} SC tumors expressed as fold change normalized to β-actin. PCR results represent Mean ±SEM of triplicate determinations. *p<0.05, **p<0.01, ***p<0.001

ITM2C Expression

Experiments on integral membrane protein 2c (ITM2C) expression were performed by undergraduate Andrew Millbridge. ITM2C expressed highly in the brain and is an inhibitor of beta-amyloid peptide production, but is known about the function of ITM2C outside the brain.

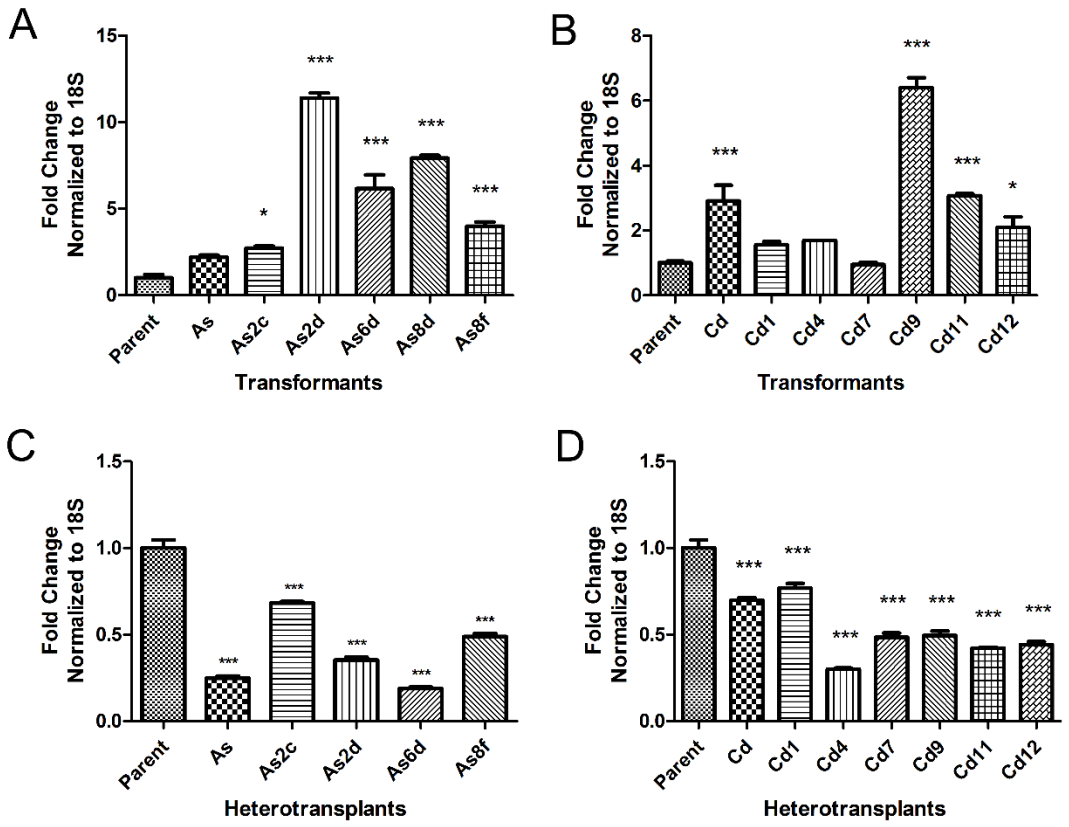

Figure 5.20 ITM2C expression is varied in As^{3+} and Cd^{2+} transformants *in vitro*, though reduced in subcutaneous tumors. Real time RT-PCR analysis of ITM2C in A) As^{3+}-transformed UROtsa cells, B) Cd^{2+}-transformed UROtsa cells, C) As^{3+} SC tumors, and D) Cd^{2+} SC tumors expressed as fold change normalized to 18S. PCR results represent Mean ±SEM of triplicate determinations. *p<0.05, **p<0.01, ***p<0.001

ABBREVIATIONS

67LR	67-kDa laminin receptor
8-oxo-dGTP	8-oxo-7,8-dihydrodeoxyguanosine triphosphate
ABC transporter	ATP-binding cassette transporter
ALDH1A1	aldehyde dehydrogenase 1 family, member A1
ANOVA	one-way analysis of variance
AP-1	activator protein 1
Ape-1	apurinic/apyrimidinic endonuclease 1
As^{3+}	arsenite
ATSDR	Agency for Toxic Substances and Disease Registry
5'-AZC	5'-azacytidine
Bmi-1	B cell-specific Moloney murine leukemia virus integration site 1
BSA	bovine serum albumin
Cd^{2+}	cadmium
$CdCl_2$	cadmium chloride
ChIP	chromatin immunoprecipitation
CK20	keratin 20
CO_2	carbon dioxide
CTBP1	c-terminal binding protein 1
DAB	3,3'-diaminobenzidine
DAPK	death-associated protein kinase
DMA(III)	dimethylarsinous acid
DMA(V)	dimethylarsinic acid

DMEM	Dulbecco's Modified Eagle Medium
DMT1	divalent metal transporter 1
DNA	deoxynucleic acid
E-cadherin	epithelial-cadherin
ECL	electrochemiluminescence
EDTA	Ethylenediaminetetraacetic acid
eEF1A2	eukaryotic translation elongation factor 1 alpha 2
EGF	epidermal growth factor
EMT	epithelial-mesenchymal transition
EPA	Environmental Protection Agency
EPHA4	ephrin receptor A4
ERK	extracellular signal-related kinase
ETV7	ets variant 7
FDA	Food and Drug Administration
GATA-4	GATA-binding factor 4
H3K9Me3	histone 3 lysine 9 trimethylation
H4Ac	histone 4 acetylation
HDACi	histone deacetylase inhibitor
HIF-2α	hypoxia-inducible factor 2 alpha
HRP	horseradish peroxidase
hrs	hours
Hsp	heat shock protein
IARC	International Agency for Research on Cancer

IHC	immunohistochemistry
IL1RN	interleukin 1 receptor antagonist
IP	intraperitoneal
ITM2C	integral membrane protein 2c
Jak	Janus family tyrosine kinase LAS-AF
LCN2	lipocalin-2
MAPK	mitogen-activated protein kinase
MDR1	multi-drug resistance
µl	microliter
µM	micromolar
min	minute
miRNA	microRNA
MMA(III)	monomethylarsonous acid
MMA(V)	monomethylarsonic acid
MMP9	matrix metallopeptidase 9
mRNA	messenger RNA
MSH	Mut S homolog
MZF1	myeloid zinc finger 1
$NaAsO_2$	sodium arsenite
N-cadherin	neuronal-cadherin
NFκB2	nuclear factor κ B
NR2F1	nuclear receptor subfamily 2, group f, member 1
NR2F2	nuclear receptor subfamily 2, group f, member 2

NRF2	nuclear factor (erythroid-derived 2)-like 2
NTF3	neurotrophin-3
NTP	National Toxicology Program
OCLN	occludin
Oct-4	octamer-binding transcription factor 4
PBS	phosphate-buffered saline
P-cadherin	placenta-cadherin
PE	phycoerythrin
PMSF	phenylmethanesulfonylfluoride
PVDF	polyvinylidene difluoride
RBPJ	recombination signal binding protein for immunoglobulin kappa J region
RECK	reversion-inducing-cysteine-rich protein with kazal motifs
RNA	ribonucleic acid
ROS	reactive oxygen species
RT-PCR	real-time polymerase chain reaction
SEM	standard error of the mean
S100P	S100 calcium binding protein P
SC	subcutaneous
SDS	sodium dodecyl sulfate
SDS-PAGE	sodium dodecyl sulfate polyacrylamide gel electrophoresis
siRNA	small interfering RNA
SLC1A2	solute carrier family 1 (glial high affinity glutamate transporter), member 2

SLC39A14	solute carrier family 39 (zinc transporter), member 14
SMAD4	SMAD family member 4
Sox2	SRY (sex-determining region Y)-box 2
Sox9	SRY (sex-determining region Y)-box 9
SPARC	secreted protein, acidic, cysteine-rich
STAT	signal transducer and activator of transcription
STEAP1	six transmembrane epithelial antigen of the prostate 1
TCF4	transcription factor 4
TGF-β	transforming growth factor beta
Tris-HCl	Tris-hydrochloride
VEGFR	vascular endothelial growth factor receptor
XPA	xeroderma pigmentosum, complementation group A
XRCC3	X-ray repair complementing defective repair in Chinese hamster cells 3
YB-1	Y-box binding protein 1
ZIP14	zrt- and irt-like protein

BIBLIOGRAPHY

Abol-Enein, H. (2008). Infection: is it a cause of bladder cancer? *Scandinavian Journal of Urology and Nephrology. Supplementum*, *42*(218), 79–84. http://doi.org/10.1080/03008880802325309

Achanzar, W. E., Achanzar, K. B., Lewis, J. G., Webber, M. M., & Waalkes, M. P. (2000). Cadmium induces c-myc, p53, and c-jun expression in normal human prostate epithelial cells as a prelude to apoptosis. *Toxicology and Applied Pharmacology*, *164*(3), 291–300. http://doi.org/10.1006/taap.1999.8907

Achanzar, W., Webber, M., & Waalkes, M. (2002). Altered apoptotic gene expression and acquired apoptotic resistance in cadmium-transformed human prostate epithelial cells. *The Prostate*, *52*(3), 236–244. http://doi.org/10.1002/pros.10106

Adam, L., Zhong, M., Choi, W., Qi, W., Nicoloso, M., Arora, A., … Dinney, C. (2009). miR-200 expression regulates epithelial-to-mesenchymal transition in bladder cancer cells and reverses resistance to epidermal growth factor receptor therapy. *Clinical Cancer Research*, *15*(16), 5060–5072. http://doi.org/10.1158/1078-0432.CCR-08-2245

Ahirwar, D. K., Agrahari, A., Mandhani, A., & Mittal, R. D. (2009). Cytokine gene polymorphisms are associated with risk of urinary bladder cancer and recurrence after BCG immunotherapy. *Biomarkers : Biochemical Indicators of Exposure, Response, and Susceptibility to Chemicals*, *14*(4), 213–218. http://doi.org/10.1080/13547500902818246

Ahlering, T. E., Dubeau, L., & Jones, P. a. (1987). A new in vivo model to study invasion and metastasis of human bladder carcinoma. *Cancer Research*, *47*(24 Pt 1), 6660–5. Retrieved from http://www.ncbi.nlm.nih.gov/pubmed/3677100

Ai, Z., Lu, W., Ton, S., Liu, H., Sou, T., Shen, Z., & Qin, X. (2007). Arsenic trioxide-mediated growth inhibition in gallbladder carcinoma cells via down-regulation of Cyclin D1 transcription mediated by Sp1 transcription factor. *Biochemical and Biophysical Research Communications*, *360*(3), 684–9. http://doi.org/10.1016/j.bbrc.2007.06.123

Aiba, I., Hossain, A., & Kuo, M. T. (2008). Elevated GSH level increases cadmium resistance through downregulation of Sp1-dependent expression of the cadmium transporter ZIP8. *Molecular Pharmacology*, *74*(3), 823–33. http://doi.org/10.1124/mol.108.046862

Al-ahmadie, H., Lin, O., & Reuter, V. E. (2011). Pathology and cytology of tumors of the urinary tract. In P. T. Scardino, W. M. Linehan, M. J. Zelefshy, & N. J. Vogelzang (Eds.), *Comprehensive Textbook of Genitourinary Oncology* (4th ed., pp. 295–316). Baltimore, MD: Lippincott Williams & Wilkins.

Alexander, N. R., Tran, N. L., Rekapally, H., Summers, C. E., Glackin, C., & Heimark, R. L. (2006). N-cadherin gene expression in prostate carcinoma is modulated by integrin-dependent nuclear translocation of Twist1. *Cancer Research*, *66*(7), 3365–9. http://doi.org/10.1158/0008-5472.CAN-05-3401

Anderson, C. M., Korkin, D., Smith, D. L., Makovets, S., Seidel, J. J., Sali, A., & Blackburn, E. H. (2008). Tel2 mediates activation and localization of ATM/Tel1 kinase to a double-strand break. *Genes & Development*, *22*(7), 854–9. http://doi.org/10.1101/gad.1646208

Andrew, A. S., Mason, R. A., Kelsey, K. T., Schned, A. R., Marsit, C. J., Nelson, H. H., & Karagas, M. R. (2009). DNA repair genotype interacts with arsenic exposure to increase bladder cancer risk. *Toxicology Letters*, *187*(1), 10–14. http://doi.org/10.1016/j.toxlet.2009.01.013

Arnér, E. S. J., & Holmgren, A. (2000). Physiological functions of thioredoxin and thioredoxin reductase. *European Journal of Biochemistry*, *267*(20), 6102–6109. http://doi.org/10.1046/j.1432-1327.2000.01701.x

Arnold, L. L., Eldan, M., Nyska, A., van Gemert, M., & Cohen, S. M. (2006). Dimethylarsinic acid: results of chronic toxicity/oncogenicity studies in F344 rats and in B6C3F1 mice. *Toxicology*, *223*, 82–100. http://doi.org/10.1016/j.tox.2006.03.013

Arnold, L. L., Suzuki, S., Yokohira, M., Kakiuchi-Kiyota, S., Pennington, K. L., & Cohen, S. M. (2014). Time course of urothelial changes in rats and mice orally administered arsenite. *Toxicologic Pathology*, *42*(5), 855–62. http://doi.org/10.1177/0192623313489778

Asmuss, M., Mullenders, L. H., Eker, A., & Hartwig, A. (2000). Differential effects of toxic metal compounds on the activities of Fpg and XPA, two zinc finger proteins involved in DNA repair. *Carcinogenesis*, *21*(11), 2097–2104. http://doi.org/10.1093/carcin/21.11.2097

ATSDR. (2007). Toxicological Profile for Arsenic. U.S. Department of Health and Human Services, Public Health Service. Atlanta, GA. Retrieved from http://dx.doi.org/10.1155/2013/286524

ATSDR. (2012). Toxicological Profile for Cadmium. U.S. Department of Health and Human Services, Public Health Service. Atlanta, GA. Retrieved from

http://www.atsdr.cdc.gov/toxprofiles/tp5.pdf\nhttp://www.ncbi.nlm.nih.gov/books/NBK158845/

Avritscher, E. B. C., Cooksley, C. D., Grossman, H. B., Sabichi, A. L., Hamblin, L., Dinney, C. P., & Elting, L. S. (2006). Clinical model of lifetime cost of treating bladder cancer and associated complications. *Urology*, *68*(3), 549–53. http://doi.org/10.1016/j.urology.2006.03.062

Baiocchi, M., Biffoni, M., Ricci-Vitiani, L., Pilozzi, E., & De Maria, R. (2010, August). New models for cancer research: Human cancer stem cell xenografts. *Current Opinion in Pharmacology*. http://doi.org/10.1016/j.coph.2010.05.002

Batson, J., Maccarthy-Morrogh, L., Archer, A., Tanton, H., & Nobes, C. D. (2014). EphA receptors regulate prostate cancer cell dissemination through Vav2-RhoA mediated cell-cell repulsion. *Biology Open*, *3*(6), 453–62. http://doi.org/10.1242/bio.20146601

Baumgart, E., Cohen, M. S., Silva Neto, B., Jacobs, M. a, Wotkowicz, C., Rieger-Christ, K. M., … Summerhayes, I. C. (2007). Identification and prognostic significance of an epithelial-mesenchymal transition expression profile in human bladder tumors. *Clinical Cancer Research : An Official Journal of the American Association for Cancer Research*, *13*(6), 1685–94. http://doi.org/10.1158/1078-0432.CCR-06-2330

Bentivegna, A., Conconi, D., Panzeri, E., Sala, E., Bovo, G., Viganò, P., … Dalprà, L. (2010). Biological heterogeneity of putative bladder cancer stem-like cell populations from human bladder transitional cell carcinoma samples. *Cancer Science*, *101*(2), 416–24. http://doi.org/10.1111/j.1349-7006.2009.01414.x

Bertin, G., & Averbeck, D. (2006). Cadmium: cellular effects, modifications of biomolecules, modulation of DNA repair and genotoxic consequences (a review). *Biochimie*, *88*(11), 1549–59. http://doi.org/10.1016/j.biochi.2006.10.001

Bhat, A., Heinzel, A., Mayer, B., Perco, P., Mühlberger, I., Husi, H., … Jankowski, V. (2015). Protein interactome of muscle invasive bladder cancer. *PloS One*, *10*(1), e0116404. http://doi.org/10.1371/journal.pone.0116404

Bialkowski, K., Bialkowska, A., & Kasprzak, K. S. (1999). Cadmium(II), unlike nickel(II), inhibits 8-oxo-dGTPase activity and increases 8-oxo-dG level in DNA of the rat testis, a target organ for cadmium(II) carcinogenesis. *Carcinogenesis*, *20*(8), 1621–1624. http://doi.org/10.1093/carcin/20.8.1621

Bid, H. K., Manchanda, P. K., & Mittal, R. D. (2006). Association of interleukin-1Ra gene polymorphism in patients with bladder cancer: case control study from North India. *Urology*, *67*(5), 1099–104. http://doi.org/10.1016/j.urology.2005.11.032

Bozdoğan, S. T., Erol, B., Dursun, a., Bozdoğan, G., Dönmez, I., Mungan, N. a., & Seydaoglu, G. (2014). The IL-1RN and IL-4 gene polymorphisms are potential

genetic markers of susceptibility to bladder cancer: a case–control study. *World Journal of Urology*, *33*(3), 389–395. http://doi.org/10.1007/s00345-014-1323-4

Bredfeldt, T. G., Kopplin, M. J., & Gandolfi, A. J. (2004). Effects of arsenite on UROtsa cells: low-level arsenite causes accumulation of ubiquitinated proteins that is enhanced by reduction in cellular glutathione levels. *Toxicology and Applied Pharmacology*, *198*(3), 412–8. http://doi.org/10.1016/j.taap.2003.10.013

Bryan, R. T. (2014). Cell adhesion and urothelial bladder cancer : the role of cadherin switching and related phenomena. *Philosophical Transactions R Soc B*, *370*, 20140042. Retrieved from http://dx.doi.org/10.1098/rstb.2014.0042

Bryan, R. T., & Tselepis, C. (2010). Cadherin switching and bladder cancer. *The Journal of Urology*, *184*(2), 423–31. http://doi.org/10.1016/j.juro.2010.04.016

Bustaffa, E., Stoccoro, A., Bianchi, F., & Migliore, L. (2014). Genotoxic and epigenetic mechanisms in arsenic carcinogenicity. *Archives of Toxicology*, *88*(5), 1043–67. http://doi.org/10.1007/s00204-014-1233-7

Cao, L., Zhou, X. D., Sens, M. A., Garrett, S. H., Zheng, Y., Dunlevy, J. R., … Somji, S. (2010). Keratin 6 expression correlates to areas of squamous differentiation in multiple independent isolates of As+3-induced bladder cancer. *Journal of Applied Toxicology*, *30*(5), 416–430. http://doi.org/10.1002/jat.1513

Capaldo, C., & Macara, I. (2007). Depletion of E-Cadherin Disrupts Establishment but Not Maintenance of Cell Junctions in Madin-Darby Canine Kidney Epithelial Cells. *Molecular Biology of the Cell*, *18*, 189–200. http://doi.org/10.1091/mbc.E06

Carballo, R., Castineiras, A., Dominguez-Martin, A., Garcia-Santos, I., & Niclos-Gutierrez, J. (2013). Solid state structures of cadmium complexes with relevance for biological systems. In A. Sigel, H. Sigel, & R. Sigel (Eds.), *Cadmium: From Toxicity to Essentiality* (1st ed., Vol. 11, pp. 145–89). Springer Netherlands. http://doi.org/10.1007/978-94-007-5179-8

Carella, C., Potter, M., Bonten, J., Rehg, J. E., Neale, G., & Grosveld, G. C. (2006). The ETS factor TEL2 is a hematopoietic oncoprotein. *Blood*, *107*(3), 1124–32. http://doi.org/10.1182/blood-2005-03-1196

Casalino, E., Sblano, C., & Landriscina, C. (1997). Enzyme activity alteration by cadmium administration to rats: the possibility of iron involvement in lipid peroxidation. *Archives of Biochemistry and Biophysics*, *346*(2), 171–9. http://doi.org/10.1006/abbi.1997.0197

Celià-Terrassa, T., Meca-Cortés, O., Mateo, F., de Paz, A. M., Rubio, N., Arnal-Estapé, A., … Thomson, T. M. (2012). Epithelial-mesenchymal transition can suppress

major attributes of human epithelial tumor-initiating cells. *The Journal of Clinical Investigation*, *122*(5), 1849–68. http://doi.org/10.1172/JCI59218

Chakraborty, P. K., Scharner, B., Jurasovic, J., Messner, B., Bernhard, D., & Thévenod, F. (2010). Chronic cadmium exposure induces transcriptional activation of the Wnt pathway and upregulation of epithelial-to-mesenchymal transition markers in mouse kidney. *Toxicology Letters*, *198*(1), 69–76. http://doi.org/10.1016/j.toxlet.2010.05.007

Chan, K. S., Espinosa, I., Chao, M., Wong, D., Ailles, L., Diehn, M., … Weissman, I. L. (2009). Identification, molecular characterization, clinical prognosis, and therapeutic targeting of human bladder tumor-initiating cells. *Proceedings of the National Academy of Sciences of the United States of America*, *106*(33), 14016–21. http://doi.org/10.1073/pnas.0906549106

Chen, C., Chiou, H., Hsueh, Y., Chen, C., Yu, H., & Pu, Y. (2009). Clinicopathological characteristics and survival outcome of arsenic related bladder cancer in Taiwan. *The Journal of Urology*, *181*(2), 547–53. http://doi.org/10.1016/j.juro.2008.10.003

Chen, C. J., Chen, C. W., Wu, M. M., & Kuo, T. L. (1992). Cancer potential in liver, lung, bladder and kidney due to ingested inorganic arsenic in drinking water. *British Journal of Cancer*, *66*(5), 888–92. Retrieved from http://www.pubmedcentral.nih.gov/articlerender.fcgi?artid=1977977&tool=pmcentrez&rendertype=abstract

Chen, C. J., Chuang, Y. C., Lin, T. M., & Wu, H. Y. (1985). Malignant neoplasms among residents of a blackfoot disease-endemic area in Taiwan: High-arsenic artesian well water and cancers. *Cancer Research*, *45*(11 II), 5895–5899. Retrieved from http://cancerres.aacrjournals.org/content/45/11_Part_2/5895.short

Chen, C. J., Chuang, Y. C., You, S. L., Lin, T. M., & Wu, H. Y. (1986). A retrospective study on malignant neoplasms of bladder, lung and liver in blackfoot disease endemic area in Taiwan. *British Journal of Cancer*, *53*(3), 399–405. Retrieved from http://www.pubmedcentral.nih.gov/articlerender.fcgi?artid=2001352&tool=pmcentrez&rendertype=abstract

Chen, C. J., & Wang, C. J. (1990). Ecological correlation between arsenic level in well water and age-adjusted mortality from malignant neoplasms. *Cancer Research*, *50*, 5470–5474.

Chen, S., Wang, Y., Hsu, J., Chang, H., Wang, C., Shen, P., … Chow, N. (2010). Nucleophosmin in the pathogenesis of arsenic-related bladder carcinogenesis revealed by quantitative proteomics. *Toxicology and Applied Pharmacology*, *242*(2), 126–35. http://doi.org/10.1016/j.taap.2009.09.016

Chen, W. T., Hung, W. C., Kang, W. Y., Huang, Y. C., & Chai, C. Y. (2007). Urothelial carcinomas arising in arsenic-contaminated areas are associated with hypermethylation of the gene promoter of the death-associated protein kinase. *Histopathology*, *51*(6), 785–792. http://doi.org/10.1111/j.1365-2559.2007.02871.x

Chen, Y., Su, H. J., Guo, Y. L., Hsueh, Y., Smith, T., Ryan, L., … Christiani, D. (2003). Arsenic methylation and bladder cancer risk in Taiwan. *Cancer Causes & Control : CCC*, *14*(4), 303–10. Retrieved from http://www.ncbi.nlm.nih.gov/pubmed/12846360

Cheng, G. Z., Zhang, W., & Wang, L. (2008). Regulation of cancer cell survival, migration, and invasion by Twist: AKT2 comes to interplay. *Cancer Research*, *68*(4), 957–60. http://doi.org/10.1158/0008-5472.CAN-07-5067

Chiou, H., Hsueh, Y., Liaw, K., Horng, S., Chiang, M., Pu, Y., … Chen, C. (1995). Incidence of internal cancers and ingested inorganic arsenic: a seven-year follow-up study in Taiwan. *Cancer Research*, *55*, 1296–1300.

Chou, W.-C., Chen, H.-Y., Yu, S.-L., Cheng, L., Yang, P.-C., & Dang, C. V. (2005). Arsenic suppresses gene expression in promyelocytic leukemia cells partly through Sp1 oxidation. *Blood*, *106*(1), 304–10. http://doi.org/10.1182/blood-2005-01-0241

Choudhury, H., Harvey, T., Thayer, W. C., Lockwood, T. F., Stiteler, W. M., Goodrum, P. E., … Diamond, G. L. (2001). Urinary cadmium elimination as a biomarker of exposure for evaluating a cadmium dietary exposure--biokinetics model. *Journal of Toxicology and Environmental Health. Part A*, *63*(5), 321–350. http://doi.org/10.1080/15287390152103643

Chu, F., Ren, X., Chasse, A., Hickman, T., Zhang, L., Yuh, J., … Burlingame, A. L. (2011). Quantitative mass spectrometry reveals the epigenome as a target of arsenic. In *Chemico-Biological Interactions* (Vol. 192, pp. 113–117). http://doi.org/10.1016/j.cbi.2010.11.003

Chung, J., Nartey, N. O., & Cherian, M. G. (1986). Metallothionein levels in liver and kidney of Canadians--a potential indicator of environmental exposure to cadmium. *Archives of Environmental Health*, *41*(5), 319–323.

Clark, A. B., & Kunkel, T. A. (2004). Cadmium inhibits the functions of eukaryotic MutS complexes. *Journal of Biological Chemistry*, *279*(52), 53903–53906. http://doi.org/10.1074/jbc.C400495200

Clarke, M. F., Dick, J. E., Dirks, P. B., Eaves, C. J., Jamieson, C. H. M., Jones, D. L., … Wahl, G. M. (2006). Cancer stem cells--perspectives on current status and future directions: AACR Workshop on cancer stem cells. *Cancer Research*, *66*(19), 9339–9344. http://doi.org/10.1158/0008-5472.CAN-06-3126

Clewell, H. J., Thomas, R. S., Kenyon, E. M., Hughes, M. F., Adair, B. M., Gentry, P. R., & Yager, J. W. (2011). Concentration- and time-dependent genomic changes in the mouse urinary bladder following exposure to arsenate in drinking water for up to 12 weeks. *Toxicological Sciences*, *123*(2), 421–432. http://doi.org/10.1093/toxsci/kfr199

Cohen, S. M., Arnold, L. L., Beck, B. D., Lewis, A. S., & Eldan, M. (2013). Evaluation of the carcinogenicity of inorganic arsenic. *Critical Reviews in Toxicology*, *43*(9), 711–52. http://doi.org/10.3109/10408444.2013.827152

Cohen, S. M., Arnold, L. L., Eldan, M., Lewis, A. S., & Beck, B. D. (2006). Methylated arsenicals: the implications of metabolism and carcinogenicity studies in rodents to human risk assessment. *Critical Reviews in Toxicology*, *36*(2), 99–133. http://doi.org/Doi 10.1080/10408440500534230

Cohen, S. M., Arnold, L. L., Uzvolgyi, E., Cano, M., St. John, M., Yamamoto, S., … Le, X. C. (2002). Possible role of dimethylarsinous acid in dimethylarsinic acid-induced urothelial toxicity and regeneration in the rat. *Chemical Research in Toxicology*, *15*(9), 1150–1157. http://doi.org/10.1021/tx020026z

Cubilla, A., Dillner, J., Schellhammer, P., Horenglas, S., Ayala, A., Reuter, V., & Krog, G. Von. (2004). Tumors of the urinary system. In J. Eble, G. Sauter, J. Epstein, & I. Sesterhenn (Eds.), *World Health Organization Classification of Tumours Pathology and Genetics of Tumours of the Urinary System and Male Genital Organs* (pp. 89–127). Lyon: IARC Press. http://doi.org/10.1016/j.urology.2004.09.048

Dally, H., & Hartwig, A. (1997). Induction and repair inhibition of oxidative DNA damage by nickel(II) and cadmium(II) in mammalian cells. *Carcinogenesis*, *18*(5), 1021–1026. http://doi.org/10.1093/carcin/18.5.1021

Dalton, T. P., He, L., Wang, B., Miller, M. L., Jin, L., Stringer, K. F., … Nebert, D. W. (2005). Identification of mouse SLC39A8 as the transporter responsible for cadmium-induced toxicity in the testis. *Proceedings of the National Academy of Sciences of the United States of America*, *102*(9), 3401–6. http://doi.org/10.1073/pnas.0406085102

Daniel, V. C., Marchionni, L., Hierman, J. S., Rhodes, J. T., Devereux, W. L., Rudin, C. M., … Watkins, D. N. (2009). A primary xenograft model of small-cell lung cancer reveals irreversible changes in gene expression imposed by culture in vitro. *Cancer Research*, *69*(8), 3364–73. http://doi.org/10.1158/0008-5472.CAN-08-4210

Demicheli, C., Frézard, F., Pereira, F. A., Santos, D. M., Mangrum, J. B., & Farrell, N. P. (2011). Interaction of arsenite with a zinc finger CCHC peptide: evidence for formation of an As-Zn-peptide mixed complex. *Journal of Inorganic Biochemistry*, *105*(12), 1753–8. http://doi.org/10.1016/j.jinorgbio.2011.09.023

Dietrich, H., & Dietrich, B. (2001). Ludwig Rehn (1849-1930)--pioneering findings on the aetiology of bladder tumours. *World Journal of Urology*, *19*(2), 151–153. http://doi.org/10.1007/s003450100211

Dodmane, P. R., Arnold, L. L., Kakiuchi-Kiyota, S., Qiu, F., Liu, X., Rennard, S. I., & Cohen, S. M. (2013). Cytotoxicity and gene expression changes induced by inorganic and organic trivalent arsenicals in human cells. *Toxicology*, *312*(1), 18–29. http://doi.org/10.1016/j.tox.2013.07.008

Dong, Z., Radinsky, R., Fan, D., Tsan, R., Bucana, C. D., Wilmanns, C., & Fidler, I. J. (1994). Organ-specific modulation of steady-state mdr gene expression and drug resistance in murine colon cancer cells. *Journal of the National Cancer Institute*, *86*(12), 913–920.

Drobná, Z., Jaspers, I., Thomas, D. J., & Stýblo, M. (2003). Differential activation of AP-1 in human bladder epithelial cells by inorganic and methylated arsenicals. *FASEB Journal : Official Publication of the Federation of American Societies for Experimental Biology*, *17*(1), 67–69. http://doi.org/10.1096/fj.02-0287fje

Drobná, Z., Walton, F. S., Paul, D. S., Xing, W., Thomas, D. J., & Stýblo, M. (2010). Metabolism of arsenic in human liver: The role of membrane transporters. *Archives of Toxicology*, *84*(1), 3–16. http://doi.org/10.1007/s00204-009-0499-7

Eblin, K. E., Bowen, M. E., Cromey, D. W., Bredfeldt, T. G., Mash, E. A., Lau, S. S., & Gandolfi, A. J. (2006). Arsenite and monomethylarsonous acid generate oxidative stress response in human bladder cell culture. *Toxicology and Applied Pharmacology*, *217*(1), 7–14. http://doi.org/10.1016/j.taap.2006.07.004

Edgecombe, A., Nguyen, B. N., Djordjevic, B., Belanger, E. C., & Mai, K. T. (2012). Utility of Cytokeratin 5/6, Cytokeratin 20, and p16 in the Diagnosis of Reactive Urothelial Atypia and Noninvasive Component of Urothelial Neoplasia. *Applied Immunohistochemistry & Molecular Morphology*, *20*(3), 264–271. http://doi.org/10.1097/PAI.0b013e3182351ed3

Eneman, J. D., Potts, R. J., Osier, M., Shukla, G. S., Lee, C. H., Chiu, J. F., & Hart, B. A. (2000). Suppressed oxidant-induced apoptosis in cadmium adapted alveolar epithelial cells and its potential involvement in cadmium carcinogenesis. *Toxicology*, *147*(3), 215–228. http://doi.org/10.1016/S0300-483X(00)00215-8

EPA. (1985). Cadmium contamination of the environment: an assessment of nationwide risk. Office of Water Regulations and Standards. Washington, D.C.

EPA. (2001). National Primary Drinking Water Regulations; Arsenic and Clarifications to Compliance and New Source Contaminants Monitoring. In *Federal Register* (Vol. 66, pp. 6976–7066).

Escudero-Lourdes, C., Medeiros, M. K., Cárdenas-González, M. C., Wnek, S. M., & Gandolfi, J. A. (2010). Low level exposure to monomethyl arsonous acid-induced the over-production of inflammation-related cytokines and the activation of cell signals associated with tumor progression in a urothelial cell model. *Toxicology and Applied Pharmacology*, *244*(2), 162–73. http://doi.org/10.1016/j.taap.2009.12.029

FDA. (2008). Total Diet Study. Elements Results Summary Statistics. Market Baskets 2006 through 2011 (Vol. 33). Center for Food Safety and Applied Nutrition. College Park, Maryland.

Feki-Tounsi, M., & Hamza-Chaffai, A. (2014). Cadmium as a possible cause of bladder cancer: a review of accumulated evidence. *Environmental Science and Pollution Research International*, *21*(18), 10561–73. http://doi.org/10.1007/s11356-014-2970-0

Feki-Tounsi, M., Olmedo, P., Gil, F., Khlifi, R., Mhiri, M.-N., Rebai, A., & Hamza-Chaffai, A. (2013a). Cadmium in blood of Tunisian men and risk of bladder cancer: interactions with arsenic exposure and smoking. *Environmental Science and Pollution Research International*, *20*(10), 7204–13. http://doi.org/10.1007/s11356-013-1716-8

Feki-Tounsi, M., Olmedo, P., Gil, F., Khlifi, R., Mhiri, M.-N., Rebai, A., & Hamza-Chaffai, A. (2013b). Low-level arsenic exposure is associated with bladder cancer risk and cigarette smoking: a case-control study among men in Tunisia. *Environmental Science and Pollution Research International*, *20*(6), 3923–31. http://doi.org/10.1007/s11356-012-1335-9

Fondrevelle, M. E., Kantelip, B., Reiter, R. E., Chopin, D. K., Thiery, J. P., Monnien, F., … Wallerand, H. (2009). The expression of Twist has an impact on survival in human bladder cancer and is influenced by the smoking status. *Urologic Oncology*, *27*(3), 268–76. http://doi.org/10.1016/j.urolonc.2007.12.012

Forman, H. J., Zhang, H., & Rinna, A. (2009). Glutathione: overview of its protective roles, measurement, and biosynthesis. *Molecular Aspects of Medicine*, *30*(1-2), 1–12. http://doi.org/10.1016/j.mam.2008.08.006

Freedman, N. D., Silverman, D. T., Hollenbeck, A. R., Schatzkin, A., & Abnet, C. C. (2011). Association between smoking and risk of bladder cancer among men and women. *JAMA*, *306*(7), 737–45. http://doi.org/10.1001/jama.2011.1142

Gao, J., Zhu, Y., Nilsson, M., & Sundfeldt, K. (2014). TGF-β isoforms induce EMT independent migration of ovarian cancer cells. *Cancer Cell International*, *14*(1), 72. http://doi.org/10.1186/s12935-014-0072-1

Garrett, S. H., Somji, S., Sens, D. A., & Zhang, K. K. (2014). Prediction of the number of activated genes in multiple independent Cd(+2)- and As(+3)-induced malignant

transformations of human urothelial cells (UROtsa). *PloS One*, *9*(1), e85614. http://doi.org/10.1371/journal.pone.0085614

Garson, K., Shaw, T. J., Clark, K. V, Yao, D.-S., & Vanderhyden, B. C. (2005). Models of ovarian cancer--are we there yet? *Molecular and Cellular Endocrinology*, *239*(1-2), 15–26. http://doi.org/10.1016/j.mce.2005.03.019

Ge, Y., Gong, Z., Olson, J. R., Xu, P., Buck, M. J., & Ren, X. (2013). Inhibition of monomethylarsonous acid (MMAIII)-induced cell malignant transformation through restoring dysregulated histone acetylation. *Toxicology*, *312*(1), 30–35. http://doi.org/10.1016/j.tox.2013.07.011

Gerlinger, M., Catto, J. W., Orntoft, T. F., Real, F. X., Zwarthoff, E. C., & Swanton, C. (2014). Intratumour Heterogeneity in Urologic Cancers: From Molecular Evidence to Clinical Implications. *European Urology*, pp. 729–37. http://doi.org/10.1016/j.eururo.2014.04.014

Gerlinger, M., & Swanton, C. (2010). How Darwinian models inform therapeutic failure initiated by clonal heterogeneity in cancer medicine. *British Journal of Cancer*, *103*(8), 1139–43. http://doi.org/10.1038/sj.bjc.6605912

Giaginis, C., Gatzidou, E., & Theocharis, S. (2006). DNA repair systems as targets of cadmium toxicity. *Toxicology and Applied Pharmacology*, *213*(3), 282–90. http://doi.org/10.1016/j.taap.2006.03.008

Girijashanker, K., He, L., Soleimani, M., Reed, J. M., Li, H., Liu, Z., … Nebert, D. W. (2008). Slc39a14 gene encodes ZIP14, a metal/bicarbonate symporter: similarities to the ZIP8 transporter. *Molecular Pharmacology*, *73*(5), 1413–23. http://doi.org/10.1124/mol.107.043588

Goodwin Jinesh, G., Willis, D. L., & Kamat, A. M. (2014). Bladder cancer stem cells: biological and therapeutic perspectives. *Current Stem Cell Research & Therapy*, *9*(2), 89–101. http://doi.org/10.2174/1574888X08666131113123051

Groen, R. W. J., de Rooij, M. F. M., Kocemba, K. A., Reijmers, R. M., de Haan-Kramer, A., Overdijk, M. B., … Spaargaren, M. (2011). N-cadherin-mediated interaction with multiple myeloma cells inhibits osteoblast differentiation. *Haematologica*, *96*(11), 1653–61. http://doi.org/10.3324/haematol.2010.038133

Grooteclaes, M. L., & Frisch, S. M. (2000). Evidence for a function of CtBP in epithelial gene regulation and anoikis. *Oncogene*, *19*(33), 3823–3828. http://doi.org/10.1038/sj.onc.1203721

Gu, X., Shin, B. H., Akbarali, Y., Weiss, A., Boltax, J., Oettgen, P., & Libermann, T. A. (2001). Tel-2 is a novel transcriptional repressor related to the Ets factor Tel/ETV-6.

The Journal of Biological Chemistry, *276*(12), 9421–36. http://doi.org/10.1074/jbc.M010070200

Gumbiner, B., Stevenson, B., & Grimaldi, A. (1988). The role of the cell adhesion molecule uvomorulin in the formation and maintenance of the epithelial junctional complex. *The Journal of Cell Biology*, *107*(4), 1575–87. Retrieved from http://www.pubmedcentral.nih.gov/articlerender.fcgi?artid=2115263&tool=pmcentrez&rendertype=abstract

Hall, M. N., Niedzwiecki, M., Liu, X., Harper, K. N., Alam, S., Slavkovich, V., … Gamble, M. V. (2013). Chronic arsenic exposure and blood glutathione and glutathione disulfide concentrations in Bangladeshi adults. *Environmental Health Perspectives*, *121*(9), 1068–74. http://doi.org/10.1289/ehp.1205727

Ham, W. S., Lee, J. H., Yu, H. S., & Choi, Y. D. (2008). Expression of chicken ovalbumin upstream promoter-transcription factor I (COUP-TFI) in bladder transitional cell carcinoma. *Urology*, *72*(4), 921–6. http://doi.org/10.1016/j.urology.2008.02.019

Han, Y. Y., Weissfeld, J. L., Davis, D. L., & Talbott, E. O. (2009). Arsenic levels in ground water and cancer incidence in Idaho: An ecologic study. *International Archives of Occupational and Environmental Health*, *82*, 843–849. http://doi.org/10.1007/s00420-008-0362-9

Hanas, J. S., & Gunn, C. G. (1996). Inhibition of transcription factor IIIA-DNA interactions by xenobiotic metal ions. *Nucleic Acids Research*, *24*(5), 924–930. http://doi.org/10.1093/nar/24.5.924

Hänze, J., Henrici, M., Hegele, A., Hofmann, R., & Olbert, P. J. (2013). Epithelial mesenchymal transition status is associated with anti-cancer responses towards receptor tyrosine-kinase inhibition by dovitinib in human bladder cancer cells. *BMC Cancer*, *13*, 589. http://doi.org/10.1186/1471-2407-13-589

Hartwig, A., Asmuss, M., Blessing, H., Hoffmann, S., Jahnke, G., Khandelwal, S., … Bürkle, A. (2002). Interference by toxic metal ions with zinc-dependent proteins involved in maintaining genomic stability. *Food and Chemical Toxicology*, *40*(8), 1179–1184. http://doi.org/10.1016/S0278-6915(02)00043-1

Hazan, R. B., Phillips, G. R., Qiao, R. F., Norton, L., & Aaronson, S. A. (2000). Exogenous expression of N-cadherin in breast cancer cells induces cell migration, invasion, and metastasis. *The Journal of Cell Biology*, *148*(4), 779–90. Retrieved from http://www.pubmedcentral.nih.gov/articlerender.fcgi?artid=2169367&tool=pmcentrez&rendertype=abstract

He, J., Pan, Y., Hu, J., Albarracin, C., Wu, Y., & Dai, J. Le. (2007). Profile of Ets gene expression in human breast carcinoma. *Cancer Biology & Therapy*, *6*(1), 76–82. Retrieved from http://www.ncbi.nlm.nih.gov/pubmed/17172821

He, X., Marchionni, L., Hansel, D., Yu, W., Sood, A., Yang, J., … Berman, D. (2009). Differentiation of a Highly Tumorigenic Basal Cell Compartment in Urothelial Carcinoma. *Stem Cells*, *27*(7), 1487–95. http://doi.org/10.1016/j.biotechadv.2011.08.021.Secreted

Hernández-Zavala, A., Valenzuela, O. L., Matousek, T., Drobná, Z., Dědina, J., García-Vargas, G. G., … Stýblo, M. (2008). Speciation of arsenic in exfoliated urinary bladder epithelial cells from individuals exposed to arsenic in drinking water. *Environmental Health Perspectives*, *116*(12), 1656–60. http://doi.org/10.1289/ehp.11503

Ho, P. L., Kurtova, A., & Chan, K. S. (2012). Normal and neoplastic urothelial stem cells: getting to the root of the problem. *Nature Reviews. Urology*, *9*(10), 583–94. http://doi.org/10.1038/nrurol.2012.142

Hopenhayn-Rich, C., Biggs, M. L., Fuchs, A., Bergoglio, R., Tello, E. E., Nicolli, H., & Smith, A. (1996). Bladder cancer mortality associated with arsenic in drinking water in Argentina. *Epidemiology (Cambridge, Mass.)*, *7*(2), 117–24. Retrieved from http://www.ncbi.nlm.nih.gov/pubmed/8834549

Horejsí, Z., Takai, H., Adelman, C. A., Collis, S. J., Flynn, H., Maslen, S., … Boulton, S. J. (2010). CK2 phospho-dependent binding of R2TP complex to TEL2 is essential for mTOR and SMG1 stability. *Molecular Cell*, *39*(6), 839–50. http://doi.org/10.1016/j.molcel.2010.08.037

Howlader, N., Noone, A., Krapcho, M., Garshell, J., Miller, D., Altekruse, S., … KA, C. (Eds.). (2014). *SEER Cancer Statistics Review, 1975-2011*. Bethesda, MD: National Cancer Institute.

Huang, C., Ke, Q., Costa, M., & Shi, X. (2004). Molecular mechanisms of arsenic carcinogenesis. *Molecular and Cellular Biochemistry*, *255*(1-2), 57–66. Retrieved from http://www.ncbi.nlm.nih.gov/pubmed/14971646

Huang, Y. C., Hung, W. C., Chen, W. T., Jiang, W. H., Yu, H. S., & Chai, C. Y. (2011). Effects of MEK and DNMT inhibitors on arsenic-treated human uroepithelial cells in relation to Cyclin-D1 and p16. *Toxicology Letters*, *200*(1-2), 59–66. http://doi.org/10.1016/j.toxlet.2010.10.015

Huang, Y., Hung, W., Chen, W., Yu, H., & Chai, C. (2011). Effects of DNMT and MEK inhibitors on the expression of RECK, MMP-9, -2, uPA and VEGF in response to arsenite stimulation in human uroepithelial cells. *Toxicology Letters*, *201*(1), 62–71. http://doi.org/10.1016/j.toxlet.2010.12.006

Hubert, R. S., Vivanco, I., Chen, E., Rastegar, S., Leong, K., Mitchell, S. C., … Afar, D. E. (1999). STEAP: a prostate-specific cell-surface antigen highly expressed in human prostate tumors. *Proceedings of the National Academy of Sciences of the United States of America*, *96*(25), 14523–8. Retrieved from http://www.pubmedcentral.nih.gov/articlerender.fcgi?artid=24469&tool=pmcentrez&rendertype=abstract

Hueper, W., Wiley, F., & Wolfe, H. (1938). Experimental production of bladder tumors in dogs by administration of beta-naphthylamine. *Journal of Industrial Hygeine and Toxicology*, *20*, 46–84.

Hughes, M. F., Kenyon, E. M., Edwards, B. C., Mitchell, C. T., Del Razo, L. M., & Thomas, D. J. (2003). Accumulation and metabolism of arsenic in mice after repeated oral administration of arsenate. *Toxicology and Applied Pharmacology*, *191*(3), 202–210. http://doi.org/10.1016/S0041-008X(03)00249-7

IARC. (1993). Beryllium, cadmium, mercury, and exposures in the glass manufacturing industry. In IARC Working Group on the Evaluation of Carcinogenic Risks to Humans (Ed.), *IARC Monographs on the Evaluation of Carcinogenic Risks to Humans* (Vol. 58). Lyon, France: Interanational Agency for Research on Cancer.

Ikenouchi, J., Matsuda, M., Furuse, M., & Tsukita, S. (2003). Regulation of tight junctions during the epithelium-mesenchyme transition: direct repression of the gene expression of claudins/occludin by Snail. *Journal of Cell Science*, *116*(Pt 10), 1959–1967. http://doi.org/10.1242/jcs.00389

Imao, T., Koshida, K., Endo, Y., Uchibayashi, T., Sasaki, T., & Namiki, M. (1999). Dominant role of E-cadherin in the progression of bladder cancer. *The Journal of Urology*, *161*(2), 692–698. http://doi.org/10.1016/S0022-5347(01)61997-9

Inaba, T., Kobayashi, E., Suwazono, Y., Uetani, M., Oishi, M., Nakagawa, H., & Nogawa, K. (2005). Estimation of cumulative cadmium intake causing Itai-itai disease. *Toxicology Letters*, *159*(2), 192–201. http://doi.org/10.1016/j.toxlet.2005.05.011

Jäger, T., Becker, M., Eisenhardt, A., Tilki, D., Tötsch, M., Schmid, K. W., … Szarvas, T. (2010). The prognostic value of cadherin switch in bladder cancer. *Oncology Reports*, *23*(4), 1125–1132. http://doi.org/10.3892/or-00000741

Jensen, T. J., Novak, P., Eblin, K. E., Gandolfi, A. J., & Futscher, B. W. (2008). Epigenetic remodeling during arsenical-induced malignant transformation. *Carcinogenesis*, *29*(8), 1500–8. http://doi.org/10.1093/carcin/bgn102

Jensen, T. J., Novak, P., Wnek, S. M., Gandolfi, A. J., & Futscher, B. W. (2009). Arsenicals produce stable progressive changes in DNA methylation patterns that are

linked to malignant transformation of immortalized urothelial cells. *Toxicology and Applied Pharmacology*, *241*(2), 221–9. http://doi.org/10.1016/j.taap.2009.08.019

Jiang, G., Gong, Z., Li, X., Cullen, W. R., & Le, X. C. (2003). Interaction of trivalent arsenicals with metallothionein. *Chemical Research in Toxicology*, *16*(7), 873–880. http://doi.org/10.1021/tx034053g

Jiang, R., Li, Y., Xu, Y., Zhou, Y., Pang, Y., Shen, L., … Liu, Q. (2013). EMT and CSC-like properties mediated by the IKKβ/IκBα/RelA signal pathway via the transcriptional regulator, Snail, are involved in the arsenite-induced neoplastic transformation of human keratinocytes. *Archives of Toxicology*, *87*(6), 991–1000. http://doi.org/10.1007/s00204-012-0933-0

Jin, T., Lu, J., & Nordberg, M. (1998). Toxicokinetics and biochemistry of cadmium with special emphasis on the role of metallothionein. *Neurotoxicology*, *19*(4-5), 529–536.

Jing, Y., Liu, L., Jiang, Y., Zhu, Y., Guo, N. L., Barnett, J., … Jiang, B. (2012). Cadmium increases HIF-1 and VEGF expression through ROS, ERK, and AKT signaling pathways and induces malignant transformation of human bronchial epithelial cells. *Toxicological Sciences : An Official Journal of the Society of Toxicology*, *125*(1), 10–9. http://doi.org/10.1093/toxsci/kfr256

Jo, W. J., Ren, X., Chu, F., Aleshin, M., Wintz, H., Burlingame, A., … Zhang, L. (2009). Acetylated H4K16 by MYST1 protects UROtsa cells from arsenic toxicity and is decreased following chronic arsenic exposure. *Toxicology and Applied Pharmacology*, *241*(3), 294–302. http://doi.org/10.1016/j.taap.2009.08.027

Johansson, S. L., & Cohen, S. M. (1997). Epidemiology and etiology of bladder cancer. *Seminars in Surgical Oncology*, *13*(5), 291–8. Retrieved from http://www.ncbi.nlm.nih.gov/pubmed/9259084

Joseph, P. (2009). Mechanisms of cadmium carcinogenesis. *Toxicology and Applied Pharmacology*, *238*(3), 272–9. http://doi.org/10.1016/j.taap.2009.01.011

Joseph, P., Muchnok, T. K., Klishis, M. L., Roberts, J. R., Antonini, J. M., Whong, W. Z., & Ong, T. M. (2001). Cadmium-induced cell transformation and tumorigenesis are associated with transcriptional activation of c-fos, c-jun, and c-myc proto-oncogenes: Role of cellular calcium and reactive oxygen species. *Toxicological Sciences*, *61*(2), 295–303. http://doi.org/10.1093/toxsci/61.2.295

Jost, S. P., Gosling, J. A., & Dixon, J. S. (1989). The morphology of normal human bladder urothelium. *Journal of Anatomy*, *167*, 103–15. Retrieved from http://www.pubmedcentral.nih.gov/articlerender.fcgi?artid=1256824&tool=pmcentrez&rendertype=abstract

Jun, J. S., Peng, G. Z., Zi, M. W., Wei, M. G., & Xiang, M. C. (2008). Identification of side population cells from bladder cancer cells by dyecycle violet staining. *Cancer Biology and Therapy*, *7*(10), 1663–1668. http://doi.org/10.4161/cbt.7.10.6637

Kaizuka, T., Hara, T., Oshiro, N., Kikkawa, U., Yonezawa, K., Takehana, K., … Mizushima, N. (2010). Tti1 and Tel2 are critical factors in mammalian target of rapamycin complex assembly. *The Journal of Biological Chemistry*, *285*(26), 20109–16. http://doi.org/10.1074/jbc.M110.121699

Kamat, A. M., Hegarty, P. K., Gee, J. R., Clark, P. E., Svatek, R. S., Hegarty, N., … Karakiewicz, P. I. (2013). ICUD-EAU international consultation on bladder cancer 2012: Screening, diagnosis, and molecular markers. *European Urology*, *63*, 4–15. http://doi.org/10.1016/j.eururo.2012.09.057

Kang, Y., Ling, J., Suzuki, R., Roife, D., Chopin-Laly, X., Truty, M. J., … Fleming, J. B. (2014). SMAD4 regulates cell motility through transcription of N-cadherin in human pancreatic ductal epithelium. *PloS One*, *9*(9), e107948. http://doi.org/10.1371/journal.pone.0107948

Kellen, E., Zeegers, M. P., Hond, E. Den, & Buntinx, F. (2007). Blood cadmium may be associated with bladder carcinogenesis: the Belgian case-control study on bladder cancer. *Cancer Detection and Prevention*, *31*(1), 77–82. http://doi.org/10.1016/j.cdp.2006.12.001

Kenyon, E. M., Hughes, M. F., Adair, B. M., Highfill, J. H., Crecelius, E. A., Clewell, H. J., & Yager, J. W. (2008). Tissue distribution and urinary excretion of inorganic arsenic and its methylated metabolites in C57BL6 mice following subchronic exposure to arsenate in drinking water. *Toxicology and Applied Pharmacology*, *232*(3), 448–455. http://doi.org/10.1016/j.taap.2008.07.018

Kitchin, K. T., & Wallace, K. (2008). The role of protein binding of trivalent arsenicals in arsenic carcinogenesis and toxicity. *Journal of Inorganic Biochemistry*, *102*(3), 532–9. http://doi.org/10.1016/j.jinorgbio.2007.10.021

Klaassen, C. D., Liu, J., & Choudhuri, S. (1999). Metallothionein: an intracellular protein to protect against cadmium toxicity. *Annual Review of Pharmacology and Toxicology*, *39*, 267–294. http://doi.org/10.1146/annurev.pharmtox.39.1.267

Klein, C. B., Leszczynska, J., Hickey, C., & Rossman, T. G. (2007). Further evidence against a direct genotoxic mode of action for arsenic-induced cancer. *Toxicology and Applied Pharmacology*, *222*(3), 289–97. http://doi.org/10.1016/j.taap.2006.12.033

Kobayashi, T., Owczarek, T., McKiernan, J., & Abate-Shen, C. (2015). Modelling bladder cancer in mice: opportunities and challenges. *Nature Reviews. Cancer*, *15*(1), 42–54.

Koizumi, T., Shirakura, H., Kumagai, H., Tatsumoto, H., & Suzuki, K. T. (1996). Mechanism of cadmium-induced cytotoxicity in rat hepatocytes: Cadmium-induced active oxygen-related permeability changes of the plasma membrane. *Toxicology*, *114*(2), 125–134. http://doi.org/10.1016/S0300-483X(96)03477-4

Kothinti, R., Blodgett, A., Tabatabai, N. M., & Petering, D. H. (2010). Zinc finger transcription factor Zn3-Sp1 reactions with Cd2+. *Chemical Research in Toxicology*, *23*(2), 405–12. http://doi.org/10.1021/tx900370u

Kubota, T. (1994). Metastatic models of human cancer xenografted in the nude mouse: the importance of orthotopic transplantation. *Journal of Cellular Biochemistry*, *56*(1), 4–8. http://doi.org/10.1002/jcb.240560103

Kuphal, S., & Bosserhoff, a K. (2006). Influence of the cytoplasmic domain of E-cadherin on endogenous N-cadherin expression in malignant melanoma. *Oncogene*, *25*(2), 248–59. http://doi.org/10.1038/sj.onc.1209054

Lamm, S. H., Engel, A., Kruse, M. B., Feinleib, M., Byrd, D. M., Lai, S., & Wilson, R. (2004). Arsenic in Drinking Water and Bladder Cancer Mortality in the United States: An Analysis Based on 133 U.S. Counties and 30 Years of Observation. *Journal of Occupational and Environmental Medicine*, *46*(3), 298–306. http://doi.org/10.1097/01.jom.0000116801.67556.8f

Lamm, S. H., Robbins, S., Chen, R., Lu, J., Goodrich, B., & Feinleib, M. (2014). Discontinuity in the cancer slope factor as it passes from high to low exposure levels – arsenic in the BFD-endemic area. *Toxicology*, *326*, 25–35. http://doi.org/10.1016/j.tox.2014.08.014

Lamouille, S., Xu, J., & Derynck, R. (2014). Molecular mechanisms of epithelial-mesenchymal transition. *Nature Reviews. Molecular Cell Biology*, *15*(3), 178–96. http://doi.org/10.1038/nrm3758

Larson, J. (2012). The UROtsa bladder cell model for heavy metal carcinogenesis: characterization with respect to the role of Beclin-1 and SPARC expression. University of North Dakota School of Medicine and Health Sciences.

Larson, J., Yasmin, T., Sens, D. A., Zhou, X. D., Sens, M. A., Garrett, S. H., … Somji, S. (2010). SPARC gene expression is repressed in human urothelial cells (UROtsa) exposed to or malignantly transformed by cadmium or arsenite. *Toxicology Letters*, *199*(2), 166–172. http://doi.org/10.1016/j.toxlet.2010.08.020

Lascombe, I., Clairotte, A., Fauconnet, S., Bernardini, S., Wallerand, H., Kantelip, B., & Bittard, H. (2006). N-cadherin as a novel prognostic marker of progression in superficial urothelial tumors. *Clinical Cancer Research*, *12*(9), 2780–7. http://doi.org/10.1158/1078-0432.CCR-05-2387

Le Mée, S., Fromigué, O., & Marie, P. J. (2005). Sp1/Sp3 and the myeloid zinc finger gene MZF1 regulate the human N-cadherin promoter in osteoblasts. *Experimental Cell Research*, *302*(1), 129–42. http://doi.org/10.1016/j.yexcr.2004.08.028

Lee, D. H., Lim, J. S., Song, K., Boo, Y., & Jacobs, D. R. (2006). Graded associations of blood lead and urinary cadmium concentrations with oxidative-stress-related markers in the U.S. population: Results from the third National Health and Nutrition Examination Survey. *Environmental Health Perspectives*, *114*(3), 350–354. http://doi.org/10.1289/ehp.8518

Lewis, D. R., Southwick, J. W., Ouellet-Hellstrom, R., Rench, J., & Calderon, R. L. (1999). Drinking water arsenic in Utah: A cohort mortality study. *Environmental Health Perspectives*, *107*(5), 359–65. Retrieved from http://www.pubmedcentral.nih.gov/articlerender.fcgi?artid=1566417&tool=pmcentrez&rendertype=abstract

Li, F., Lan, Y., Wang, Y., Wang, J., Yang, G., Meng, F., … Yang, X. (2011). Endothelial Smad4 maintains cerebrovascular integrity by activating N-cadherin through cooperation with Notch. *Developmental Cell*, *20*(3), 291–302. http://doi.org/10.1016/j.devcel.2011.01.011

Li, F., Tiede, B., Massagué, J., & Kang, Y. (2007). Beyond tumorigenesis: cancer stem cells in metastasis. *Cell Research*, *17*(1), 3–14. http://doi.org/10.1038/sj.cr.7310118

Li, Y., Kimura, T., Huyck, R. W., Laity, J. H., & Andrews, G. K. (2008). Zinc-induced formation of a coactivator complex containing the zinc-sensing transcription factor MTF-1, p300/CBP, and Sp1. *Molecular and Cellular Biology*, *28*(13), 4275–84. http://doi.org/10.1128/MCB.00369-08

Lin, B., Chen, G., Xiao, D., & Kumar, S. (2000). Orphan Receptor COUP-TF Is Required for Induction of Retinoic Acid Receptor β , Growth Inhibition , and Apoptosis by Retinoic Acid in Cancer Cells Orphan Receptor COUP-TF Is Required for Induction of Retinoic Acid Receptor ␣ , Growth Inhibition , and Apop. http://doi.org/10.1128/MCB.20.3.957-970.2000.Updated

Lin, S., Del Razo, L. M., Styblo, M., Wang, C., Cullen, W. R., & Thomas, D. J. (2001). Arsenicals inhibit thioredoxin reductase in cultured rat hepatocytes. *Chemical Research in Toxicology*, *14*(3), 305–311. http://doi.org/10.1021/tx0001878

Liu, B., Miyake, H., Nishikawa, M., & Fujisawa, M. (2015). Expression profile of epithelial-mesenchymal transition markers in non–muscle-invasive urothelial carcinoma of the bladder: Correlation with intravesical recurrence following transurethral resection. *Urologic Oncology: Seminars and Original Investigations*, *33*(3), 110.e11–110.e18. http://doi.org/10.1016/j.urolonc.2014.08.012

Liu, C., Huang, H., Wang, C., Kong, Y., & Zhang, H. (2014). Involvement of ephrin receptor A4 in pancreatic cancer cell motility and invasion. *Oncology Letters*, *7*(6), 2165–2169. http://doi.org/10.3892/ol.2014.2011

Liu, J., Liu, Y., Habeebu, S. S., & Klaassen, C. D. (1998). Susceptibility of MT-null mice to chronic CdCl2-induced nephrotoxicity indicates that renal injury is not mediated by the CdMT complex. *Toxicological Sciences : An Official Journal of the Society of Toxicology*, *46*(1), 197–203. http://doi.org/10.1006/toxs.1998.2541

Liu, L., Qiu, M., Tan, G., Liang, Z., Qin, Y., Chen, L., … Liu, J. (2014). miR-200c Inhibits invasion, migration and proliferation of bladder cancer cells through down-regulation of BMI-1 and E2F3. *Journal of Translational Medicine*, *12*(1), 305. http://doi.org/10.1186/s12967-014-0305-z

Liu, W., Qi, L., Lv, H., Zu, X., Chen, M., Wang, J., … Li, Y. (2015). MiRNA-141 and miRNA-200b are closely related to invasive ability and considered as decision-making biomarkers for the extent of PLND during cystectomy. *BMC Cancer*, *15*(1), 92. http://doi.org/10.1186/s12885-015-1110-7

Liu, Z., Shen, J., Carbrey, J. M., Mukhopadhyay, R., Agre, P., & Rosen, B. P. (2002). Arsenite transport by mammalian aquaglyceroporins AQP7 and AQP9. *Proceedings of the National Academy of Sciences of the United States of America*, *99*(9), 6053–8. http://doi.org/10.1073/pnas.092131899

Lotan, Y., Shariat, S. F., Schmitz-Dräger, B. J., Sanchez-Carbayo, M., Jankevicius, F., Racioppi, M., … Grossman, H. B. (2010). Considerations on implementing diagnostic markers into clinical decision making in bladder cancer. *Urologic Oncology*, *28*(4), 441–448. http://doi.org/10.1016/j.urolonc.2009.11.004

Lu, S. C. (2009). Regulation of glutathione synthesis. *Molecular Aspects of Medicine*, *30*(1-2), 42–59. http://doi.org/10.1016/j.mam.2008.05.005

Lützen, A., Liberti, S. E., & Rasmussen, L. J. (2004). Cadmium inhibits human DNA mismatch repair in vivo. *Biochemical and Biophysical Research Communications*, *321*(1), 21–5. http://doi.org/10.1016/j.bbrc.2004.06.102

MacIntosh, D. L., Williams, P. L., Hunter, D. J., Sampson, L. A., Morris, S. C., Willett, W. C., & Rimm, E. B. (1997). Evaluation of a food frequency questionnaire-food composition approach for estimating dietary intake of inorganic arsenic and methylmercury. *Cancer Epidemiology Biomarkers and Prevention*, *6*(12), 1043–1050.

Maeda, M., Johnson, K. R., & Wheelock, M. J. (2005). Cadherin switching: essential for behavioral but not morphological changes during an epithelium-to-mesenchyme transition. *Journal of Cell Science*, *118*(Pt 5), 873–887. http://doi.org/10.1242/jcs.01634

Maeda, O., Ando, T., Ohmiya, N., Ishiguro, K., Watanabe, O., Miyahara, R., … Goto, H. (2014). Alteration of gene expression and DNA methylation in drug-resistant gastric cancer. *Oncology Reports*, *31*(4), 1883–90. http://doi.org/10.3892/or.2014.3014

Malats, N., & Real, F. X. (2015). Epidemiology of Bladder Cancer. *Hematology/Oncology Clinics of North America*, *29*(2), 177–189. http://doi.org/10.1016/j.hoc.2014.10.001

Marshall, G., Ferreccio, C., Yuan, Y., Bates, M. N., Steinmaus, C., Selvin, S., … Smith, A. (2007). Fifty-year study of lung and bladder cancer mortality in Chile related to arsenic in drinking water. *Journal of the National Cancer Institute*, *99*(12), 920–8. http://doi.org/10.1093/jnci/djm004

Martiáñez, T., Lamarca, A., Casals, N., & Gella, A. (2013). N-cadherin expression is regulated by UTP in schwannoma cells. *Purinergic Signalling*, *9*(2), 259–70. http://doi.org/10.1007/s11302-012-9348-x

Matos, J. M., Witzmann, F. A., Cummings, O. W., & Schmidt, C. M. (2009). A pilot study of proteomic profiles of human hepatocellular carcinoma in the United States. *The Journal of Surgical Research*, *155*(2), 237–43. http://doi.org/10.1016/j.jss.2008.06.008

Matsui, Y., Assi, K., Ogawa, O., Raven, P. a, Dedhar, S., Gleave, M. E., … So, A. I. (2012). The importance of integrin-linked kinase in the regulation of bladder cancer invasion. *International Journal of Cancer. Journal International Du Cancer*, *130*(3), 521–31. http://doi.org/10.1002/ijc.26008

McNeill, D. R., Narayana, A., Wong, H. K., & Wilson, D. M. (2004). Inhibition of Ape1 nuclease activity by lead, iron, and cadmium. *Environmental Health Perspectives*, *112*(7), 799–804. http://doi.org/10.1289/ehp.7038

Medeiros, M., Zheng, X., Novak, P., Wnek, S. M., Chyan, V., Escudero-Lourdes, C., & Gandolfi, A. J. (2012). Global gene expression changes in human urothelial cells exposed to low-level monomethylarsonous acid. *Toxicology*, *291*(1-3), 102–12. http://doi.org/10.1016/j.tox.2011.11.002

Medici, D., Hay, E. D., & Olsen, B. R. (2008). Snail and Slug promote epithelial-mesenchymal transition through beta-catenin-T-cell factor-4-dependent expression of transforming growth factor-beta3. *Molecular Biology of the Cell*, *19*(11), 4875–87. http://doi.org/10.1091/mbc.E08-05-0506

Meliker, J. R., Slotnick, M. J., AvRuskin, G. A., Schottenfeld, D., Jacquez, G. M., Wilson, M. L., … Nriagu, J. O. (2010). Lifetime exposure to arsenic in drinking water and bladder cancer: a population-based case-control study in Michigan, USA. *Cancer Causes & Control : CCC*, *21*(5), 745–57. http://doi.org/10.1007/s10552-010-9503-z

Meliker, J. R., Wahl, R. L., Cameron, L. L., & Nriagu, J. O. (2007). Arsenic in drinking water and cerebrovascular disease, diabetes mellitus, and kidney disease in Michigan: a standardized mortality ratio analysis. *Environmental Health : A Global Access Science Source*, *6*, 4. http://doi.org/10.1186/1476-069X-6-4

Méplan, C., Mann, K., & Hainaut, P. (1999). Cadmium induces conformational modifications of wild-type p53 and suppresses p53 response to DNA damage in cultured cells. *Journal of Biological Chemistry*, *274*(44), 31663–31670. http://doi.org/10.1074/jbc.274.44.31663

Michailidi, C., Hayashi, M., Datta, S., Sen, T., Zenner, K., Oladeru, O., … Hoque, M. O. (2015). Involvement of Epigenetics and EMT-Related miRNA in Arsenic-Induced Neoplastic Transformation and Their Potential Clinical Use. *Cancer Prevention Research (Philadelphia, Pa.)*, *8*(3), 208–221. http://doi.org/10.1158/1940-6207.CAPR-14-0251

Mikhailova, M. V, Littlefield, N. A., Hass, B. S., Poirier, L. A., & Chou, M. W. (1997). Cadmium-induced 8-hydroxydeoxyguanosine formation, DNA strand breaks and antioxidant enzyme activities in lymphoblastoid cells. *Cancer Letters*, *115*(2), 141–148. http://doi.org/10.1016/S0304-3835(97)04720-4

Moreaux, J., Kassambara, A., Hose, D., & Klein, B. (2012). STEAP1 is overexpressed in cancers: a promising therapeutic target. *Biochemical and Biophysical Research Communications*, *429*(3-4), 148–55. http://doi.org/10.1016/j.bbrc.2012.10.123

Mostafa, M. H., Sheweita, S. A., & O'Connor, P. J. (1999). Relationship between schistosomiasis and bladder cancer. *Clinical Microbiology Reviews*, *12*(1), 97–111. Retrieved from http://www.pubmedcentral.nih.gov/articlerender.fcgi?artid=88908&tool=pmcentrez&rendertype=abstract

Muramaki, M., Miyake, H., Terakawa, T., Kumano, M., Sakai, I., & Fujisawa, M. (2012). Expression profile of E-cadherin and N-cadherin in non-muscle-invasive bladder cancer as a novel predictor of intravesical recurrence following transurethral resection. *Urologic Oncology*, *30*(2), 161–6. http://doi.org/10.1016/j.urolonc.2010.01.005

Muramaki, M., Miyake, H., Terakawa, T., Kusuda, Y., & Fujisawa, M. (2011). Expression profile of E-cadherin and N-cadherin in urothelial carcinoma of the upper urinary tract is associated with disease recurrence in patients undergoing nephroureterectomy. *Urology*, *78*(6), 1443.e7–12. http://doi.org/10.1016/j.urology.2011.07.1388

Nesnow, S., Roop, B. C., Lambert, G., Kadiiska, M., Mason, R. P., Cullen, W. R., & Mass, M. J. (2002). DNA damage induced by methylated trivalent arsenicals is

mediated by reactive oxygen species. *Chemical Research in Toxicology*, *15*(12), 1627–1634. http://doi.org/10.1021/tx025598y

Nigam, D., Shukla, G. S., & Agarwal, A. K. (1999). Glutathione depletion and oxidative damage in mitochondria following exposure to cadmium in rat liver and kidney. *Toxicology Letters*, *106*(2-3), 151–157. http://doi.org/10.1016/s0378-4274(99)00059-4

Ning, Z.-F., Huang, Y.-J., Lin, T.-X., Zhou, Y.-X., Jiang, C., Xu, K.-W., … Huang, J. (2009). Subpopulations of stem-like cells in side population cells from the human bladder transitional cell cancer cell line T24. *The Journal of International Medical Research*, *37*(3), 621–630. http://doi.org/10.1177/147323000903700304

NTP. (2011). Cadmium and cadmium compounds. In U.S. Department of Health and Human Services Public Service (Ed.), *Report on Carcinogens* (13th ed., Vol. 100 C, pp. 121–145). Research Triangle Park, NC. http://doi.org/10.1002/14356007.a04

O'Toole, C., Price, Z. H., Ohnuki, Y., & Unsgaard, B. (1978). Ultrastructure, karyology and immunology of a cell line originated from a human transitional-cell carcinoma. *British Journal of Cancer*, *38*(1), 64–76.

Oki, M., Yamamoto, H., Taniguchi, H., Adachi, Y., Imai, K., & Shinomura, Y. (2008). Overexpression of the receptor tyrosine kinase EphA4 in human gastric cancers. *World Journal of Gastroenterology : WJG*, *14*(37), 5650–6. Retrieved from http://www.pubmedcentral.nih.gov/articlerender.fcgi?artid=2748198&tool=pmcentrez&rendertype=abstract

Oottamasathien, S., Williams, K., Franco, O. E., Thomas, J. C., Saba, K., Bhowmick, N. a., … Pope IV, J. C. (2006). Bladder tissue formation from cultured bladder urothelium. *Developmental Dynamics*, *235*(10), 2795–2801. http://doi.org/10.1002/dvdy.20886

Panda, D. K., Miao, D., Lefebvre, V., Hendy, G. N., & Goltzman, D. (2001). The Transcription Factor SOX9 Regulates Cell Cycle and Differentiation Genes in Chondrocytic CFK2 Cells. *Journal of Biological Chemistry*, *276*(44), 41229–41236. http://doi.org/10.1074/jbc.M104231200

Park, J. D., Cherrington, N. J., & Klaassen, C. D. (2002). Intestinal absorption of cadmium is associated with divalent metal transporter 1 in rats. *Toxicological Sciences*, *68*(2), 288–294. http://doi.org/10.1093/toxsci/68.2.288

Peinado, H., Olmeda, D., & Cano, A. (2007). Snail, Zeb and bHLH factors in tumour progression: an alliance against the epithelial phenotype? *Nature Reviews. Cancer*, *7*(6), 415–28. http://doi.org/10.1038/nrc2131

Petzoldt, J. L., Leigh, I. M., Duffy, P. G., Sexton, C., & Masters, J. R. W. (1995). Immortalisation of human urothelial cells. *Urological Research*, *23*(6), 377–380. http://doi.org/10.1007/BF00698738

Polyak, K., & Weinberg, R. a. (2009). Transitions between epithelial and mesenchymal states: acquisition of malignant and stem cell traits. *Nature Reviews. Cancer*, *9*(4), 265–273. http://doi.org/10.1038/nrc2620

Popenoe, E. A., & Schmaeler, M. A. (1979). Interaction of human DNA polymerase beta with ions of copper, lead, and cadmium. *Archives of Biochemistry and Biophysics*, *196*(1), 109–120.

Potts, R. J., Bespalov, I. A., Wallace, S. S., Melamede, R. J., & Hart, B. A. (2001). Inhibition of oxidative DNA repair in cadmium-adapted alveolar epithelial cells and the potential involvement of metallothionein. *Toxicology*, *161*(1-2), 25–38. http://doi.org/10.1016/S0300-483X(00)00419-4

Pratesi, G., Manzotti, C., Tortoreto, M., Audisio, R. A., & Zunino, F. (1991). Differential efficacy of flavone acetic against liver versus lung metastases in a human tumour xenograft. *British Journal of Cancer*, *63*(1), 71–4. Retrieved from http://www.pubmedcentral.nih.gov/articlerender.fcgi?artid=1971638&tool=pmcentrez&rendertype=abstract

Price, D. J., & Joshi, J. G. (1983). Ferritin. Binding of beryllium and other divalent metal ions. *Journal of Biological Chemistry*, *258*, 10873–10880.

Qi, J., Chen, N., Wang, J., & Siu, C.-H. (2005). Transendothelial migration of melanoma cells involves N-cadherin-mediated adhesion and activation of the beta-catenin signaling pathway. *Molecular Biology of the Cell*, *16*(9), 4386–97. http://doi.org/10.1091/mbc.E05-03-0186

Qu, W., Diwan, B. a, Reece, J. M., Bortner, C. D., Pi, J., Liu, J., & Waalkes, M. P. (2005). Cadmium-induced malignant transformation in rat liver cells: role of aberrant oncogene expression and minimal role of oxidative stress. *International Journal of Cancer. Journal International Du Cancer*, *114*(3), 346–55. http://doi.org/10.1002/ijc.20736

Qu, W., Tokar, E. J., Kim, A. J., Bell, M. W., & Waalkes, M. P. (2012). Chronic cadmium exposure in vitro causes acquisition of multiple tumor cell characteristics in human pancreatic epithelial cells. *Environmental Health Perspectives*, *120*(9), 1265–71. http://doi.org/10.1289/ehp.1205082

Rehn, L. (1895). Blasengeschwuelste bei Fuchsinarbeitern. *Arch Klin*, *50*, 588–600.

Rieger-Christ, K. M., Cain, J. W., Braasch, J. W., Dugan, J. M., Silverman, M. L., Bouyounes, B., … Summerhayes, I. C. (2001). Expression of classic cadherins type

I in urothelial neoplastic progression. *Human Pathology*, *32*(1), 18–23. http://doi.org/10.1053/hupa.2001.21140

Rieger-Christ, K. M., Lee, P., Zagha, R., Kosakowski, M., Moinzadeh, A., Stoffel, J., … Summerhayes, I. C. (2004). Novel expression of N-cadherin elicits in vitro bladder cell invasion via the Akt signaling pathway. *Oncogene*, *23*(27), 4745–53. http://doi.org/10.1038/sj.onc.1207629

Rosen, B. P. (2002). Biochemistry of arsenic detoxification. *FEBS Letters*, *529*(1), 86–92. http://doi.org/10.1016/S0014-5793(02)03186-1

Ross, M. H., & Pawlina, W. (2011). *Histology: A text and atlas* (6th ed.). Baltimore, MD.

Rossi, M. R., Masters, J. R., Park, S., Todd, J. H., Garrett, S. H., Sens, M. a, … Sens, D. a. (2001). The immortalized UROtsa cell line as a potential cell culture model of human urothelium. *Environmental Health Perspectives*, *109*(8), 801–8. Retrieved from http://www.pubmedcentral.nih.gov/articlerender.fcgi?artid=1240407&tool=pmcentrez&rendertype=abstract

Rossi, M. R., Somji, S., Garrett, S. H., Sens, M. A., Nath, J., & Sens, D. a. (2002). Expression of hsp 27, hsp 60, hsc 70, and hsp 70 stress response genes in cultured human urothelial cells (UROtsa) exposed to lethal and sublethal concentrations of sodium arsenite. *Environmental Health Perspectives*, *110*(12), 1225–32. Retrieved from http://www.pubmedcentral.nih.gov/articlerender.fcgi?artid=1241110&tool=pmcentrez&rendertype=abstract

Rubin, P., & Hansen, J. T. (2012). Urinary Bladder. In *TNM Staging Atlas with Oncoanatomy* (2nd ed.). Philadelphia, PA: Lippincott Williams & Wilkins. http://doi.org/10.1016/S0094-0143(05)70198-1

Russell, P. J., Raghavan, D., Gregory, P., Philips, J., Wills, E. J., Jelbart, M., … Vincent, P. C. (1986). Bladder cancer xenografts: a model of tumor cell heterogeneity. *Cancer Res*, *46*(4 Pt 2), 2035–2040. Retrieved from http://www.ncbi.nlm.nih.gov/pubmed/2418959

Said, N., Frierson, H. F., Sanchez-Carbayo, M., Brekken, R. A., & Theodorescu, D. (2013). Loss of SPARC in bladder cancer enhances carcinogenesis and progression. *Journal of Clinical Investigation*, *123*(2), 751–66. http://doi.org/10.1172/JCI64782

Santra, A., Maiti, A., Chowdhury, A., & Mazumder, D. N. (2000). Oxidative stress in liver of mice exposed to arsenic-contaminated water. *Indian Journal of Gastroenterology : Official Journal of the Indian Society of Gastroenterology*, *19*(3), 112–115.

Satarug, S., Baker, J. R., Reilly, P. E. B., Moore, M. R., & Williams, D. J. (2002). Cadmium levels in the lung, liver, kidney cortex, and urine samples from Australians without occupational exposure to metals. *Archives of Environmental Health*, *57*(1), 69–77. http://doi.org/10.1080/00039890209602919

Satarug, S., & Moore, M. R. (2004). Adverse health effects of chronic exposure to low-level cadmium in foodstuffs and cigarette smoke. *Environmental Health Perspectives*, *112*(10), 1099–1103. http://doi.org/10.1289/ehp.6751

Scaggiante, B., Dapas, B., Bonin, S., Grassi, M., Zennaro, C., Farra, R., … Grassi, G. (2012). Dissecting the expression of EEF1A1/2 genes in human prostate cancer cells: the potential of EEF1A2 as a hallmark for prostate transformation and progression. *British Journal of Cancer*, *106*(1), 166–73. http://doi.org/10.1038/bjc.2011.500

Schulte, J., Weidig, M., Balzer, P., Richter, P., Franz, M., Junker, K., … Berndt, A. (2012). Expression of the E-cadherin repressors Snail, Slug and Zeβ1 in urothelial carcinoma of the urinary bladder: Relation to stromal fibroblast activation and invasive behaviour of carcinoma cells. *Histochemistry and Cell Biology*, *138*(6), 847–860. http://doi.org/10.1007/s00418-012-0998-0

Scott, N., Hatlelid, K. M., MacKenzie, N. E., & Carter, D. E. (1993). Reactions of arsenic(III) and arsenic(V) species with glutathione. *Chemical Research in Toxicology*, *6*(1), 102–106. http://doi.org/10.1021/tx00031a016

Sen, B., Wang, A., Hester, S. D., Robertson, J. L., & Wolf, D. C. (2005). Gene expression profiling of responses to dimethylarsinic acid in female F344 rat urothelium. *Toxicology*, *215*(3), 214–26. http://doi.org/10.1016/j.tox.2005.07.008

Sens, D., Park, S., Gurel, V., Sens, M. A., Garrett, S. H., & Somji, S. (2004). Inorganic cadmium- and arsenite-induced malignant transformation of human bladder urothelial cells. *Toxicological Sciences : An Official Journal of the Society of Toxicology*, *79*(1), 56–63. http://doi.org/10.1093/toxsci/kfh086

Sens, D., Rossi, M., Park, S., Gurel, V., Nath, J., Garrett, S., … Somji, S. (2003). Metallothionein isoform 1 and 2 gene expression in a human urothelial cell line (UROtsa) exposed to CdCl2 and NaAsO2. *Journal of Toxicology and Environmental Health. Part A*, *66*(21), 2031–2046. Retrieved from http://www-ncbi-nlm-nih-gov.ezproxy.undmedlibrary.org/pubmed/14555400

Seo, S.-K., Kim, J.-H., Choi, H.-N., Choe, T.-B., Hong, S.-I., Yi, J.-Y., … Park, I.-C. (2014). Knockdown of TWIST1 enhances arsenic trioxide- and ionizing radiation-induced cell death in lung cancer cells by promoting mitochondrial dysfunction. *Biochemical and Biophysical Research Communications*, *449*(4), 490–5. http://doi.org/10.1016/j.bbrc.2014.05.030

Shi, H., Shi, X., & Liu, K. J. (2004). Oxidative mechanism of arsenic toxicity and carcinogenesis. *Molecular and Cellular Biochemistry*, *255*(1-2), 67–78. http://doi.org/10.1023/B:MCBI.0000007262.26044.e8

Shih, C. M., Ko, W. C., Wu, J. S., Wei, Y. H., Wang, L. F., Chang, E. E., … Chen, C. T. (2004). Mediating of caspase-independent apoptosis by cadmium through the mitochondria-ROS pathway in MRC-5 fibroblasts. *Journal of Cellular Biochemistry*, *91*(2), 384–397. http://doi.org/10.1002/jcb.10761

Shimazui, T., Schalken, J. a, Giroldi, L. a, Jansen, C. F., Akaza, H., Koiso, K., … Bringuier, P. P. (1996). Prognostic value of cadherin-associated molecules (alpha-, beta-, and gamma-catenins and p120cas) in bladder tumors. *Cancer Research*, *56*(18), 4154–4158.

Shiota, M., Izumi, H., Onitsuka, T., Miyamoto, N., Kashiwagi, E., Kidani, A., … Kohno, K. (2008). Twist promotes tumor cell growth through YB-1 expression. *Cancer Research*, *68*(1), 98–105. http://doi.org/10.1158/0008-5472.CAN-07-2981

Siemiatycki, J., Dewar, R., Louise, N., & Gérin, M. (1997). Occupational risk factors for bladder cancer: results from a case-control study in Montreal, Quebec, Canada. *American Journal of Epidemiology*, *140*(12), 1061–80.

Simeonova, P. P., Wang, S., Kashon, M. L., Kommineni, C., Crecelius, E., & Luster, M. I. (2001). Quantitative relationship between arsenic exposure and AP-1 activity in mouse urinary bladder epithelium. *Toxicological Sciences*, *60*(2), 279–284. http://doi.org/10.1093/toxsci/60.2.279

Simeonova, P. P., Wang, S., Toriuma, W., Kommineni, V., Matheson, J., Unimye, N., … Luster, M. I. (2000). Arsenic mediates cell proliferation and gene expression in the bladder epithelium association with activating protein-1 transactivation. *Cancer Research*, *60*(13), 3445–3453.

Simon, R., Jones, P., Sidransky, D., Cordon-Cardo, C., Cairns, P., Amin, M., … Knowles, M. (2004). Genetics and predictive factors of non-invasive urothelial neoplasias. In A. Cubilla, J. Dillner, P. Schellhammer, S. Horenglas, A. Ayala, V. Reuter, & G. Von Krog (Eds.), *World Health Organization Classification of Tumours Pathology and Genetics of Tumours of the Urinary System and Male Genital Organs* (pp. 120–3). Lyon.

Sjöblom, T. (2008). Systematic analyses of the cancer genome: lessons learned from sequencing most of the annotated human protein-coding genes. *Current Opinion in Oncology*, *20*(1), 66–71. http://doi.org/10.1097/CCO.0b013e3282f31108

Smith, A. H., Goycolea, M., Haque, R., & Biggs, M. Lou. (1998). Marked increase in bladder and lung cancer mortality in a region of Northern Chile due to arsenic in

drinking water. *American Journal of Epidemiology*, *147*(7), 660–669. http://doi.org/10.1093/oxfordjournals.aje.a009507

Smith, C., Livingston, S., & Doolittle, D. (1997). An international literature survey of "IARC group I carcinogens" reported in mainstream cigarette smoke. *Food and Chemical Toxicology*, *35*, 1107–1130. http://doi.org/10.1016/S0278-6915(97)00063-X

Sobrado, V. R., Moreno-Bueno, G., Cubillo, E., Holt, L. J., Nieto, M. A., Portillo, F., & Cano, A. (2009). The class I bHLH factors E2-2A and E2-2B regulate EMT. *Journal of Cell Science*, *122*(Pt 7), 1014–1024. http://doi.org/10.1242/jcs.028241

Soh, M., Dunlevy, J. R., Garrett, S. H., Allen, C., Sens, D. A., Zhou, X. D., … Somji, S. (2012). Increased neuron specific enolase expression by urothelial cells exposed to or malignantly transformed by exposure to Cd 2+ or As 3+. *Toxicology Letters*, *212*(1), 66–74. http://doi.org/10.1016/j.toxlet.2012.05.003

Somji, S., Bathula, C. S., Zhou, X. D., Sens, M. A., Sens, D. A., & Garrett, S. H. (2008). Transformation of human urothelial cells (UROtsa) by As3+ and Cd2+ induces the expression of keratin 6a. *Environmental Health Perspectives*, *116*(4), 434–440. http://doi.org/10.1289/ehp.10279

Somji, S., Cao, L., Mehus, A., Zhou, X. D., Sens, M. A., Dunlevy, J. R., … Sens, D. a. (2011). Comparison of expression patterns of keratin 6, 7, 16, 17, and 19 within multiple independent isolates of As+3- and Cd+2-induced bladder cancer. *Cell Biology and Toxicology*, *27*(6), 381–96. http://doi.org/10.1007/s10565-010-9169-z

Somji, S., Zhou, X. D., Garrett, S. H., Sens, M. A., & Sens, D. a. (2006). Urothelial cells malignantly transformed by exposure to cadmium (Cd+2) and arsenite (As+3) have increased resistance to Cd+2 and As+3-induced cell death. *Toxicological Sciences*, *94*(2), 293–301. http://doi.org/10.1093/toxsci/kfl108

Somji, S., Zhou, X. D., Mehus, A., Sens, M. A., Garrett, S. H., Lutz, K. L., … Sens, D. A. (2010). Variation of keratin 7 expression and other phenotypic characteristics of independent isolates of cadmium transformed human urothelial cells (UROtsa). *Chemical Research in Toxicology*, *23*(2), 348–356. http://doi.org/10.1021/tx900346q

Steinmaus, C. M., Ferreccio, C., Romo, J. A., Yuan, Y., Cortes, S., Marshall, G., … Smith, A. H. (2013). Drinking water arsenic in northern chile: high cancer risks 40 years after exposure cessation. *Cancer Epidemiology, Biomarkers & Prevention : A Publication of the American Association for Cancer Research, Cosponsored by the American Society of Preventive Oncology*, *22*(4), 623–30. http://doi.org/10.1158/1055-9965.EPI-12-1190

Stemmler, M. P., Hecht, A., Kinzel, B., & Kemler, R. (2003). Analysis of regulatory elements of E-cadherin with reporter gene constructs in transgenic mouse embryos. *Developmental Dynamics : An Official Publication of the American Association of Anatomists*, *227*(2), 238–245. http://doi.org/10.1002/dvdy.10301

Styblo, M., Del Razo, L. M., Vega, L., Germolec, D. R., LeCluyse, E. L., Hamilton, G. a., … Thomas, D. J. (2000). Comparative toxicity of trivalent and pentavalent inorganic and methylated arsenicals in rat and human cells. *Archives of Toxicology*, *74*(6), 289–299. http://doi.org/10.1007/s002040000134

Su, C.-C., Lu, J.-L., Tsai, K.-Y., & Lian, I.-B. (2011). Reduction in arsenic intake from water has different impacts on lung cancer and bladder cancer in an arseniasis endemic area in Taiwan. *Cancer Causes & Control : CCC*, *22*(1), 101–8. http://doi.org/10.1007/s10552-010-9679-2

Su, Y., Qiu, Q., Zhang, X., Jiang, Z., Leng, Q., Liu, Z., … Jiang, F. (2010). Aldehyde dehydrogenase 1 A1-positive cell population is enriched in tumor-initiating cells and associated with progression of bladder cancer. *Cancer Epidemiology, Biomarkers & Prevention : A Publication of the American Association for Cancer Research, Cosponsored by the American Society of Preventive Oncology*, *19*(2), 327–37. http://doi.org/10.1158/1055-9965.EPI-09-0865

Suggitt, M., & Bibby, M. C. (2005). 50 Years of preclinical anticancer drug screening: Empirical to target-driven approaches. *Clinical Cancer Research*.

Sumino, K., Hayakawa, K., Shibata, T., & Kitamura, S. (1975). Heavy metals in normal Japanese tissues. Amounts of 15 heavy metals in 30 subjects. *Archives of Environmental Health*, *30*(10), 487–494.

Suyama, K., Shapiro, I., Guttman, M., & Hazan, R. B. (2002). A signaling pathway leading to metastasis is controlled by N-cadherin and the FGF receptor. *Cancer Cell*, *2*(4), 301–314. http://doi.org/10.1016/S1535-6108(02)00150-2

Svatek, R. S., Hollenbeck, B. K., Holmäng, S., Lee, R., Kim, S. P., Stenzl, A., & Lotan, Y. (2014). The economics of bladder cancer: Costs and considerations of caring for this disease. *European Urology*, *66*, 253–262. http://doi.org/10.1016/j.eururo.2014.01.006

Takai, H., Wang, R. C., Takai, K. K., Yang, H., & de Lange, T. (2007). Tel2 regulates the stability of PI3K-related protein kinases. *Cell*, *131*(7), 1248–59. http://doi.org/10.1016/j.cell.2007.10.052

Takeichi, M. (2007). The cadherin superfamily in neuronal connections and interactions. *Nature Reviews. Neuroscience*, *8*(1), 11–20. http://doi.org/10.1038/nrn2043

Thiery, J. P., Acloque, H., Huang, R. Y. J., & Nieto, M. A. (2009). Epithelial-Mesenchymal Transitions in Development and Disease. *Cell*, *139*(5), 871–890. http://doi.org/10.1016/j.cell.2009.11.007

Tokar, E. J., Diwan, B. A., & Waalkes, M. P. (2010). Arsenic exposure transforms human epithelial stem/progenitor cells into a cancer stem-like phenotype. *Environmental Health Perspectives*, *118*(1), 108–15. http://doi.org/10.1289/ehp.0901059

Tokar, E. J., Diwan, B. A., Ward, J. M., Delker, D. A., & Waalkes, M. P. (2011). Carcinogenic effects of "whole-life" exposure to inorganic arsenic in CD1 mice. *Toxicological Sciences : An Official Journal of the Society of Toxicology*, *119*(1), 73–83. http://doi.org/10.1093/toxsci/kfq315

Tokar, E. J., Qu, W., Liu, J., Liu, W., Webber, M. M., Phang, J. M., & Waalkes, M. P. (2010). Arsenic-specific stem cell selection during malignant transformation. *Journal of the National Cancer Institute*, *102*(9), 638–49. http://doi.org/10.1093/jnci/djq093

Tsai, S. Y., & Tsai, M. J. (1997). Chick ovalbumin upstream promoter-transcription factors (COUP-TFs): Coming of age. *Endocrine Reviews*. http://doi.org/10.1210/er.18.2.229

Tseng, W. P. (1977). Effects and dose response relationships of skin cancer and blackfoot disease with arsenic. *Environmental Health Perspectives*, *Vol.19*(August), 109–119. http://doi.org/10.1289/ehp.7719109

Tsuji, J. S., Alexander, D. D., Perez, V., & Mink, P. J. (2014). Arsenic exposure and bladder cancer: quantitative assessment of studies in human populations to detect risks at low doses. *Toxicology*, *317*, 17–30. http://doi.org/10.1016/j.tox.2014.01.004

Tsuji, T., Ibaragi, S., Shima, K., Hu, M. G., Katsurano, M., Sasaki, A., & Hu, G. (2008). Epithelial-mesenchymal transition induced by growth suppressor p12CDK2-AP1 promotes tumor cell local invasion but suppresses distant colony growth. *Cancer Research*, *68*(24), 10377–86. http://doi.org/10.1158/0008-5472.CAN-08-1444

Ueda, F., Seki, H., Fujiwara, H., Ebara, K., Minomiya, S., & Shimaki, Y. (1987). Interacting effects of zinc and cadmium on the cadmium distribution in the mouse. *Veterinary and Human Toxicology*, *29*(5), 367–72. Retrieved from http://www.ncbi.nlm.nih.gov/pubmed/3686816

Vahter, M. (2002). Mechanisms of arsenic biotransformation. *Toxicology*, *181-182*, 211–217. http://doi.org/10.1016/S0300-483X(02)00285-8

Van der Horst, G., Bos, L., & van der Pluijm, G. (2012). Epithelial plasticity, cancer stem cells, and the tumor-supportive stroma in bladder carcinoma. *Molecular Cancer Research : MCR*, *10*(8), 995–1009. http://doi.org/10.1158/1541-7786.MCR-12-0274

Van Roy, F. (2014). Beyond E-cadherin: roles of other cadherin superfamily members in cancer. *Nature Reviews. Cancer*, *14*(2), 121–34. http://doi.org/10.1038/nrc3647

Verhoeven, R. H. a, Louwman, M. W. J., Buntinx, F., Botterweck, A. M., Lousbergh, D., Faes, C., & Coebergh, J. W. W. (2011). Variation in cancer incidence in northeastern Belgium and southeastern Netherlands seems unrelated to cadmium emission of zinc smelters. *European Journal of Cancer Prevention : The Official Journal of the European Cancer Prevention Organisation (ECP)*, *20*(6), 549–55. http://doi.org/10.1097/CEJ.0b013e3283498e9c

Vesey, D. A. (2010). Transport pathways for cadmium in the intestine and kidney proximal tubule: focus on the interaction with essential metals. *Toxicology Letters*, *198*(1), 13–9. http://doi.org/10.1016/j.toxlet.2010.05.004

Vineis, P., & Pirastu, R. (1997). Aromatic amines and cancer. *Cancer Causes and Control*, *8*(3), 346–355. http://doi.org/10.1023/A:1018453104303

Waalkes, M. P., Liu, J., Ward, J. M., & Diwan, B. A. (2006). Enhanced urinary bladder and liver carcinogenesis in male CD1 mice exposed to transplacental inorganic arsenic and postnatal diethylstilbestrol or tamoxifen. *Toxicology and Applied Pharmacology*, *215*(3), 295–305. http://doi.org/10.1016/j.taap.2006.03.010

Wadhwa, S. K., Kazi, T. G., Afridi, H. I., Tüzen, M., & Citak, D. (2013). Arsenic in water, food and cigarettes: a cancer risk to Pakistani population. *Journal of Environmental Science and Health. Part A, Toxic/hazardous Substances & Environmental Engineering*, *48*(14), 1776–82. http://doi.org/10.1080/10934529.2013.823332

Waisberg, M., Joseph, P., Hale, B., & Beyersmann, D. (2003, November). Molecular and cellular mechanisms of cadmium carcinogenesis. *Toxicology*. http://doi.org/10.1016/S0300-483X(03)00305-6

Wallerand, H., Cai, Y., Wainberg, Z. a, Garraway, I., Lascombe, I., Nicolle, G., … Reiter, R. R. (2010). Phospho-Akt pathway activation and inhibition depends on N-cadherin or phospho-EGFR expression in invasive human bladder cancer cell lines. *Urologic Oncology*, *28*(2), 180–8. http://doi.org/10.1016/j.urolonc.2008.09.041

Wang, G. Z., Zhang, W., Fang, Z. T., Zhang, W., Yang, M. J., Yang, G. W., … Qu, X. D. (2014). Arsenic trioxide: Marked suppression of tumor metastasis potential by inhibiting the transcription factor Twist in vivo and in vitro. *Journal of Cancer Research and Clinical Oncology*, *140*(7), 1125–1136. http://doi.org/10.1007/s00432-014-1659-6

Wang, H. H., Wu, M. M., Chan, M. W. Y., Pu, Y. S., Chen, C. J., & Lee, T. C. (2014). Long-term low-dose exposure of human urothelial cells to sodium arsenite activates

lipocalin-2 via promoter hypomethylation. *Archives of Toxicology*, *88*(8), 1549–1559. http://doi.org/10.1007/s00204-014-1214-x

Wang, L., Chen, F., Zhang, Z., Chen, G., Luo, J., & Shi, X. (2012). Cancer stem cells in the mechanism of metal carcinogenesis. *Journal of Environmental Pathology, Toxicology and Oncology : Official Organ of the International Society for Environmental Toxicology and Cancer*, *31*(3), 245–63. Retrieved from http://www.ncbi.nlm.nih.gov/pubmed/23339699

Wang, T.-C., Jan, K.-Y., Wang, A. S. S., & Gurr, J.-R. (2007). Trivalent arsenicals induce lipid peroxidation, protein carbonylation, and oxidative DNA damage in human urothelial cells. *Mutation Research*, *615*(1-2), 75–86. http://doi.org/10.1016/j.mrfmmm.2006.10.003

Wang, X.-J., Sun, Z., Chen, W., Eblin, K. E., Gandolfi, J. A., & Zhang, D. D. (2007). Nrf2 protects human bladder urothelial cells from arsenite and monomethylarsonous acid toxicity. *Toxicology and Applied Pharmacology*, *225*(2), 206–13. http://doi.org/10.1016/j.taap.2007.07.016

Watkin, R. D., Nawrot, T., Potts, R. J., & Hart, B. A. (2003). Mechanisms regulating the cadmium-mediated suppression of Sp1 transcription factor activity in alveolar epithelial cells. *Toxicology*, *184*(2-3), 157–178. http://doi.org/10.1016/S0300-483X(02)00577-2

Wei, M., Wanibuchi, H., Morimura, K., Iwai, S., Yoshida, K., Endo, G., … Fukushima, S. (2002). Carcinogenicity of dimethylarsinic acid in male F344 rats and genetic alterations in induced urinary bladder tumors. *Carcinogenesis*, *23*(8), 1387–1397.

Wei, M., Wanibuchi, H., Yamamoto, S., Li, W., & Fukushima, S. (1999). Urinary bladder carcinogenicity of dimethylarsinic acid in male F344 rats. *Carcinogenesis*, *20*(9), 1873–1876. http://doi.org/10.1093/carcin/20.9.1873

Wheelock, M. J., Shintani, Y., Maeda, M., Fukumoto, Y., & Johnson, K. R. (2008). Cadherin switching. *Journal of Cell Science*, *121*(Pt 6), 727–735. http://doi.org/10.1242/jcs.000455

Wolf, C., Strenziok, R., & Kyriakopoulos, A. (2009). Elevated metallothionein-bound cadmium concentrations in urine from bladder carcinoma patients, investigated by size exclusion chromatography-inductively coupled plasma mass spectrometry. *Analytica Chimica Acta*, *631*(2), 218–22. http://doi.org/10.1016/j.aca.2008.10.035

Wolff, N. a, Abouhamed, M., Verroust, P. J., & Thévenod, F. (2006). Megalin-dependent internalization of cadmium-metallothionein and cytotoxicity in cultured renal proximal tubule cells. *The Journal of Pharmacology and Experimental Therapeutics*, *318*(2), 782–791. http://doi.org/10.1124/jpet.106.102574

Worst, T. S., Reiner, V., Gabriel, U., Weiß, C., Erben, P., Martini, T., & Bolenz, C. (2014). IL1RN and KRT13 Expression in Bladder Cancer: Association with Pathologic Characteristics and Smoking Status. *Advances in Urology*, *2014*, 184602. http://doi.org/10.1155/2014/184602

Wu, K., Zeng, J., Zhou, J., Fan, J., Chen, Y., Wang, Z., … He, D. (2012). Slug contributes to cadherin switch and malignant progression in muscle-invasive bladder cancer development. *Urologic Oncology*. http://doi.org/10.1016/j.urolonc.2012.02.001

Xie, S.-H., Liu, A.-L., Chen, Y.-Y., Zhang, L., Zhang, H.-J., Jin, B.-X., … Lu, W.-Q. (2010). Analysis of genomic dose-response information on arsenic to inform key events in a mode of action for carcinogenicity. *Environmental and Molecular Mutagenesis*, *51*(June 2009), 229–235. http://doi.org/10.1002/em

Xu, Y., Li, Y., Pang, Y., Ling, M., Shen, L., Yang, X., … Liu, Q. (2012). EMT and stem cell-like properties associated with HIF-2α are involved in arsenite-induced transformation of human bronchial epithelial cells. *PloS One*, *7*(5), e37765. http://doi.org/10.1371/journal.pone.0037765

Xu, Y., Tokar, E. J., Person, R. J., Orihuela, R. G., Ngalame, N. N. O., & Waalkes, M. P. (2013). Recruitment of normal stem cells to an oncogenic phenotype by noncontiguous carcinogen-transformed epithelia depends on the transforming carcinogen. *Environmental Health Perspectives*, *121*(8), 944–950. http://doi.org/10.1289/ehp.1306714

Xue, G., Restuccia, D. F., Lan, Q., Hynx, D., Dirnhofer, S., Hess, D., … Hemmings, B. a. (2012). Akt/PKB-mediated phosphorylation of Twist1 promotes tumor metastasis via mediating cross-talk between PI3K/Akt and TGF-β signaling axes. *Cancer Discovery*, *2*(3), 248–259. http://doi.org/10.1158/2159-8290.CD-11-0270

Yager, J. W., Gentry, P. R., Thomas, R. S., Pluta, L., Efremenko, A., Black, M., … Clewell, H. J. (2013). Evaluation of gene expression changes in human primary uroepithelial cells following 24-Hr exposures to inorganic arsenic and its methylated metabolites. *Environmental and Molecular Mutagenesis*, *54*(2), 82–98. http://doi.org/10.1002/em.21749

Yamamoto, S., Konishi, Y., Matsuda, T., Murai, T., Shibata, M. a., Matsui-Yuasa, I., … Fukushima, S. (1995). Cancer induction by an organic arsenic compound, dimethylarsinic acid (cacodylic acid), in F344/DuCrj rats after pretreatment with five carcinogens. *Cancer Research*, *55*, 1271–1276.

Yamamoto, T., Tamura, Y., Kobayashi, J.-I., Kamiguchi, K., Hirohashi, Y., Miyazaki, A., … Sato, N. (2013). Six-transmembrane epithelial antigen of the prostate-1 plays a role for in vivo tumor growth via intercellular communication. *Experimental Cell Research*, *319*(17), 2617–26. http://doi.org/10.1016/j.yexcr.2013.07.025

Yan, H., Wang, N., Weinfeld, M., Cullen, W. R., & Le, X. C. (2009). Identification of arsenic-binding proteins in human cells by affinity chromatography and mass spectrometry. *Analytical Chemistry*, *81*(10), 4144–4152. http://doi.org/10.1021/ac900352k

Yang, C.-Y., Chiu, H.-F., Chang, C.-C., Ho, S.-C., & Wu, T.-N. (2005). Bladder cancer mortality reduction after installation of a tap-water supply system in an arsenious-endemic area in southwestern Taiwan. *Environmental Research*, *98*(1), 127–32. http://doi.org/10.1016/j.envres.2004.07.013

Yang, F., Sun, L., Li, Q., Han, X., Lei, L., Zhang, H., & Shang, Y. (2012). SET8 promotes epithelial-mesenchymal transition and confers TWIST dual transcriptional activities. *The EMBO Journal*, *31*(1), 110–23. http://doi.org/10.1038/emboj.2011.364

Yang, S. W., Becker, F. F., & Chan, J. Y. (1996). Inhibition of human DNA ligase I activity by zinc and cadmium and the fidelity of ligation. *Environmental and Molecular Mutagenesis*, *28*(1), 19–25. http://doi.org/doi: 10.1002/(sici)1098-2280(1996)28:1%3C19::aid-em5%3E3.0.co;2-9

Yang, Y. M., & Chang, J. W. (2008). Bladder cancer initiating cells (BCICs) are among EMA-CD44v6+ subset: novel methods for isolating undetermined cancer stem (initiating) cells. *Cancer Investigation*, *26*(7), 725–33. http://doi.org/10.1080/07357900801941845

Yeung, C., Dinh, T., & Lee, J. (2014). The Health Economics of Bladder Cancer: An updated Review of the Published Literature. *PharmacoEconomics*, *32*, 1093–1104. http://doi.org/10.1007/s40273-014-0194-2

Youn, C. K., Kim, S. H., Lee, D. Y., Song, S. H., Chang, I. Y., Hyun, J. W., … You, H. J. (2005). Cadmium down-regulates human OGG1 through suppression of Sp1 activity. *Journal of Biological Chemistry*, *280*(26), 25185–25195. http://doi.org/10.1074/jbc.M412793200

Zeegers, M., Tan, F., Dorant, E., & Van Den Brandt, P. (2000). The impact of characteristics of cigarette smoking on urinary tract cancer risk: a meta-analysis of epidemiologic studies. *Cancer*, *89*, 630–639.

Zhang, C., Awasthi, N., Schwarz, M. A., & Schwarz, R. E. (2013). Establishing a peritoneal dissemination xenograft mouse model for survival outcome assessment of experimental gastric cancer. *The Journal of Surgical Research*, *182*(2), 227–34. http://doi.org/10.1016/j.jss.2012.10.052

Zhang, H., Toyofuku, T., Kamei, J., & Hori, M. (2003). GATA-4 regulates cardiac morphogenesis through transactivation of the N-cadherin gene. *Biochemical and*

Biophysical Research Communications, *312*(4), 1033–1038. http://doi.org/10.1016/j.bbrc.2003.11.019

Zhang, Y., Sun, M., Shi, W., Yang, Q., Chen, C., Wang, Z., & Zhou, X. (2015). Arsenic trioxide suppresses transcription of hTERT through down-regulation of multiple transcription factors in HL-60 leukemia cells. *Toxicology Letters*, *232*(2), 481–9. http://doi.org/10.1016/j.toxlet.2014.11.028

Zhao, J., Dong, D., Sun, L., Zhang, G., & Sun, L. (2014). Prognostic significance of the epithelial-tomesenchymal transition markers e-cadherin, vimentin and twist in bladder cancer. *International Braz J Urol*, *40*(2), 179–189. http://doi.org/10.1590/S1677-5538.IBJU.2014.02.07

Zhou, X. D., Sens, D. a, Sens, M. A., Namburi, V. B. R. K., Singh, R. K., Garrett, S. H., & Somji, S. (2006). Metallothionein-1 and -2 expression in cadmium- or arsenic-derived human malignant urothelial cells and tumor heterotransplants and as a prognostic indicator in human bladder cancer. *Toxicological Sciences*, *91*(2), 467–75. http://doi.org/10.1093/toxsci/kfj174

Zhou, X. D., Sens, M. A., Garrett, S. H., Somji, S., Park, S., Gurel, V., & Sens, D. a. (2006). Enhanced expression of metallothionein isoform 3 protein in tumor heterotransplants derived from As+3- and Cd+2-transformed human urothelial cells. *Toxicological Sciences*, *93*(2), 322–30. http://doi.org/10.1093/toxsci/kfl065

Zhou, X., Sun, X., Cooper, K. L., Wang, F., Liu, K. J., & Hudson, L. G. (2011). Arsenite interacts selectively with zinc finger proteins containing C3H1 or C4 motifs. *Journal of Biological Chemistry*, *286*(26), 22855–22863. http://doi.org/10.1074/jbc.M111.232926